DISSERTATION

MODULATION OF OPIOID PHARMACOKINETICS AND PHARMACODYNAMICS, *IN VIVO*

Submitted by

Iman Elkiweri

Department of Biomedical Sciences

In partial fulfillment of the requirements

For the Degree of Doctor of Philosophy

Colorado State University

Fort Collins, Colorado

Fall 2005

COLORADO STATE UNIVERSITY

October 6, 2005

WE HEREBY RECOMMEND THAT THE DISSERTATION PREPARED UNDER OUR SUPERVISION BY IMAN ELKIWERI TITLED MODULATION OF OPIOID PHARMACOKINETICS AND PHARMACODYNAMICS, *IN VIVO.* BE ACCEPTED AS FULFILLING INPART REQUIREMENTS FOR THE DEGREE OF DOCTOR OF PHILOSOPHY.

Committee on Graduate Work
(Please print name under signature)

Anne E. Wagner

Charles W. Miller

Douglas N. Ishi

Richard A. Bowen

Martha Tissot van Patot
Adviser

Co-Adviser (if applicable)

Barbara M. Sanborn
Department Head/Director

ABSTRACT OF DISSERTATION

MODULATION OF OPIOID PHARMACOKINETICS AND PHARMACODYNAMICS, *IN VIVO*

Inter-individual variability in response to opioid anesthesia complicates optimal and effective anesthetic management. Extensive first-pass pulmonary uptake of opioids has a significant impact on the central effect. Because a greater understanding of the mechanisms controlling opioid transport into the lung and brain is essential to developing dosage strategies, we investigated the role of opioid transport inhibitors in lung and brain of Sprague Dawley rats using pharmacokinetic and pharmacodynamic modeling techniques. First, we evaluated the effect of verapamil, a P-glycoprotein (P-gp) efflux transporter inhibitor, on fentanyl and loperamide partitioning in lung (P_L) and brain (P_B) and central effect by a continuously processed electroencephalogram (EEG), *in vivo* and hypothesized differential effects of verapamil on these processes. Our results showed that verapamil slightly decreased P_B for fentanyl, whereas P_L and P_B of loperamide increased to a much larger extent. Central effect was reduced with verapamil-induced reduction of fentanyl P_B, while verapamil increased loperamide central effect. Also, this is the first report of loperamide crossing the blood brain barrier and eliciting a central effect. We then investigated the effect of opioids on verapamil disposition in lung and brain, *in vivo*. We found that fentanyl slightly reduced verapamil P_B but slightly increased P_L; in contrast, loperamide increased P_L and P_B. These results confirm that verapamil and loperamide are substrates of the efflux transporter P-gp and suggest that verapamil and fentanyl may be substrates of an as yet unidentified inward transporter. Because our study showed that verapamil had only slight effect on fentanyl partitioning and clearance, we hypothesized that inhibition of uptake by organic anion transport polypeptides (Oatp) using

pravastatin or naloxone may reduce P_L and P_B of fentanyl, *in vivo*. We report that co-administration of fentanyl with pravastatin or naloxone reduces P_L and P_B of fentanyl in Sprague Dawley rats. In conclusion, Oatp inhibition modulates fentanyl lung and brain concentration; whereas loperamide concentrations in lung and brain are closely controlled by P-gp.

Iman Elkiweri
Department of Biomedical Sciences
Colorado State University
Fort Collins, Colorado 80523
Fall 2005

Dedicated to

Khaled Ibn El Walid ElKiweri

1959-2005

&

Omar Mehdawi

1987-2005

TABLE OF CONTENTS

CHAPTER 1

Introduction and Literature Review

Drug effects are largely determined by the concentration of drug at the site of action. During the past few years it has been recognized that there is considerable variation among individuals' response to similar doses of drug. This inter-individual variability is largely the result of variability in drug concentration at the receptor site (pharmacokinetic variability); some of this variability is also the result of differences in drug sensitivity (pharmacodynamic variability) (Wood, 1997). For drugs with rapid onset of effect, like the opioid analgesic fentanyl, early pharmacokinetic events are of great importance in determining the drug concentrations at the sites of action. The timing and intensity of the onset of drug effect immediately after rapid intravenous drug administration are influenced by factors that affect the early arterial drug concentrations versus time profile. These factors include pulmonary uptake, intravascular mixing, distribution to highly perfused tissues, and, rarely, rapid metabolism (Krejcie et al., 1994). Drug uptake by pulmonary tissue, if extensive, markedly reduces peak systemic arterial concentrations in the moments after rapid intravenous drug administration. Thus, for drugs with rapid onsets of action, pulmonary drug uptake could act to reduce peak drug effect.

Pulmonary Uptake

The lungs are anatomically unique in that they are located between the systemic venous and arterial circulations, and they are perfused by nearly the entire cardiac output (Boer, 2003). In addition, the pulmonary circulation contains almost half of the entire endothelium in the body (Bakhle, 1990). The pulmonary circulation has important functions other than gas exchange, including a pharmacokinetic function in which pulmonary endothelium accumulated a wide variety of biogenic and xenobiotic substances (Bakhle, 1990; Roerig et al., 1994; Boer, 2003).

Many drugs, especially basic lipophilic amines such as the opioid analgesics fentanyl (Roerig et al., 1987; Taeger et al., 1988) and sufentanil (Boer et al., 1995), are known to have significant, reversible, pulmonary uptake following intravenous administration. The calcium channel blocker verapamil (Roerig et al., 1989b), the local anesthetics lidocaine (Krejcie et al., 1997) and bupivacaine (Ohmura et al., 1993), and the beta-blocker propranolol (Howell and Lanken, 1992) have also been shown to exhibit extensive pulmonary uptake. The endothelial cell is the primary cell involved in the pulmonary uptake of drugs as the first cell encountered by blood-borne substrates (Bakhle, 1990; Boer, 2003).

It has long been maintained that pulmonary uptake is the result of simple diffusion from the intravascular space into lung tissues (Roerig et al., 1987). However, pulmonary uptake of the opioid analgesic fentanyl has been recently shown to be the result of both passive diffusion and saturable specific uptake mechanisms (Henthorn et al., 1998; Waters et al., 1999; Waters et al., 2000). Numerous transporters responsible for substrate import and export have been identified, and many more remain to be identified, one of

which may be responsible for transport of the opioid analgesic fentanyl as well as other substances in the lungs. After uptake, some drugs may be metabolized, but metabolism is insignificant for most drugs used in anesthesia (Bakhle, 1990; Boer, 2003). Since pulmonary tissue does not metabolize these drugs to any appreciable extent, the kinetics of this uptake process is one of extensive partitioning between blood and lung tissues that manifests itself as a greatly reduced and delayed initial peak arterial blood concentration followed by slow release of the drug from the pulmonary tissue when blood concentrations fall below those in the lung (Roerig et al., 1994).

For drugs with extensive pulmonary uptake, like the opioid analgesic fentanyl, the initial arterial fentanyl concentrations delivered to the brain depend on the extent of pulmonary uptake.

Brain uptake

The blood- brain barrier (BBB) is an important interface between blood and brain that is formed by endothelial cells lining the brain capillaries and is thought to protect the brain from xenobiotics and regulate brain homeostasis. Throughout most of the brain the capillary endothelial cells are tightly linked to each other by tight junctions, completely covering the wall of the blood vessels. In combination with a lack of fenestrae and pinocytosis in the endothelial cells, this makes for a nearly continuous physical barrier (Begley and Brightman, 2003; Ballabh et al., 2004). As a consequence of this barrier, hydrophilic compounds which are not small enough to pass the tight junctions by passive diffusion will be excluded from the brain unless they are translocated across the endothelial cells by specific carrier systems. However, hydrophobic compounds can cross the blood-brain barrier by passive diffusion and enter the brain compartment. In fact, it

has been found that for most compounds the degree of lipophilicity as measured by the octanol-water partition correlates with the capacity of these compounds to enter the brain (Levin, 1980; Kastin et al., 1999). In addition to passive diffusion, a number of other mechanisms such as transcytosis, receptor mediated endocytosis, and facilitated active transporters permit the entry or exit of various nutrients and substrates including pharmacological agents into the brain (Ayrton and Morgan, 2001). The presence of an inward-directed transporter for substances like the basic lipophilic amine fentanyl at the endothelial cell layer of the BBB would affect its pharmacodynamics (i.e., onset time and plasma-apparent EC_{50}) (Henthorn et al., 1999).

Novel, multi-specific, organic anion transporter polypeptides (Oatp/OATP) have been found in endothelial cells lining the brain (Gao et al., 1999) and lung (Hagenbuch and Meier, 2003) capillaries of rats and humans. They may represent an important influx system for a wide range of substrates including analgesic opioids, in the brain (Gao et al., 2000) and lung

Organic anion transporting polypeptides

Origin and Structure

Organic anion transporting polypeptides (rodent: Oatps, human: OATPs) are a group of membrane solute carriers with a wide spectrum of amphipathic transport substrates. Currently, 11 rat, 8 mouse and 9 human Oatp/OATPs have been identified. Their genes are currently classified within the solute carrier family 21A (rodents: Slc21a; humans: SLC21A) of the human and mouse genome nomenclature database (Hagenbuch and Meier, 2003; Kim, 2003).

In general, these proteins possess 12 putative transmembrane domains with large hydrophobic loops between the first and second, and the sixth and seventh domains. N-glycosylation sites are predicted on the hydrophobic loop between the first and second transmembrane domain as well as several phosphorylation sites on the loop between the sixth and seventh domains (Hagenbuch and Meier, 2003; Kim, 2003) (Figure 1.1).

Location

Most Oatp/OATPs are expressed in various normal rat and human tissues as well as in human cancer cell lines. Rat Oatps as well as human OATPs are found in the BBB, lung, choroid plexus, heart, intestine, kidney, placenta, and testis (Gao et al., 1999; Hagenbuch and Meier, 2003; Kim, 2003). Rat Oatp2 and human OATP-8 have been localized along both the luminal and abluminal membranes of brain endothelial cells (Gao et al., 1999).

Mechanism of action

It is well accepted that Oatps/OATPs represent sodium-independent bile salt and organic anion transport systems and are believed to have influx *and* efflux capabilities at the BBB (Ayrton and Morgan, 2001). The driving force for Oatp/OATP-mediated transport has not been investigated in detail for all transporters, but for Oatp1 and Oatp2 physiologic efflux of glutathione (GSH) may represent an important driving force for substrate uptake by these transporters (Hagenbuch and Meier, 2003).

Substrates and inhibitors

In general Oatp/OATP substrates are compounds with a steroid nucleus or small linear and cyclic peptides. Their substrates include a wide range of amphipathic organic compounds including bile salts, steroid hormones and their conjugates, thyroid hormones, and even organic cations. In addition to endogenous and exogenous amphipathic

compounds, Oatps/OATPs can mediate the transport of numerous drugs including the receptor antagonist BQ-123, the δ opioid receptor agonists deltorphin II and [D-Pen(2),D-Pen(5)] enkephalin, the HMG-CoA reductase pravastatin and the antihistamine fexofenadine (Hsiang et al., 1999; Gao et al., 2000; Hagenbuch and Meier, 2003; Kim, 2003) (Table 1.1). The nonselective opiate antagonist naloxone is an inhibitor to the uptake of deltorphin II (Gao et al., 2000). Interestingly, a number of the Oatps/OATPs transporters appear to have shared drug substrates with the efflux transporter P-glycoprotein (P-gp). Moreover, they are co-expressed in organs important to drug disposition such as the intestine and liver, or organs with known barrier function such as the brain. Thus Oatp/OATP and P-gp may play an important role to determine the net cellular entry or efflux of shared substrates (Cvetkovic et al., 1999; Dagenais et al., 2001; Su et al., 2004) (Figures 1.2 and 1.3).

P-glycoprotein

Origin and structure

P-glycoproteins are transport proteins members of the ATP-binding cassette (ABC) transporter superfamily. They are widely distributed in many endothelia and act to create and maintain tissue/plasma gradients of lipophilic xenobiotics that would not be produced by simple passive processes alone (Schinkel and Jonker, 2003). The ATP-dependent efflux transporter P-gp is expressed in a number of barrier tissues involved in the biodisposition of xenobiotics, and is encoded by the multidrug resistant (mdr) genes in rodents (mdr1a and mdr1b) and humans (MDR1) (Schinkel, 1997). Its importance was first recognized with the occurrence of multidrug resistance during chemotherapy of tumors. Tumor cells are protected against various cytostatic agents due to over expression

of P-gp (Fardel et al., 1996). These large (150-170 kDa) transmembrane proteins also reside in plasma membrane of normal cells and may have evolved along with various cytochrome P-450s, as part of the body's defense against plant toxins. The drug transporting P-glycoproteins are N-glycosylated membrane proteins of about 1280 amino acids. The polypeptide chain consists of two homologous domains each containing six putative transmembrane segments and an intracellular ATP binding site (Demeule et al., 2002) (Figure 1.4).

Location

P-glycoprotein is found in endothelial cells comprising the blood-brain barrier (Bendayan et al., 2002) and human capillary endothelial cells of lung and bronchi (Lechapt-Zalcman et al., 1997). P-gp is also present in placenta and endometrium of the pregnant uterus, testis, the apical membrane of intestinal epithelial cells of small and large intestine, the biliary canalicular membrane of hepatocytes, the luminal membrane of proximal tubular epithelial cells of the kidney, and adrenal glands of humans and mice (but not rats) possess high levels of P-gp diffusely distributed in both the cortex and medulla (Schinkel and Jonker, 2003).

Mechanism of action

It is suggested that P-gp can protect against toxic xenobiotic compounds by excreting these compounds into urine, bile, and the intestinal lumen, and by preventing their accumulation in critical organs, such as the brain or testis. The transport of compounds by P-gp is an active process requiring ATP. The exact mechanism by which P-gp extrudes substrates from the cell cytoplasm remains unresolved. According to the classical model of a typical substrate-enzyme interaction, substrates bind to a cytoplasmic region of P-gp

resulting in an energy-dependent conformational change that shuttles the drug to the outside of the plasma membrane. On the other hand, recent evidence suggests that P-gp act as a "flippase" where membrane bound drug is relocated between inner and outer lipid leaflets of the plasma membrane, which would result in a net efflux of drug. Whatever the precise molecular mechanism of drug transport, P-gp can mediate very effective extrusion of drugs penetrating the plasma membrane, which result in very low intracellular drug levels (Higgins and Gottesman, 1992; Sharom, 1997) (Figure 1.5).

Substrates and inhibitors

P-glycoprotein substrates and/or inhibitors include a broad variety of structurally diverse compounds (Ford, 1995; Fardel et al., 1996). Although these compounds share only broad structural similarities, the majority is lipophilic and many are heterocyclic, positively charged molecules. P-gp substrates include various anticancer agents such as Vinca alkaloids, and anthracyclines, also many other drugs such as cardiac drugs, calcium channel blockers, β-adrenoceptors antagonists, HIV protease inhibitors, antibiotics, immunosuppressants, histamine H_1 receptor antagonists, and opioids (Schinkel, 1997; Schinkel and Jonker, 2003) (Table 1.2). Most of these P-gp substrates are also substrates of the major drug metabolizing enzyme cytochrome P450 3A4 (CYP3A4). This may be important in the gut leading to a drug efflux-metabolism alliance through repeated cycles of metabolism and efflux. However, this overlap is not complete because some drugs are P-gp substrates but are not metabolized by CYP3A4 (digioxin) and some drugs are CYP3A4 substrates but are not P-gp substrates (midazalom). Also, recent data indicate a lack of co-regulation of CYP3A4 and P-gp in human small intestine(Kim et al., 1999). P-gp inhibitors are also structurally diverse, including

quinolines, immunosuppressive agents, antibiotics, calcium channel blockers, calmodulin antagonists, HIV-1 protease inhibitors among others (Schinkel and Jonker, 2003) (Table 1.2). Some of these inhibitors act as P-gp substrates. This inhibition could involve competitive mechanisms where the inhibitor binds to the substrate binding site or non-competitive mechanisms where the inhibitor binds other binding sites that cause allosteric changes in the P-gp protein resulting in inhibition of substrate binding (Schinkel, 1997). The administration of P-gp blockers can enhance the penetration of many drugs into organs such as the brain (Bendayan et al., 2002; Sun et al., 2003). The injection of very high concentrations (0.05-0.5 mM) of the P-gp blocker verapamil in a rat brain *in situ* perfusion model has been shown to increase the brain uptake of hydrophobic peptides (Chikhale et al., 1995). Furthermore, the P-gp knockout mouse (mdr1a (-/-) mouse) has provided a significant pharmacologic tool to examine the function of P-gp in the BBB *in vivo*(Dagenais et al., 2004). P-gp is completely absent in the BBB of the mdr1a (-/-) mouse. An intravenous bolus injection of 0.2 mg/kg [^{3}H] digoxin (P-gp substrate and Oatp substrate) in mdr1a (-/-) mice resulted in 100-fold higher brain concentrations in comparison with wild-type mice indicating that Oatp2 which express high affinity to digoxin might be responsible for the extensive uptake and accumulation of digoxin in brain tissue of these mdr1a (-/-) mice.

Oatp/OATP and P-pg transport in lung

As discussed above, the lung plays an important role in regulating the arterial blood concentrations of opioids. Immediately after intravenous injection, high pulmonary uptake moderates peak concentrations of opioids during the first pass through the systemic circulation and thus other organ systems (Roerig et al., 1994; Boer, 2003). The

high pulmonary uptake of the opioid analgesic fentanyl observed *in vivo* is due to drug uptake into the vascular endothelium by both a passive and a saturable active uptake process. The active uptake mechanism of fentanyl in the lungs is specific, and is due to uptake by an inward transporter (Henthorn et al., 1998; Waters et al., 1999; Waters et al., 2000).

Because OATP-A/Oatp2 (human/rat) are present in the lungs (Hagenbuch and Meier, 2003) and opioid peptides are substrates of these influx transporters (Gao et al., 2000), OATP-A/Oatp2 may play an important role in pulmonary uptake of fentanyl.

The efflux transporter P-gp is found in pulmonary endothelial cells (Lechapt-Zalcman et al., 1997) and is responsible for efflux of fentanyl from the pulmonary endothelium. However, the outward-mediated extrusion of fentanyl by P-gp in bovine pulmonary artery endothelial cells (BPAECs) is small compared to its facilitated uptake (Waters et al., 1999).

Although the increased pulmonary tissue/plasma partitioning of fentanyl may affect observed drug effect after rapid intravenous administration, the presence of a similar uptake phenomenon at the BBB would have even more immediate pharmacodynamic implications. Firstly, if fentanyl concentration at its site(s) of action is controlled by an endothelial transporter, not passive diffusion, then intra- and inter-individual potency variability may not be solely dependent on μ receptor differences, but on variable plasma/brain partitioning. Secondly, if fentanyl transport is inward at the brain

endothelium, then such a mechanism may be exploitable for reducing fentanyl effects or enhancing the central nervous system effects of other drugs (Henthorn et al., 1999).

Oatp/OATP and P-pg transport in the brain

The major factor governing the uptake of fentanyl into bovine brain micro vascular endothelial cells (BBMECs) is active carrier-mediated transport not passive diffusion (Henthorn et al., 1999).

Because the BBB rat Oatp2 and human OATP-A transporters have been localized along both the luminal and abluminal membranes of brain endothelial cells (Gao et al., 1999) and human OATP-A transports two opioid peptides, deltorphin II and [D-Pen(2),D-Pen(5)] enkephalin, other opioids may also be substrates of these two influx transporters in humans and rats (Gao et al., 2000). Hence, human OATP-A and rat Oatp2 may play an important role in the uptake of fentanyl in the human and rat BBB.

P-gp is present at high concentrations in the apical membrane of the endothelial cells of the brain capillaries as demonstrated by immunostaining with various monoclonal and polyclonal antibodies in cultured polarized mouse, bovine and human brain endothelial cells and by studies with cultured brain endothelial cells (Lee et al., 2001; Bendayan et al., 2002; Lee and Bendayan, 2004). Fentanyl is a substrate of P-gp in BBMECs, but the active P-gp mediated extrusion of fentanyl in these cells is overshadowed by an active inward transport process (Henthorn et al., 1999).

Opioids

Fentanyl

Fentanyl is a widely used potent synthetic opioid analgesic which has been introduced into clinical practice in the early 1960s and represented a major increase in potency in

comparison with clinically important opiate agonists of the time. Fentanyl acts at the μ-opioid receptor and is widely used as analgesic to supplement general anesthesia for various surgical procedures or as a primary anesthetic agent in very high doses during cardiac surgery. Fentanyl is administered via infusion for long-term analgesia and sedation in intensive care patients. The pharmacokinetics of fentanyl have been studied in detail (Roerig et al., 1987; Roerig et al., 1989a; Bjorkman et al., 1993). The peak plasma concentration of fentanyl immediately following identical intravenous bolus administration varies at least 16-fold among patients (Reilly et al., 1985). Fentanyl undergoes significant reversible pulmonary uptake following intravenous administration (Roerig et al., 1994). This has been an area of great interest because significant alterations in the pulmonary uptake process will result in significant changes in the blood drug concentrations in the initial minutes following intravenous administration.

Fentanyl transport in lung

The high pulmonary uptake of fentanyl has been thought to be determined by a drug's physicochemical properties such as octanol-water partitioning and protein binding (Roerig et al., 1987). However, fentanyl concentration in the pulmonary endothelial cells is higher at lower fentanyl supernatant concentrations than would be expected if uptake occurred by diffusion alone, indicating that first-pass pulmonary uptake of fentanyl *in vivo* is attributable to both a passive and saturable active uptake processes. The outward-mediated extrusion of fentanyl by P-glycoprotein in the pulmonary endothelial cells is small compared to the facilitated uptake by an inward transporter, and both can be blocked by verapamil *in vitro*. Furthermore, the active uptake mechanism of fentanyl in

the lungs is specific, as alfentanil uptake into pulmonary endothelial cells is not facilitated (Henthorn et al., 1998; Waters et al., 1999; Waters et al., 2000).

Fentanyl transport in brain

The major factor governing fentanyl uptake in bovine brain micro vascular endothelial cells (BBMEC), is active carrier-mediated transport, not passive diffusion. Fentanyl is a substrate of P-gp in BBMECs and the active P-gp mediated extrusion of fentanyl in these cells is overshadowed by an active inward transport process. Verapamil can block both the inward and outward transporters in BBMEC (Henthorn et al., 1999).

Loperamide

Loperamide is a potent opioid that is widely used for treatment of diarrhea. It primarily acts through activation of opioid receptors in the intestinal tract (Heel et al., 1978).

Loperamide transport in lung

Classically, loperamide is administered orally and is not exposed to pulmonary endothelium in a first pass manner, as is fentanyl. In the following studies, loperamide was administered intravenously, allowing contact with the pulmonary endothelium.

We believe that an uptake process similar to fentanyl uptake in lungs might be responsible for loperamide pulmonary uptake. Because loperamide is a known P-gp substrate, we believe that P-gp may also have a role in the efflux of the drug from the lungs.

Loperamide transport in brain

Loperamide has been shown to be actively extruded from the brain by P-gp. Loperamide elicits potent centrally mediated opiate-like effects and evidences increased brain accumulation in P-gp-deficient mice as compared to transport-competent animals

(Dagenais et al., 2004). Pronounced morphine-like CNS side effects have been observed after administration of loperamide to mdr1a (-/-) mice, which is probably caused by increased concentration of this drug in the CNS. Administration of [^{3}H] loperamide to mdr1a (-/-) mice resulted in 13-fold higher radioactivity in the brain, whereas the plasma levels have been shown to be only 2-fold higher than that in the wild-type mice (Schinkel et al., 1996). Also, when healthy volunteers were given a single oral dose of loperamide with and without the P-gp inhibitor quinidine, a central effect of loperamide (change in ventilatory response to increasing carbon dioxide concentrations) was only observed during co-administration of the P-gp inhibitor (Sadeque et al., 2000).

Why loperamide?

Because loperamide is a potent opioid which has never been used in anesthesia and it is a substrate of the efflux transporter P-gp, we wanted to study the pharmacokinetics and pharmacodynamics of intravenous loperamide and compare it to that of the widely used anesthetic fentanyl in the presence and absence of the P-gp inhibitor verapamil.

Verapamil

Verapamil is a calcium channel blocker and a basic lipophilic amine. It is widely used in the treatment of cardiovascular disorders such as arrhythmias, hypertension and angina pectoris. Important to our studies, is its further function as a P-gp inhibitor (Chikhale et al., 1995).

Verapamil transport in lung

Verapamil undergoes significant pulmonary uptake in human lung following intravenous bolus administration with about 50% of the drug accumulating in lung tissue during first pass. This extensive first-pass uptake of verapamil has been thought to be due its high

lipid solubility. Also, this significant pulmonary uptake may play a role in the initial pharmacokinetics of verapamil immediately after intravenous administration (Roerig et al., 1989b).

Verapamil is a substrate of P-gp and is one of the first P-gp modulators discovered. It has been used in many clinical trials with anticancer drugs transported by P-gp (Sinicrope et al., 1992). The observed interaction between verapamil and digoxin is due to decreased elimination of digoxin resulting from the inhibition of P-gp activity caused by verapamil (Verschraagen et al., 1999).

Verapamil transport in brain

Verapamil is a classic P-gp substrate/competitive inhibitor. It is also a substrate of the fentanyl uptake transporter in the BBB (Henthorn et al., 1999).

Pharmacokinetics and pharmacodynamics (pk-pd)

The dose-response relationship is governed by the pharmacokinetics (pk) and the pharmacodynamics (pd) of the drug in question (Camu et al., 1998; Shafer, 1998) (Figure 1.6). Knowledge of a drug's pk-pd allows development of dosing strategies to achieve the desired degree of drug effect rapidly, maintaining that effect as long as needed, and allowing rapid recovery from the effect (Camu et al., 1998).

Physiological or compartmental models are used in pk analysis of drugs. Physiological pharmacokinetic models determine the distribution of drug to the organs or organ groups by tissue volumes, blood flow and tissue/blood partition coefficients. Limitations of these models are that, it is impossible to determine regional blood flow and the tissue volume of each organ. Compartmental pharmacokinetic modeling techniques are an alternative concept for the distribution of a drug by using virtual volumes of homogenous, well

mixed compartments. These compartments are a mathematical concept that allows envisioning a structure in the body to account for the decrease in plasma concentration of a drug. The central compartment represents the initial mixing volume into which the drug is injected and some fraction of the plasma and the very rapidly equilibrating tissues. The other peripheral compartments could represent less vessel-rich tissues. One, two, three or more compartments may be utilized by this technique (Figure 1.7).

Basic assumptions for compartmental pharmacokinetic analysis are that the volume of each compartment remains constant, each compartment is well stirred so that the concentrations are homogenous at all times and the exchange of drug between compartments are first order and occurs by concentration differences thus the proportional rate along each pathway remains constant so that the resulting change in concentration is exponential (Shafer, 1998). Recirculatory models are an alternative to physiological and compartmental models. Henthorn and colleagues (Krejcie et al., 1994; Krejcie et al., 1997) introduced recirculatory models for the description of drug kinetics. This model allows for uptake in a central circuit and into two parallel peripheral compartments. The model can be used to describe the kinetics of several drugs and indicators.

In this study, the pharmacokinetics were analyzed using the SAAM II software (SAAM Institute, Seattle, WA) which was adapted to fit a two compartment model for the opioids, fentanyl and loperamide, and a one compartment model for verapamil.

To study the pharmacodynamics of the opioids, fentanyl and loperamide, we measured a processed electroencephalogram (EEG) signal. The primary utility of the processed EEG as a measure of opioid effect is that it is a continuous measure that allows

pharmacodynamic quantitations. By application of pharmacokinetic-pharmacodynamic, the value of certain EEG parameters can be directly related the concentration at the effect site on the basis of the sigmoidal E_{max} pharmacodynamic model (Lemmens et al., 1994; Egan et al., 1996).

Prior research by the Principal Investigator

Pulmonary fentanyl transport

Previous research by Henthorn et al. (Henthorn et al., 1998; Waters et al., 1999) established that pulmonary uptake of fentanyl is via active as well as passive transport by pulmonary endothelial cells, in cultured bovine pulmonary endothelial monolayers. They also found that, although there is outwardly directed P-gp mediated extrusion of fentanyl, it was small compared with facilitated uptake. Thus, investigators speculated that P-gp-like transporter was responsible for facilitation of fentanyl uptake into the pulmonary vascular endothelium.

Follow up investigations examining fentanyl transport in the brain showed that fentanyl was transported bi-directionally in bovine brain micro vascular endothelial cells by two different transporters (Henthorn et al., 1999). Uptake of fentanyl occurred via a carrier-mediated, active transporter and similar to pulmonary fentanyl uptake, brain fentanyl uptake supersedes efflux. Furthermore, while verapamil blocked both uptake and efflux of fentanyl, it was clearly shown that P-gp was exclusively an outward transporter and there is an unidentified active inward transporter capable of transporting both fentanyl and verapamil.

Because previous reports indicate that both inward transport of fentanyl and outward transport of loperamide are inhibited by verapamil, we propose that opioid transport may

be exploited for either reducing (fentanyl) or enhancing (loperamide) central nervous system effects. The following studies have been designed to establish the effect of verapamil inhibition on lung and brain opioid concentrations (pharmacokinetics) and opioid effects on the central nervous system (pharmacodynamics), *in vivo*. Because both inward and outward transporters, Oatp2 and P-gp, are known to be present in Sprague Dawley rat lung and brain endothelium, this animal model was used for all studies outlined below. Our initial approach was to develop a method for quantifying opioids in minute quantities of plasma and tissue using LC/LC-MS/MS.

Hypothesis and Specific Aims

Hypothesis. Because active uptake transport of fentanyl overshadows P-gp mediated efflux *in vitro*, yet intracellular loperamide concentration is primarily mediated by P-gp *in vitro*, and both uptake and efflux are blocked by verapamil, we hypothesized that verapamil will decrease fentanyl concentrations in lung and brain and intrinsic central effect, yet increase loperamide lung and brain concentrations and intrinsic central effect, *in vivo*.

Furthermore, we also hypothesized that Oatp substrate pravastatin and Oatp inhibitor naloxone will decrease fentanyl concentrations in lung and brain, *in vivo*.

Specific Aim 1. Hypothesis: Co-administration of verapamil and opioids fentanyl or loperamide will decrease lung and brain partitioning of fentanyl and increase that of loperamide.

Aim 1. Determine fentanyl and loperamide plasma: brain and plasma: lung partition ratios as well as the global pk parameters of volume of

distribution and elimination clearance in absence and presence of verapamil.

Specific Aim 2. Hypothesis: Co-administration of verapamil with opioids will decrease fentanyl effect and increase loperamide effect.

Aim 2A. Determine the time course of the onset and offset of opioid effect as measured continuously by a processed EEG in rats treated with fentanyl or loperamide with and without verapamil.

Aim 2B. Determine correlations between opiate brain partitioning and EEG, using pk/pd modeling.

Specific Aim 3. Hypothesis: Opioids fentanyl and loperamide will alter lung and brain partitioning of verapamil.

Aim 3. Determine verapamil plasma: brain and plasma: lung partition ratios as well as the global pk parameters of volume of distribution and elimination clearance in the absence and presence of fentanyl or loperamide.

Specific Aim 4. Hypothesis: We hypothesized that specific inhibition of Oatp would reduce lung and brain.

Aim 4. Determine fentanyl plasma: brain and plasma: lung partition ratios as well as the global pk parameters of volume of distribution and elimination clearance in the absence and presence of Oatp substrate pravastatin and inhibitor naloxone.

Table 1.1. Tissue distribution and Substrates of Organic Anion Transporter polypeptide protein (Oatp/OATP) (Hagenbuch and Meier, 2003).

Transporter	Tissue Distribution	Substrates
Human		
OATP-A	Brain (capillary endothelial cells)	Bile acids, bromosulophthalein, APD-ajmalinium, N-mehtyl-quindine, N-mehtyl-quinine, fexofenadine, rocuronium, D-penicillamine enkephalin (DPDPE), deltrphin II
OATP-B	Liver, Kidney, intestine, lung, placenta	Estrone-3-sulfate, bromosulfophthalein
OATP-C	Liver	Bile Acids, conjucated steroids (dehydroepiandrosterone sulfate, estradiol-17β-glucuronide, estrone-3 sulfate), eicosanoids (PGE2, TXB2, LTC4, LTE4), thyroid hormones(T4, T3) , pravastatin, rifampin
OATP-8	Liver	Dehydroeoiandrosterone sulfate, estrone-3-sulfate, coristol, APD-ajmalinum. Fexofenadine
Rat		
OATP 1	Liver, brain (choroids plexus), kidney	Enalpril, temocaprilat, ochratoxin A, BQ-123, CRC 220, bromosulfophthlein, estradiol-17β-glucuronide, ouabain, aldosterone, estrone-3-sulfate, coristol, APD-ajmalinium, fexofenadine
OATP 2	Liver, brain (capillary endothelial cells)	Pravastatin, BQ-123, thyroid hormones (T4, T3), digoxin, ouabain, estradiol, estrone-3-sulfate, estradiol-17β-glucuronide, fexofenadine
OATP 3	Kidney, retina , small intestine	Taurocholate, Cholecystokinin, thyroid hormones (T4, T3), fexofenadine
OATP 4	Liver	Taurocholate, Cholecystokinin, dehydroepiandrosterone sulfate, estradiol-17β-glucuronide, estrone-3-sulfate, LTC4, BQ-123, DPDPE

Table 1.2. P-glycoprotein Substrates and Inhibitors (Demeule et al., 2002).

P-gp substrates	P-gp inhibitors
Cancer Drugs Doxorubicin, Daunorbicin, Viblastine Vincristine, Paciltaxel, Etopside	Cyclopropylibenzosuberane LY335979
Immunosuppressive drugs Cyclosprin A, Fk506	Immunosuppressant Cyclosporin A, Valspodar (PSC833)
Lipid Lowering Agent Lovastatin	**Calcium channel blocker** **Verpamil**
Steroids Aldosterone, Coristol Corticosterone, Dexamethasone	Progesterone antagonist Mefipristone (RU486)
HIV protease inhibitors Amprenaviar, Indinavir, Nelfinavir Ritonavir, Saquinavir	Antiarrthmic agent Quinidine
Cardiac Drugs Dixogin, Quidine	Antifungal agent Ketoconazole
Opioids **Morphine** **Loperamide** **Fentanyl**	Acridonecarboxamide derivative GG918 (GF120918)
Anti-gout agent Colchicine	Peptide chemosensitizers Reversin 121 Reversin 125
Anti-tuberculous agent Erythromyccin	Topoisomerase Xenova (XR 5944)
Anti-helminthic agent Ivermectin	
Anti-tuberculous agent Rifampin	
Fluorescent dye Rhodamine	

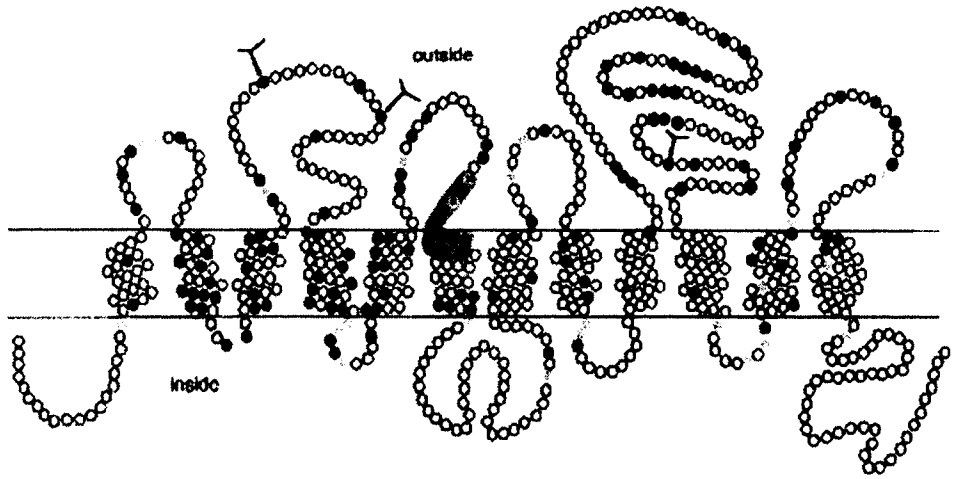

Figure 1.1. Predicted 12 transmembrane domain model of rat Oatp1. Three potential *N*-glycosylation sites (Y) are present on extracellular protein loops (Hagenbuch and Meier, 2003).

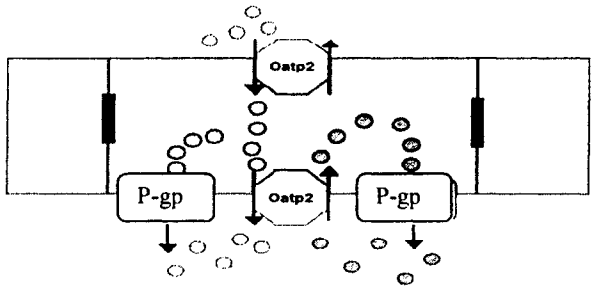

Figure 1.2. Shows normal function of the various transporters located within the BBB. Pay particular attention to the function of p-gp. The gray molecules are pumped in through OATP, but P-gp quickly pumps them back out.
Modified from http://student.biology.arizona.edu/honors2003/group02/transporters.gif

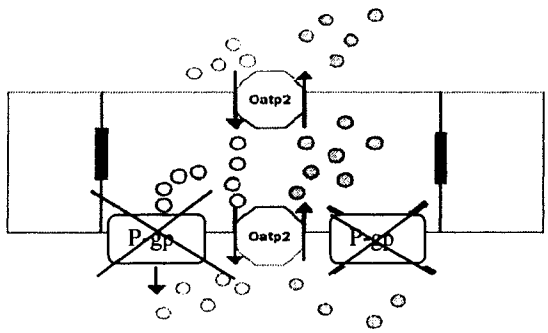

Figure 1.3. Here we see P-gp being knocked out. When this transporter is nonfunctional, the intracellular concentration of gray molecules increases and they are moved across into the cerebrospinal fluid by OATP.
Modified from http://student.biology.arizona.edu/honors2003/group02/transporters.gif

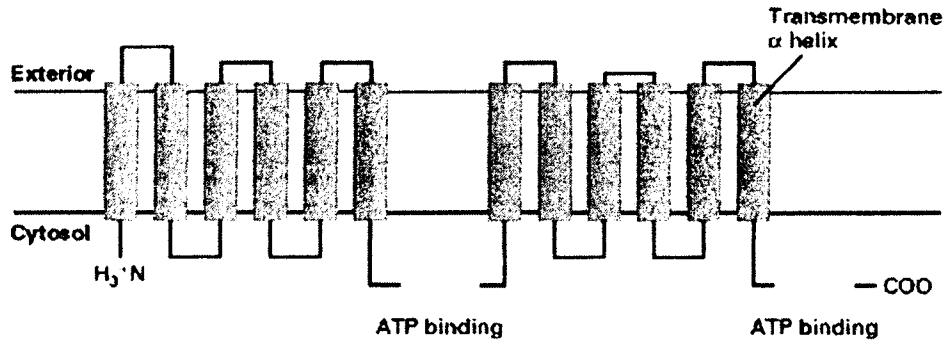

Figure 1.4. Schematic structural model for mammalian P-gp. In this member of the ABC super family, the two transmembrane domains and two cytosolic ATP-binding domains are part of a single polypeptide. Each transmembrane domain contains six a helices. The two halves of this 1280-aa protein have similar amino acid sequences.
This figure is from http://www.ncbi.nlm.nih.gov/books/bookres.fcgi/mcb/ch15f16.gif

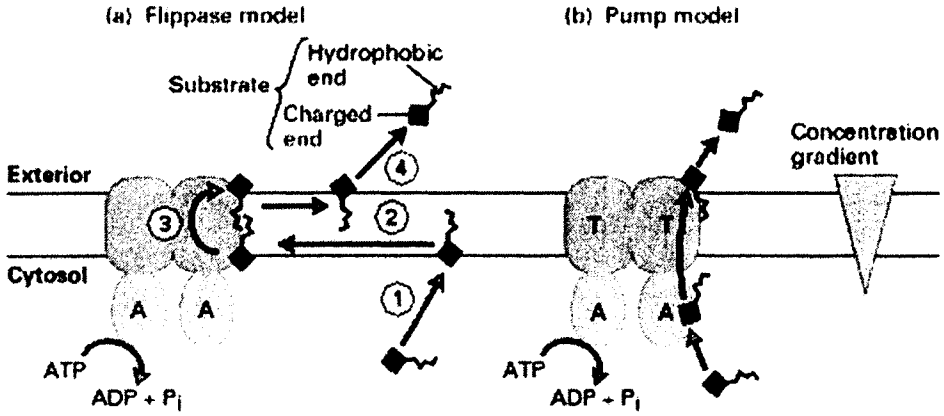

Figure 1.5. Possible mechanisms of action of the P-gp. (a) The flippase model proposes that a lipid-soluble molecule first dissolves in the cytosolic-facing leaflet of the plasma membrane (1) and then diffuses in the membrane until binding to a site on the P-gp that is within the bilayer (2). Powered by ATP hydrolysis, the substrate molecule flips into the exoplasmic leaflet (3), from which it can move directly into the aqueous phase on the outside of the cell (4). (b) According to the pump model, P-gp has a single multisubstrate binding site and transports molecules by a mechanism similar to that of other ATP-powered pumps.
This figure is from http://www.ncbi.nlm.nih.gov/books/bookres.fcgi/mcb/ch15f17.gif

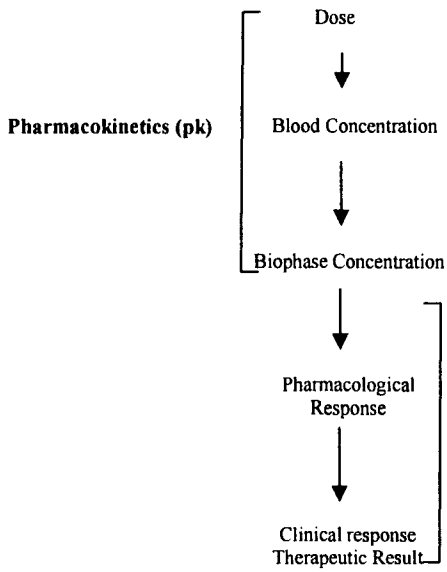

Figure 1.6. The relationship between drug dose, concentrations in the blood and the biophase, and effect (Camu et al., 1998).

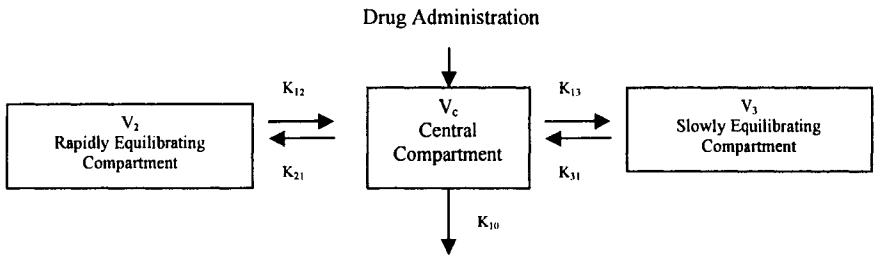

Figure 1.7. Representation of a three-compartment pharamacokinetic model. Vc, V_2 and V_3 represent the compartment volumes, k_{10}, k_{12}, k_{21}, k_{13} and k_{31} represent the transfer constants between compartments (Shafer, 1998).

REFERENCES

Ayrton A and Morgan P (2001) Role of transport proteins in drug absorption, distribution and excretion. *Xenobiotica* **31**:469-497.

Bakhle YS (1990) Pharmacokinetic and metabolic properties of lung. *British Journal of Anaesthesia* **65**:79-93.

Ballabh P, Braun A and Nedergaard M (2004) The blood-brain barrier: an overview: structure, regulation, and clinical implications. *Neurobiology of Disease* **16**:1-13.

Begley DJ and Brightman MW (2003) Structural and functional aspects of the blood-brain barrier. *Progress in Drug Research* **61**:39-78.

Bendayan R, Lee G and Bendayan M (2002) Functional expression and localization of P-glycoprotein at the blood brain barrier. *Microscopy Research & Technique* **57**:365-380.

Bjorkman S, Stanski DR, Harashima H, Dowrie R, Harapat SR, Wada DR and Ebling WF (1993) Tissue distribution of fentanyl and alfentanil in the rat cannot be described by a blood flow limited model. *Journal of Pharmacokinetics & Biopharmaceutics* **21**:255-279.

Boer F (2003) Drug handling by the lungs. *British Journal of Anaesthesia* **91**:50-60.

Boer F, Engbers FH, Bovill JG, Burm AG and Hak A (1995) First-pass pulmonary retention of sufentanil at three different background blood concentrations of the opioid. *British Journal of Anaesthesia* **74**:50-55.

Camu F, Lauwers M and Vanlersberghe C (1998) Basic principles of pharmacokinetics and pharmacodynamics for the anesthesiologist. *Acta Anaesthesiologica Belgica* **49**:55-64.

Chikhale EG, Burton PS and Borchardt RT (1995) The effect of verapamil on the transport of peptides across the blood-brain barrier in rats: kinetic evidence for an apically polarized efflux mechanism. *Journal of Pharmacology & Experimental Therapeutics* **273**:298-303.

Cvetkovic M, Leake B, Fromm MF, Wilkinson GR and Kim RB (1999) OATP and P-glycoprotein transporters mediate the cellular uptake and excretion of fexofenadine. *Drug Metabolism & Disposition* **27**:866-871.

Dagenais C, Ducharme J and Pollack GM (2001) Uptake and efflux of the peptidic delta-opioid receptor agonist. *Neuroscience Letters* **301**:155-158.

Dagenais C, Graff CL and Pollack GM (2004) Variable modulation of opioid brain uptake by P-glycoprotein in mice. *Biochemical Pharmacology* **67**:269-276.

Demeule M, Regina A, Jodoin J, Laplante A, Dagenais C, Berthelet F, Moghrabi A and Beliveau R (2002) Drug transport to the brain: key roles for the efflux pump P-glycoprotein in the blood-brain barrier. *Vascular Pharmacology* **38**:339-348.

Egan TD, Minto CF, Hermann DJ, Barr J, Muir KT and Shafer SL (1996) Remifentanil versus alfentanil: comparative pharmacokinetics and pharmacodynamics in healthy adult male volunteers.[erratum appears in Anesthesiology 1996 Sep;85(3):695]. *Anesthesiology* **84**:821-833.

Fardel O, Lecureur V and Guillouzo A (1996) The P-glycoprotein multidrug transporter. *General Pharmacology* **27**:1283-1291.

Ford JM (1995) Modulators of multidrug resistance. Preclinical studies. *Hematology - Oncology Clinics of North America* **9**:337-361.

Gao B, Hagenbuch B, Kullak-Ublick GA, Benke D, Aguzzi A and Meier PJ (2000) Organic anion-transporting polypeptides mediate transport of opioid peptides across blood-brain barrier. *Journal of Pharmacology & Experimental Therapeutics* **294**:73-79.

Gao B, Stieger B, Noe B, Fritschy JM and Meier PJ (1999) Localization of the organic anion transporting polypeptide 2 (Oatp2) in capillary endothelium and choroid plexus epithelium of rat brain. *Journal of Histochemistry & Cytochemistry* **47**:1255-1264.

Hagenbuch B and Meier PJ (2003) The superfamily of organic anion transporting polypeptides. *Biochimica et Biophysica Acta* **1609**:1-18.

Heel RC, Brogden RN, Speight TM and Avery GS (1978) Loperamide: a review of its pharmacological properties and therapeutic efficacy in diarrhoea. *Drugs* **15**:33-52.

Henthorn TK, Krejcie TC, Avram MJ, Jensen TR and Waters CM (1998) Transporter-mediated pulmonary endothelial uptake of fentanyl. *International Journal of Clinical Pharmacology & Therapeutics* **36**:74-75.

Henthorn TK, Liu Y, Mahapatro M and Ng KY (1999) Active transport of fentanyl by the blood-brain barrier. *Journal of Pharmacology & Experimental Therapeutics* **289**:1084-1089.

Higgins CF and Gottesman MM (1992) Is the multidrug transporter a flippase? *Trends in Biochemical Sciences* **17**:18-21.

Howell RE and Lanken PN (1992) Pulmonary accumulation of propranolol in vivo: sites and physiochemical mechanism. *Journal of Pharmacology & Experimental Therapeutics* **263**:130-135.

Hsiang B, Zhu Y, Wang Z, Wu Y, Sasseville V, Yang WP and Kirchgessner TG (1999) A novel human hepatic organic anion transporting polypeptide (OATP2). Identification of a liver-specific human organic anion transporting polypeptide and identification of rat and human hydroxymethylglutaryl-CoA reductase inhibitor transporters. *Journal of Biological Chemistry* **274**:37161-37168.

Kastin AJ, Pan W, Maness LM and Banks WA (1999) Peptides crossing the blood-brain barrier: some unusual observations. *Brain Research* **848**:96-100.

Kim RB (2003) Organic anion-transporting polypeptide (OATP) transporter family and drug disposition. *European Journal of Clinical Investigation* **33 Suppl 2**:1-5.

Kim RB, Wandel C, Leake B, Cvetkovic M, Fromm MF, Dempsey PJ, Roden MM, Belas F, Chaudhary AK, Roden DM, Wood AJ and Wilkinson GR (1999) Interrelationship between substrates and inhibitors of human CYP3A and P-glycoprotein. *Pharmaceutical Research* **16**:408-414.

Krejcie TC, Avram MJ, Gentry WB, Niemann CU, Janowski MP and Henthorn TK (1997) A recirculatory model of the pulmonary uptake and pharmacokinetics of lidocaine based on analysis of arterial and mixed venous data from dogs. *Journal of Pharmacokinetics & Biopharmaceutics* **25**:169-190.

Krejcie TC, Henthorn TK, Shanks CA and Avram MJ (1994) A recirculatory pharmacokinetic model describing the circulatory mixing, tissue distribution and elimination of antipyrine in dogs. *Journal of Pharmacology & Experimental Therapeutics* **269**:609-616.

Lechapt-Zalcman E, Hurbain I, Lacave R, Commo F, Urban T, Antoine M, Milleron B and Bernaudin JF (1997) MDR1-Pgp 170 expression in human bronchus. *European Respiratory Journal* **10**:1837-1843.

Lee G and Bendayan R (2004) Functional expression and localization of P-glycoprotein in the central nervous system: relevance to the pathogenesis and treatment of neurological disorders. *Pharmaceutical Research* **21**:1313-1330.

Lee G, Dallas S, Hong M and Bendayan R (2001) Drug transporters in the central nervous system: brain barriers and brain parenchyma considerations. *Pharmacological Reviews* **53**:569-596.

Lemmens HJ, Dyck JB, Shafer SL and Stanski DR (1994) Pharmacokinetic-pharmacodynamic modeling in drug development: application to the investigational opioid trefentanil. *Clinical Pharmacology & Therapeutics* **56**:261-271.

Levin VA (1980) Relationship of octanol/water partition coefficient and molecular weight to rat brain capillary permeability. *Journal of Medicinal Chemistry* **23**:682-684.

Ohmura S, Yamamoto K, Kobayashi T and Murakami S (1993) Displacement of lidocaine from the lung after bolus injection of bupivacaine. *Canadian Journal of Anaesthesia* **40**:676-680.

Reilly CS, Wood AJ and Wood M (1985) Variability of fentanyl pharmacokinetics in man. Computer predicted plasma concentrations for three intravenous dosage regimens. *Anaesthesia* **40**:837-843.

Roerig DL, Ahlf SB, Dawson CA, Linehan JH and Kampine JP (1994) First pass uptake in the human lung of drugs used during anesthesia. *Advances in Pharmacology* **31**:531-549.

Roerig DL, Kotrly KJ, Ahlf SB, Dawson CA and Kampine JP (1989a) Effect of propranolol on the first pass uptake of fentanyl in the human and rat lung. *Anesthesiology* **71**:62-68.

Roerig DL, Kotrly KJ, Dawson CA, Ahlf SB, Gualtieri JF and Kampine JP (1989b) First-pass uptake of verapamil, diazepam, and thiopental in the human lung. *Anesthesia & Analgesia* **69**:461-466.

Roerig DL, Kotrly KJ, Vucins EJ, Ahlf SB, Dawson CA and Kampine JP (1987) First pass uptake of fentanyl, meperidine, and morphine in the human lung. *Anesthesiology* **67**:466-472.

Sadeque AJ, Wandel C, He H, Shah S and Wood AJ (2000) Increased drug delivery to the brain by P-glycoprotein inhibition. *Clinical Pharmacology & Therapeutics* **68**:231-237.

Schinkel AH (1997) The physiological function of drug-transporting P-glycoproteins. *Seminars in Cancer Biology* **8**:161-170.

Schinkel AH and Jonker JW (2003) Mammalian drug efflux transporters of the ATP binding cassette (ABC) family: an overview. *Advanced Drug Delivery Reviews* **55**:3-29.

Schinkel AH, Wagenaar E, Mol CA and van Deemter L (1996) P-glycoprotein in the blood-brain barrier of mice influences the brain penetration and pharmacological activity of many drugs. *Journal of Clinical Investigation* **97**:2517-2524.

Shafer SL (1998) Pharmacokinetics and pharmacodynamics in anesthetic drug development. *Acta Anaesthesiologica Belgica* **49**:65-78.

Sharom FJ (1997) The P-glycoprotein efflux pump: how does it transport drugs?[see comment]. *Journal of Membrane Biology* **160**:161-175.

Sinicrope FA, Dudeja PK, Bissonnette BM, Safa AR and Brasitus TA (1992) Modulation of P-glycoprotein-mediated drug transport by alterations in lipid fluidity of rat liver canalicular membrane vesicles. *Journal of Biological Chemistry* **267**:24995-25002.

Su Y, Zhang X and Sinko PJ (2004) Human organic anion-transporting polypeptide OATP-A (SLC21A3) acts in concert with P-glycoprotein and multidrug resistance protein 2 in the vectorial transport of Saquinavir in Hep G2 cells. *Molecular Pharmaceutics* **1**:49-56.

Sun H, Dai H, Shaik N and Elmquist WF (2003) Drug efflux transporters in the CNS. *Advanced Drug Delivery Reviews* **55**:83-105.

Taeger K, Weninger E, Schmelzer F, Adt M, Franke N and Peter K (1988) Pulmonary kinetics of fentanyl and alfentanil in surgical patients. *British Journal of Anaesthesia* **61**:425-434.

Verschraagen M, Koks CH, Schellens JH and Beijnen JH (1999) P-glycoprotein system as a determinant of drug interactions: the case of digoxin-verapamil. *Pharmacological Research* **40**:301-306.

Waters CM, Avram MJ, Krejcie TC and Henthorn TK (1999) Uptake of fentanyl in pulmonary endothelium. *Journal of Pharmacology & Experimental Therapeutics* **288**:157-163.

Waters CM, Krejcie TC and Avram MJ (2000) Facilitated uptake of fentanyl, but not alfentanil, by human pulmonary endothelial cells. *Anesthesiology* **93**:825-831.

Wood M (1997) Drug distribution: less passive, more active?[comment]. *Anesthesiology* **87**:1274-1276.

CHAPTER 2

Development and Validation of an Assay for the Simultaneous Quantification of Opioids in Biological Samples by LC/LC-MS/MS

Yan Ling Zhang, Iman ElKiweri, Martha Tissot van Patot, Ka-Yun Ng,
Thomas Henthorn, and Uwe Christians

Clinical Research and Development, Department of Anesthesiology, University of Colorado Health Sciences Center, Denver, Colorado

Submitted to: Therapeutic Drug Monitoring

Type: Original Article

Key words: automated sample preparation, column-switching, simultaneous quantification, opioids

Supported by grant No. R01- GM47502.09 from the National Institutes of Health and in part by the Nema Foundation, Malaysia.

Introduction

Opioids are a family of drugs that have morphine-like effects. Fentanyl, alfentanil, remifentanil, and sufentanil are structurally similar, and are currently the most frequently used opioid analgesics in clinical anesthesia. The structurally related loperamide is used as an anti-diarrhea drug and is sold over-the-counter. Chemical structures of these five opioids are shown in Figure 2.1.

Recent surveys suggest that the abuse of opioids, often in combination, is pervasive throughout society (Cone et al., 2004), including medical professionals. Due to their efficacy at low doses, the concentrations of opioids in biological samples fall rapidly below the limit of detection of most assay procedures. Thus, analytical methods for quantification in biological samples used for pharmacokinetic studies and drug monitoring will require high sensitivity. Several quantification methods for opioid analysis in biological matrices have been developed, such as radioimmunoassay (RIA) (Woestenborghs et al., 1994), enzyme-linked immuno-sorbent assay (ELISA), liquid chromatography with ultraviolet absorbance detection (HPLC-UV) (Lambropoulos et al., 1999) (Kumar et al., 1996a), solid-phase extraction (SPE) combined with HPLC-UV (SPE-HPLC-UV) (Kabbaj and Varin, 2003) and gas chromatography with mass selective detection (GC/MS) (Woestenborghs et al., 1994; Szeitz et al., 1996; Anderson and Muto, 2000; Metz et al., 2000b; Ropero-Miller et al., 2002; Kuhlman et al., 2003). Recently, also LC/MS and LC-MS/MS assays for the quantification of fentanyl in human plasma have been reported (Shou and al, 2001; Weng and al, 2002; Day and al, 2003).

Most assays require complex sample preparation and are limited to the quantification of one opioid. RIA and ELISA are the most common techniques for pharmacokinetic

studies and screening of fentanyl and sufentanil in human urine and plasma samples (palleschi et al., 2003). But those methods are lacking specificity due to cross-reactivity of the antibodies with metabolites and have low precision. GC/MS methods require multi-step extractions and derivatization (Wasels and Belleville, 1994; Darwin et al., 2003). We developed an analytical platform based on semi-automated online extraction and LC-MS/MS that allows for the quantification of opioids in different matrices such as plasma and tissues. The assay was validated for alfentanil, fentanyl, loperamide, remifentanil, and sufentanil in rat plasma, rat brain, rat lung and human plasma.

Material and Methods

Materials and Reagents

All solvents used for the HPLC mobile phase and extraction (water and methanol) were of HPLC grade. All solvents and formic acid (88%) was from Fisher Scientific (Fair Lawn, NJ, USA) and zinc sulfate was obtained from Sigma-Aldrich (St. Louis, MO, USA). Fentanyl citrate was purchased from Abbott Laboratories (North Chicago, IL). Loperamide was obtained from Sigma Aldrich Inc. (St. Louis, MO). Alfentanil, remifentanil and sufentanil were obtained from Abbott Laboratories (North Chicago, IL.

The use of blood samples from healthy volunteers for assay development and validation purposes received "exempt" status from our institutional review board, the Colorado Multi-Institutional Review Board (COMIRB).

All rat studies including the collection of blank tissues and blood for assay development and validation was approved by the local Institutional Animal Care and Use Committee (IACUC). Animals received humane care following current guidelines such as the "Guide for the Care and Use of Laboratory Animals" prepared by the National Institute of

Sciences and published by the National Institutes of Health (NIH publication No. 80-123, revised 1985).

Sample Extraction

Plasma. One of the opioids, usually loperamide, not contained in the samples was used as internal standard. For loperamide analysis alfentanil was used as internal standard. The internal standard was added to the protein precipitation solution to yield a final concentration of 10 ng/mL. One hundred µL plasma from each sample was pipetted into the well of a 96-well plate (1 mL well volume, Agilent, Palo Alto, CA). Four-hundred µL methanol/ 0.2 M $ZnSO_4$ (7:3, v/v) containing the internal standard were added to 100 µL plasma. The 96-well plates were covered, vortexed (2.5 min), centrifuged (4°C, 8000g, 5 min), and placed into the auto sampler. The auto sampler needle height was adjusted to aspire only the supernatant and none of the precipitated proteins.

Tissues. Tissue samples were thawed, weighed and homogenized with 2 mL KH_2PO_4 buffer pH 7.4 (1 M) using a teflon-glass manual homogenizer. The assay was found to accommodate tissue samples between 5- 80 mg without the need to adjust buffer volumes. One-hundred µL of the sample was transferred into a 96-well plate and were processed as described for plasma samples above.

Chromatography Conditions and On-Line Extraction

Samples were extracted using online extraction and were quantified using an API4000 tandem quadrupole mass spectrometer as detector (Applied Biosystems, Foster City, CA). Two linked HPLC systems (LC/LC), one for extract (I) and one for analytical separation (II), were comprised of the following components: HPLC I: Agilent G1312A binary pump, G1322A degasser and Leap Technologies HTS PAL auto sampler (CTC Analytics,

Zwingen, Switzerland) equipped with a cooled stack temperature controller, a 6-port LC injection valve and a fast wash station; HPLC II: Agilent G1312A binary pump, a G1316A column thermostat and an API4000 mass spectrometer. The two HPLC systems were connected *via* a motorized 6-port column switching valve (Rheodyne, Cotati, CA). The mass spectrometer, HPLC components, LEAP auto sampler were controlled and all data was processed by Applied Biosystems Analyst software version 1.3. (Applied Biosystems, Foster City, CA).

The HPLC mobile phase consisted of 0.1 % formic acid and methanol. After extraction, supernatants were loaded onto the extraction column (4.6 × 12.5 mm, 5 μm particle size, Eclipse XDB-C8, Agilent, Palo Alto, CA) and were washed with a high flow of 5 mL/min, 80% 0.1% formic acid/ 20% methanol for 1 min. Then the switching valve was activated and the analytes were back-flushed onto the C8 analytical column (4.6 × 12.5 mm, 5 μm particle size, Eclipse XDB-C8, Agilent). A linear gradient was used: methanol increased from 55% to 100% in 4 min and was kept at 100% methanol for 1 min. The flow rate was 1 mL/min and the injection volume was 100 μL. Column temperature was maintained at 40°C.

Quantification by MS/MS.

After elution form the HPLC column, analytes were introduced into the turbo-ion spray source. Zero-grade air for the nebulizing and turbo gasses was provided by a Zero Air Generator (Analytical Gas Systems). Nitrogen of >99.999% purity was used as Collision Activated Dissociation (CAD) gas. Positive ions were monitored using Multiple Reaction Monitoring (MRM). MRM parameters for each analyte were adjusted by directly infusing each compound and the mixture of all five compounds (0.1 μg/mL, 80% methanol/ 20%

0.1% formic acid) into the electro spray source using a syringe infusion pump ((KD Scientific, Holliston, MA). The following MRM parameters were found to give the best sensitivities: the source temperature was set to 480°C, and the ion spray voltage was 5000V, gases were set at 20 for nebulizer gas, 15 for turbo gas, curtain gas was 15 and the collision activated dissociation (CAD) gas was 8 (all arbitrary units as used in the Analyst software). The declustering potential (DP) was 50V. The dwell time for each transition was 200 ms. Data were collected and the major product ion resulting from fragmentation was monitored at the ion transitions fentanyl: *m/z* 337.5 → 188.4, remifentanil: *m/z* 377.4 → 228.4, sufentanil: *m/z* 387.5 → 238.4, alfentanil: *m/z* 417.4 → 197.3, and lopermide: *m/z* 477.5 → 266.1. Peak area ratios of analytes to IS were plotted *versus* nominal concentration, and calibration curves were constructed using non-weighted linear regression.

Standard Curves and Quality Control Samples.

Individual stock solutions of 1 mg/mL for all five opioids were prepared in methanol and formic acid (80% methanol/ 20% 0.1% formic acid). All stock solutions were stored at -80°C until use. Dilutions of the stock solutions ranging from 1 ng/mL to 1000 ng/mL were freshly prepared using the aforementioned methanol/ formic acid solution. Calibration standards and quality control samples were prepared in drug-free plasma or drug-free rat tissue samples homogenized in 1 M KH_2PO_4 (5 mg tissue/ mL, *vide supra*). Samples were spiked with opioids and incubated at 37°C for 30 min to allow for distribution and binding of the opioids to proteins. Pooled calibration standards at concentrations of 0.017, 0.033, 0.083, 0.17, 0.33, 0.83, 1.67, 3.33, 8.33, 16.67, 33.33 and 83.33 ng/mL were prepared in rat plasma and rat tissue homogenates (lung and brain).

For human plasma, the calibration standards at the following concentration levels were prepared: 0.0125, 0.025, 0.05, 0.125, 0.25, 0.5, 1.25, 0.5, 1.25, 2.5, 5, 12.5, 25 and 50 ng/mL.

For quality control samples, opioid-free rat tissue homogenates (lung and brain) and plasma were spiked with opioid standard solutions to result in final concentrations at the LLOQ, 2-fold the LLOQ, and ULOQ. All calibrators and quality control samples were stored frozen at -80°C prior to and during LC/LC-MS/MS analysis.

Assay Development and Validation

Assay performance was established following current guidelines of the United States Federal Drug Administration (FDA), the following criteria were evaluated: range of linear response, limit of detection (LOD), LLOQ, ULOQ, intra- and inter-day precisions and accuracies, absolute recovery, stabilities, matrix interferences, ion suppression, carry over, and dilution integrity.

Validation strategy. The assay was completely validated using spiked human plasma samples, including inter-day performance and stability. Hereafter, the validation was extended to rat plasma and tissues using an abbreviated validation strategy since the only change was the matrix. Parameters determined for abbreviated validation included lower limit of quantitation, upper limit of quantitation, linearity, intra-day accuracy and precision.

Pre-defined acceptance criteria. The assay was considered acceptable if precision (coefficient of variance, CV %) at each concentration was ≤ 15% for intra-day and day-to-day precision. The accuracy compared with the nominal value had to be within ± 15%

for both intra- and day-to-day accuracy. The calibration curve had to have a correlation coefficient r of 0.99 or better. The absolute recovery had to exceed 60%.

LOD, LLOQ and ULOQ. The LOD was defined as a signal to noise ratio of 3:1. The LLOQ was determined as the lowest quantity consistently achieving an intra-day accuracy $\leq \pm 20\%$ of the nominal concentration, an intra-day precision $\leq 20\%$, and a signal-to-noise ratio greater than 10:1. The ULOQ was defined as the highest concentration that consistently showed an intra-day accuracy $\leq \pm 20\%$ of the nominal concentration, and an intra-day precision $\leq 20\%$. At higher concentrations the calibration curve usually started to plateau so that in all cases a loss of accuracy was found to be the limiting factor.

Precision and accuracy. Accuracies and precisions were established in all four matrices and at four different concentration levels over the dynamic range. The specific concentrations tested for each compound are given in Table 2.1. Intra-day precision and accuracy were assessed based on six samples per concentration level. For the determination of inter-day precisions and accuracies six replicates per concentration were extracted and analyzed on three different days (total: n = 18/ concentration level and matrix). Precisions are reported as coefficient of variance in % and accuracies in % of the nominal concentration.

Recoveries. Absolute recoveries were determined by comparing the detector signal of the opioids obtained after extraction of quality control samples at all four concentration levels with the signal after injection of the respective nominal amount from standard solutions. Prior "break-through" experiments had demonstrated that no analyte was lost during online extraction under the conditions described above.

Matrix interferences, ion suppression and carry-over effects. To exclude interferences in the matrices, blank plasma and tissue samples from 10 different subjects or animals were extracted and analyzed. The lack of ion suppression at the time of elution of the analyte and its internal standard from the HPLC column was established following the procedure described by Müller *et al.* In brief: Analysis of ion suppression was set up by continuously infusion of each analyte solution (10 μg/mL) separately by a syringe pump (KD Scientific, USA) at a flow rate of 20 L/min *via* a PEEK T-connector into the elute from the LC column. The effect of injecting opioid-free extracted samples (n = 10 for each matrix, from 10 different individuals or animals) on the continuous signal produced by post-column infusion of the analyte was analyzed. A potential carry-over effect was assessed by alternately analyzing blank blood samples (n = 6) and plasma samples containing concentrations of opioids 10-fold higher than the upper limit of quantitation (n = 6).

Stability studies. The freeze-and-thaw stability of the opioids was determined during five freeze-and-thaw cycles using human plasma spiked with the 5 opioids at the following concentrations: alfentanil: 10 ng/mL, fentanyl: 20 ng/mL, lopermide: 5 ng/mL, remifentanil: 60 ng/mL, and sufentanil: 10 ng/mL. Samples were kept frozen at -80°C and thawed at room temperature. Within-batch stability of the opioids after protein precipitation was studied at room temperature and +4°C in the autosampler for 24 h. Samples (n = 6/ concentration) were compared with freshly prepared samples at the same concentration levels.

Results

Assay Development

Chromatography. The five opioids were separated within 5.0 minutes. Representative ion chromatograms are shown in Figure 2.2. As demonstrated by analysis of 10 blank samples (for each matrix, all samples from different individuals or rats), no matrix interferences with the analyte peaks were found.

MS/MS Detection. For the determination of the MS/MS conditions giving the best sensitivity, each compound was directly infused into the electro spray source using a syringe pump (*vide supra*). All opioids predominantly formed protonated quasi-molecular ions in our mobile phase resulting in the following $[M+H]^+$: alfentanil: m/z = 417.4, fentanyl: m/z = 337.5, loperamide: m/z = 477.3, remifentanil: m/z = 377.2, and sufentanil: m/z = 387.1. The fragment patterns produced by collision-activated dissociation are shown in Figure 2.3. The most intense product ions observed in MS/MS spectra were chosen for MRM and were in most cases the result of the neutral loss of *N*-phenyl-*N*-propanamide. The only exception was loperamide. Here the cleavage of the 4-(*p*-chlorophenyl)-4-hydroxyl-1-piperidine group gave the most intense fragment at m/z = 266.1.

Carryover. During method development, carry-over of loperamide turned out to be a significant potential problem. No carryover for any of the other opioids was observed. Carryover of loperamide was avoided after washing steps with methanol (2 times) and water (2 times) for both injector and injection valve through the Leap washing station were added after sample injection (Figure 2.4). Those washing steps were carried out during sample analysis and, thus, did not negatively affect sample turnover.

Ion Suppression. Ion suppression was found in the ion chromatograms of all 5 analytes and all matrices between 1.6 min to 1.9 min (Figure 2.5). No significant ion suppression was detected at any other time after injection of extracted blank matrices. Remifentanil has the shortest retention time, but the peak was unaffected by ion suppression caused by the non-retained materials underlying the injection peak (Figure 2.5).

Matrix interferences. No interference in the retention time range for any of the analytes was find for any of the matrices tested (n = 10 different individuals/ matrix).

Validation

Lower Limits of Quantitation and Range of Linear Response. The lower limits of quantitation (LLOQ) on column were 3.3 pg for most compounds in rat plasma and rat tissue homogenates (brain and lung). Fentanyl in lung and brain homogenates, loperamide in plasma and lung homogenates and sufentanil in lung homogenates showed better sensitivity with LLOQs of 1.7 pg on column (Figure 2.2). LLOQs in human plasma were 1.25 pg on column for alfentanil, lopermide, and sufentanil and 2.5 pg on column for fentanyl and remifentanil. For rat plasma and tissue homogenates (lung and brain), the linear ranges varied depending on opioid and matrix and ranged from 0.017- 16.67 ng/mL (e.g. fentanyl in plasma) to 0.083- 33.3 ng/mL (e.g. loperamide in brain tissue homogenate). Details are shown in Table 2.1. In human plasma, ranges of the linear response were between 0.0125- 6.25 ng/mL (loperamide) and 0.025- 25 ng/mL (remifentanil) (Table 2.2). The regression coefficients (r) were always better than 0.999.

Accuracies and Precisions. At the LLOQ, intra-day accuracies were between 81.8% (sufentanil, in rat brain homogenates) and 119.7 (loperamide in rat plasma) and intra-day precisions ranged between 0.6% loperamide in rat brain and 16.2% (remifentanil in rat

lung homogenates) (Table 2.3). At the upper limit of quantitation (ULOQ), intra-day accuracies were between 98.7% (loperamide in rat brain homogenates) and 100.7% (sufentanil in human plasma) and intra-day precisions were between 0.9% (alfentanil in rat plasma) - 3.9% (remifentanil in rat lung homogenates) (Table 2.3). At the LLOQ, inter-day accuracies ranged between 80.5% (loperamide in rat brain homogenates) and 119.5% (fentanyl in rat lung homogenates) and inter-day precisions were between 3.6% (fentanyl in rat brain homogenates) and 18.0% (remifentanil in rat lung homogenates). At the ULQ, inter-day accuracies were found between 99% (loperamide in rat brain homogenates) and 100.8% (remifentanil in rat lung homogenates), and between 2.1% (e.g. fentanyl in rat brain homogenates) and 3.8% (loperamide in human plasma) (Table 2.3).

Processed Sample Stability and Stability During Freeze/Thaw Cycles.

Processed validation samples at low, middle and high concentrations were kept at 4°C in the auto sampler for 48h, and then re-analyzed, quantified and compared with samples immediately quantified after extraction and with their nominal values (Table 2.4). The mean accuracy and precision for determination of all opioids of human plasma in the extracted stored samples after 48h ranged from 88.4 - 111.2% and 0.2 - 10.8%, respectively, and were within the acceptance limits and not significantly different from extracted samples immediately analyzed.

Alfentanil, fentanyl, sufentanil and loperamide were found stable during five freeze/ thaw cycles with analytical recoveries between 97.1 to 105.8% (Figure 2.6). However, sufentanil was only stable for three freeze/thaw cycles showing acceptable recovery (≥ 97.2%). During the fourth cycle, recovery dropped to a mean 78.6% and thus below the acceptance range (Figure 2.6).

Discussion

Due to the specificity of mass spectrometers used as HPLC detectors, there has recently been a trend towards developing assays for groups of drugs with similar treatment indications instead of assays for only single drugs. Due to the increasing number of drugs for specific indications and the combination of drugs, the drug analysis laboratory is challenged with samples only few of which contain the same drugs. Frequent switching between methods including change of columns and solvents, as well as analysis of calibrators and quality controls only to measure a few clinical samples is economically not feasible. The alternative is to wait until an acceptable number of samples have accumulated. However, the result of this strategy is poor turn-around times. Especially in the case of opioids, fast turn around is required in most cases and in case of the diagnosis of a potential abuse, there is also a need for screening since the administered opioid may be unknown. Several assays have described the quantitative analysis of single opioids and/or their main metabolite in biological samples using LC/MS (Shou et al., 2001; Day et al., 2003; Koch et al., 2004). Although simultaneous analysis of two or three opioids such as fentanyl and remifentanil using GC (Bjorksten et al., 2002), fentanyl and alfentanil using HPLC (Kumar et al., 1996b), fentanyl, alfentanil and sufentanil using HPLC (Lambropoulos et al., 2000), and fentanyl, alfentanil and sufentanil by GC/MS (Metz et al., 2000a) has been reported, no broadly applicable analysis strategy has been developed that also allows for analysis in different matrices such as tissues. In addition, most published methods involved multi-step manual extraction procedures. Thus, we developed an HPLC-MS/MS-based analytical platform that was validated for 5 commonly used opioids in human and rat plasma as well as in rat lung and brain, both

tissues that are of high interest during drug development and for research studies. This analytical platform includes fast semi-automated sample extraction and can easily be adapted to the quantification of other opioids and their metabolites as well as other matrices. Our assay also uses the same platform (online extraction, same columns and solvents) as other assays developed and used in our laboratory for other groups of drugs such as immunosuppressants (Christians, 2000) and anti-human immunodeficiency virus (HIV) drugs (Jacobsen, 2004). This means that samples containing those drugs can be run in the same batch as the opioids and all that is required is the automatic download of a different Analyst method.

It must be noted that our method was developed to give the highest sensitivity to detect trace amounts in potential human and veterinary abuse cases and during pharmacokinetic and tissue distribution studies in rats. As demonstrated by our dilution integrity studies, samples that contain higher concentrations can easily and reliably be diluted so that the concentrations fall into the ranges of linear response. Also, LLOQ, linearity, and range of linear response for tissues were reported in ng/mL homogenate rather than in ng/mg tissue. To keep sample processing the same for all tissue samples, our extraction procedure uses the same volume of homogenization buffer. Thus, if the sensitivity of the assay had been reported on a ng/mg basis, it would have depended on the amount of tissue used. Reporting ng/mL tissue homogenate results is more generally applicable.

The stability of opioids in biological matrices, stock solutions and after extraction has been studied by other investigators. Fentanyl stock solutions were stable for at least 147 days at 4°C (Shou et al., 2001) and 29 days at room temperature while protected from light (Lambropoulos et al., 1999). Fentanyl in biological matrices and extracts were

found stable for 24 h - 4 days at room temperature and for 105 days if stored at - 20°C (Lambropoulos et al., 2000). Fentanyl samples proved to be stable during 3 freeze/thaw cycles (Shou et al., 2001). Sufentanil stability in plasma was established in the dark at - 20°C for 4 weeks. Sufentanil and alfentanil stock solutions and extracts were stable for at least 4 days when stored at room temperature (Lambropoulos et al., 2000). Remifentanil's poor stability has always been a matter of concern (Kabbaj and Varin, 2003). The stability of Remi in freshly spiked dog plasma was found to be only 4 h when kept on ice (Kabbaj and Varin, 2003). The addition of citric acid can prevent remifentanil hydrolysis, allowing blood samples to be safely stored for at least 20 h at room temperature and for at least 1 year when frozen. Acidified samples were also found to be stable through 3 freeze-thaw cycles (Selinger et al., 1994). The stability of loperamide was established in stock solutions (30 days at 4°C), in the auto sampler after extraction (24 h at 20°C), in human plasma samples (24 h at 20°C), during long-term storage of human plasma samples (5 months at -80°C) and during 3 freeze/thaw cycles (Tu et al., 1989). Based on the data in the literature, we decided that stock solution; bench top and long-term storage stability was well established and did not need to be studied again. The stability of extracted samples in the auto sampler depends on the extraction procedure and thus data from the literature could not be extrapolated. Also we know from other assays in our laboratory which use a similar extraction procedure (Christians, 2000; Jacobsen 2004) that matrix degradation during freeze-thaw cycles may lead to significantly reduced absolute recovery during the protein precipitation step. As shown by our stability studies, all opioids were stable in the auto sampler after extraction for at least 48h and could undergo at least 3 freeze thaw cycles.

Column-switching techniques for automated on-line sample preparation have been used for HPLC analyses for decades (Huber&Zech). However, their application was limited to drugs with specific UV-absorption maxima. During recent years, on-line sample preparation has experienced a revival due to the increased use of mass spectrometers as HPLC detectors and their superior specificity and selectivity compared to UV detectors. In our laboratory, the use of online extraction using column switching has significantly improved intra and inter-day precisions (Christians 2000; Jacobsen 2004). In our experience, the use of 96-well plates instead of single HPLC auto sampler vials has not only the advantage that a multi-pipette can be used to dispense the protein precipitation solution to speed up and streamline the manual part of our extraction procedure, it also significantly reduced the number of non-systematic errors due to pipetting errors or accidental switching of vials. However, as aforementioned, it is critical that the injector needle height is adjusted to avoid drawing the precipitate at the well bottom. Also, abrupt movements of the 96-well plate after centrifugation should be avoided to prevent shearing particles from the precipitate that potentially may clog the injector needle, capillaries or the extraction columns. So far, we used our assay for more than 5000 plasma and tissue samples without loosing a single sample due to clogging or degradation of the online extraction columns. As a precaution, we change the online extraction column every 500 injections and the analytical column every 2000 analyses.

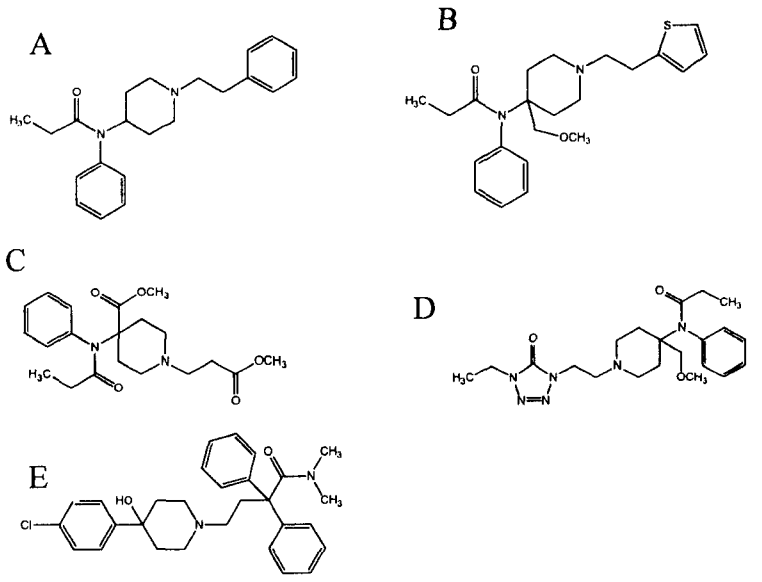

Figure 2.1. Structures of five opioids. A. Fentanyl, B. Sufentanil, C. Remifentanil, D. Alfentanil and D. Loperamide.

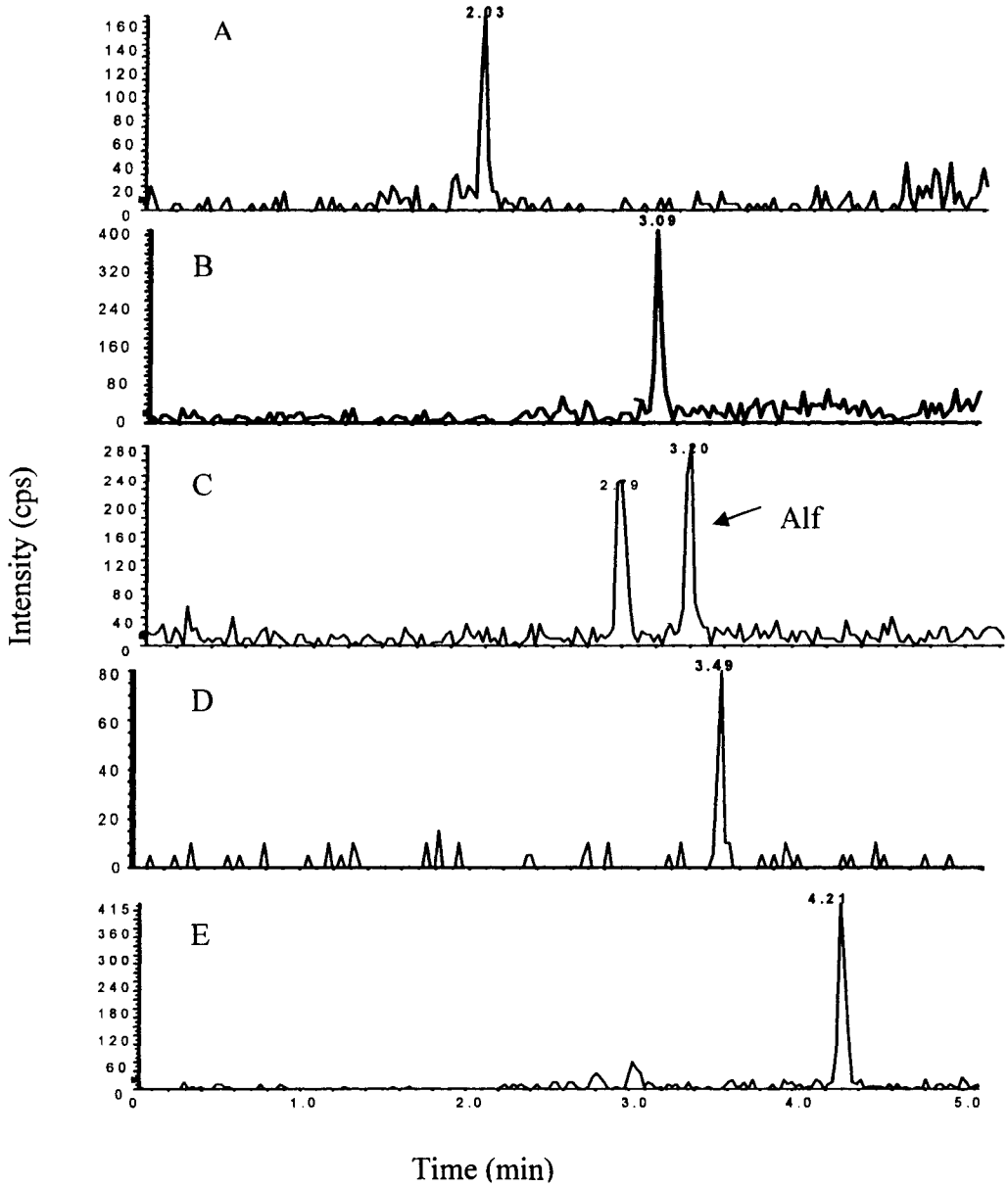

Figure 2.2. Representative blank ion chromatogram and ion chromatograms of blank matrix samples spiked at the lower limit of quantitation. A. remifentanil (0.033 ng/mL) in rat lung; B.fentanyl (0.033 ng/mL) in rat brain; C.alfentanil (0.033 ng/mL) in rat plasma; D. sufentanil (0.017 ng/mL) in rat lung and E. loperamide (0.017 ng/mL) in rat plasma. To determine the lower limit of quantitation (LLOQ), blank matrices were spiked with the opioids (n = 5 per matrix and opioid). LLOQ was defined as the lowest concentration at which both accuracy and precision were $\leq 20\%$.

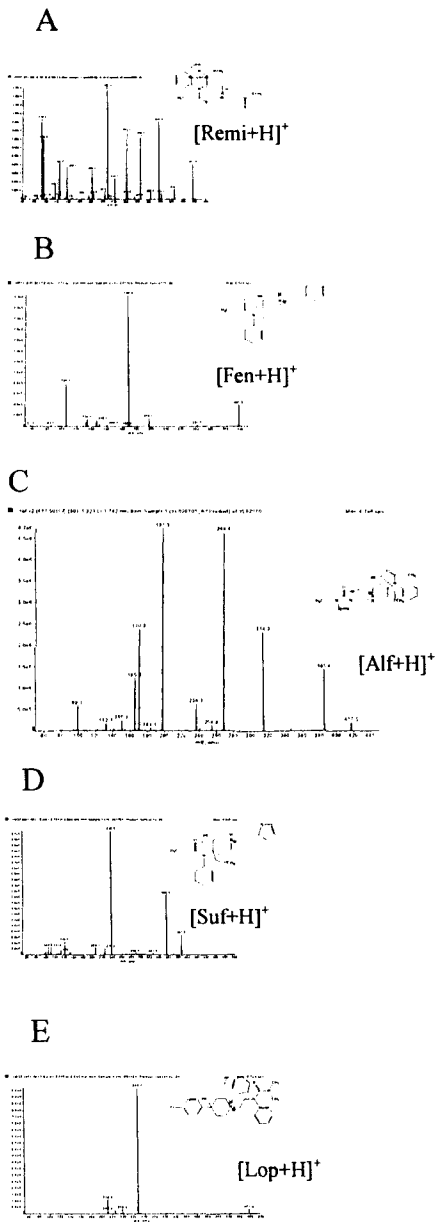

Figure 2.3. Spectra of product ion and the proposed pattern of fragmentation. A. remifentanil; B. fentanyl; C. alfentanil; D. sufentanil, and E. loperamide.

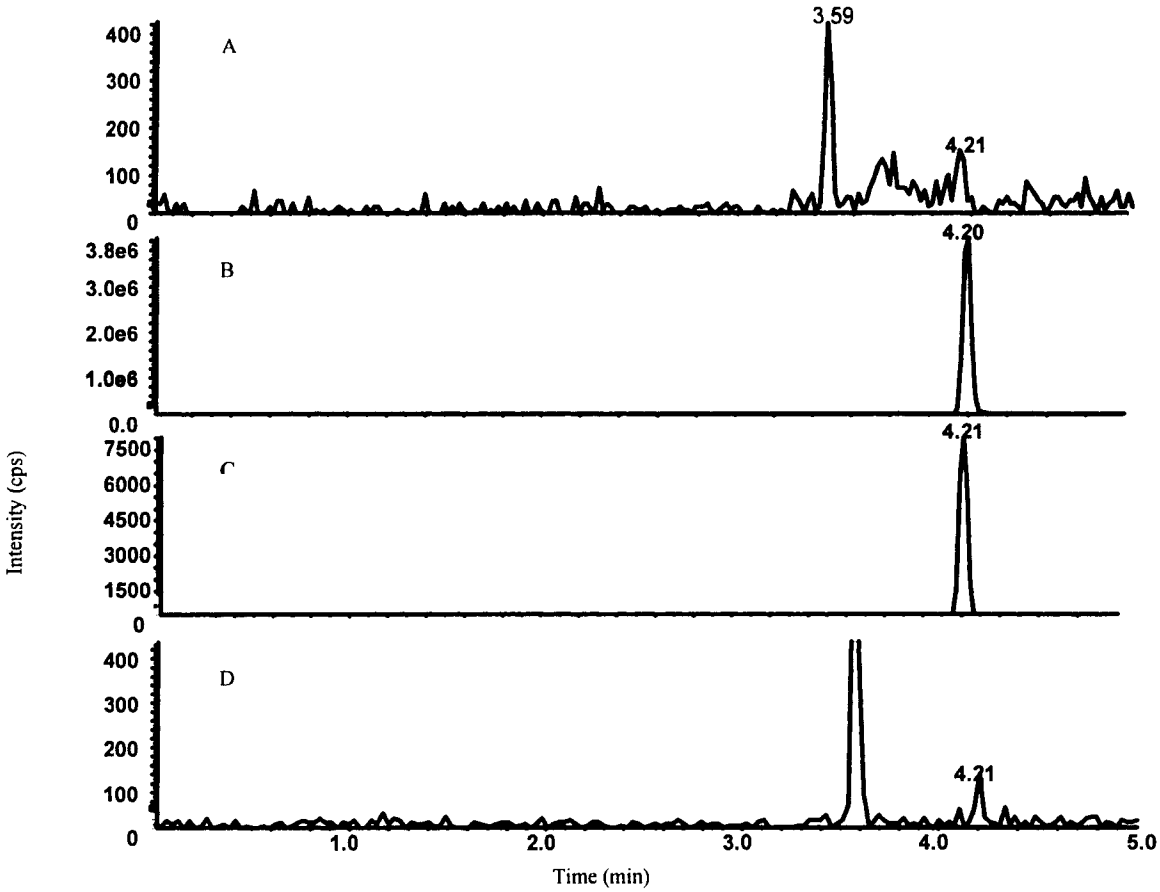

Figure 2.4. Loperamide carryover, A. Blank human plasma, B. Spiked human plasma (100 ng/mL) and C. Solvent (MeOH) blank after injection of B without wash step added. D. Human plasma after injection B with wash step program added. Representative ion chromatograms of a total of n = 6 experiments are shown.

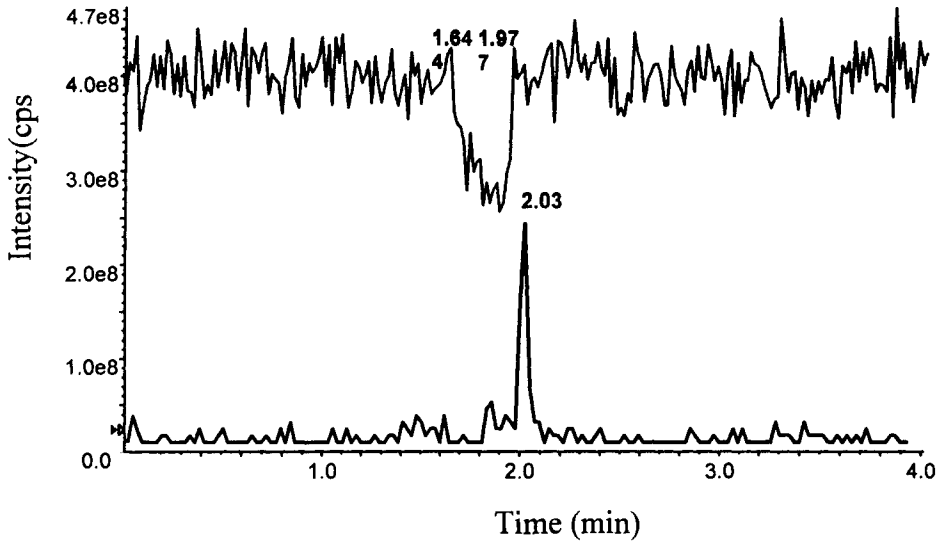

Figure 2.5. A representative ion suppression experiment: remifentanil. Ion suppression was tested for each of the opioids and matrices with n = 10 blank matrix preparations collected from 10 different individuals.

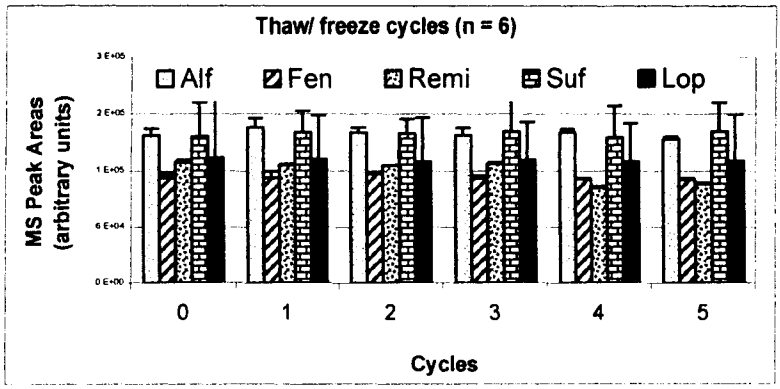

Figure 2.6. Stability of the five opioids tested during five freeze/thaw cycles in human plasma. Each bar represents the mean ± standard deviation n = 6.

Table 2.1. Summary of the calibration curve parameters in rat plasma (P), lung tissue homogenate (L) and brain tissue homogenate (B)

	Fentanyl			Loperamide			Sufentanil			Alfentanil			Remifentanil		
	P	L	B	P	L	B	P	L	B	P	L	B	P	L	B
Linearity Range (ng/mL)	0.033-16.67	0.017-16.67	0.017-16.67	0.017-16.67	0.017 - 16.67	0.08-33.3	0.033-16.67	0.017 - 16.67	0.03-16.6	0.033-33.33	0.08 - 33.3	0.033-33.33	-	0.033-33.33	0.033-16.67
LOD (ng/mL)	0.0083	0.003	0.083	0.008	0.003	0.03	0.017	0.008	0.01	0.008	0.03 3	0.008	-	0.017	0.017
LLOQ (ng/mL)	0.033	0.017	0.017	0.017	0.017	0.08	0.033	0.017	0.03	0.033	0.08	0.033	-	0.033	0.033
ULOQ (ng/mL)	16.67	16.67	16.67	16.67	16.67	33.3	16.67	16.67	16.6	33.33	33.3	33.33	-	33.33	16.67
Standard Curve	y=0.00424x-0.000346 (P) y=0.00562x+0.000342 (L) y=0.0138x+0.00238 (B)			y=0.031x-0.00132 (P) y=0.0263x+0.00281 (L) y=0.0185x+0.00773 (B)			y=0.00536x-0.0000182 (P) y=0.00589x-0.0000662 (L) y=0.00568x+0.000191 (B)			y=0.0262x+0.00483 (P) y=0.0117x+0.00149 (L) y=0.00325x+0.000071 (B)			y=0.000253x+0.000175 (L) y=0.000773x+0.000365 (B)		
Regression Coefficient (r)	0.9994 (P) 0.9996 (L) 0.9995 (B)			0.9994 (P) 0.9994 (L) 0.9989 (B)			0.9993 (P) 0.9993 (L) 0.9991 (B)			0.9995 (P) 0.9993 (L) 0.9992 (B)			0.9991 (L) 0.9992 (B)		

Each calibration curve was measured with n = 6.

Table 2.2. Summary of the calibration curve parameters in human plasma

	Fentanyl	Loperamide	Sufentanil	Alfentanil	Remifentanil
Linearity Range (ng/mL)	0.025-12.5	0.0125- 6.25	0.0125-6.25	0.0125-12.5	0.025-25
LOD (ng/mL)	0.0125	0.0025	0.0025	0.0025	0.0125
LLOQ (ng/mL)	0.025	0.0125	0.0125	0.0125	0.025
ULOQ (ng/mL)	12.5	6.25	6.25	12.5	25
Standard Curve	y = 5.16e+003X + 11.4	y = 1.44e+005X + 5.35e+ 003	y = 7.73e+004X -3.75e+003	y = 1.6e+004X+ 191	y = 2.69e+003 X - 129
Regression Coefficient (r)	0.9990, 0.9993, 0.9998	0.9990, 0.9997, 0.9985	0.9994, 0.9993, 0.9996	0.9990, 0.9996, 0.9996	0.9991, 0.9994, 0.9987

Each calibration curve was measured with n = 6.

Table 2.3. Intra- and inter-assay precision and accuracy

Matrix		Intra-day (n = 6)				Inter-day (n = 18)			
		Accuracy (%)		Precision (%)		Accuracy (%)		Precision (%)	
		LLOQ ng/mL*	0.083 ULOQ	LLOQ ng/mL*	0.083 ULOQ	LLOQ ng/mL*	0.083 ULOQ	LLOQ ng/mL*	0.083 ULOQ
Rat Plasma	Fen	99.0	101.1	2.3	1.9	105.7	105.6	6.8	10.4
	Lop	100.2		3.3		100.0		2.4	
	Suf	119.7	111.6	6.5	7.9	117.2	110.6	5.2	6.3
	Alf	100.3		3.9		100.3		2.7	
	Remi	118.0	116.7	6.5	7.2	93.8	102.5	15.9	9.0
		100.0		3.5		99.9		2.6	
		87.2	87.5	6.7	4.3	85.8	89.4	11.3	8.2
		100.2		0.9		99.7		2.1	
		-- -- --		-- -- --		-- -- --		-- -- --	
Rat Lung	Fen	95.5	95.9	12.8	4.0	119.5	105.6	5.7	3.9
	Lop	99.6		2.8		100.0		2.6	
	Suf	113.4	101.0	6.4	7.1	117.0	102.6	10.1	5.3
	Alf	100.1		2.7		100.3		2.9	
	Remi	89.1	99.9	16.0	3.4	91.2	102.0	16.3	3.7
		100.3		3.5		100.2		3.0	
		82.1	82.1	6.4	6.4	82.0	82.0	7.6	7.6
		99.7		1.7		99.9		3.4	
		91.3	97.1	16.2	12.3	99.2	97.7	18.0	14.4
		100.0		3.9		100.8		3.3	
Rat Brain	Fen	118.7	104.5	7.4	3.0	111.5	101.4	3.6	4.6
	Lop	99.8		2.9		100.0		2.1	
	Suf	90.0	90.0	0.6	0.6	80.5	81.7	9.9	9.9
	Alf	98.7		2.7		99.0		2.6	
	Remi	81.8	92.1	6.1	3.4	89.4	94.4	6.9	4.4
		99.4		3.7		99.7		3.5	
		82.6	91.7	8.5	1.4	102.5	100.0	10.8	4.8
		99.6		2.9		100.2		3.2	
		84.2	86.7	11.1	13.7	107.9	101.3	8.7	9.2
		99.6		1.9		100.4		2.2	
***Human Plasma**	Fen	115.1	108.8	10.5	8.6	91.7	94.7	8.6	5.9
	Lop	100.1		3.4		99.9		2.8	
	Suf	82.8	84.8	6.2	5.7	82.9	87.5	10.4	6.5
	Alf	99.7		3.7		99.8		3.8	
	Remi	119.5	109.8	4.6	5.7	118.1	106.4	4.6	4.9
		100.7		3.2		100.4		3.2	
		93.0	91.6	16.1	15.7	87.1	95.0	14.4	8.5
		100.4		3.7		100.0		2.6	
		114.7	91.9	6.8	9.4	108.1	98.3	11.6	6.2
		99.6		3.4		99.8		2.7	

*For human plasma, this data was 2 * LLOQ.
Fen: fentanyl, lop: lopermide, suf: sufentanil, alf: alfentanil, remi: remifentanil.

Table 2.4. Stability of opioids after extraction from human plasma in the autosampler at 4°C for 48 hours n = 6 for each data point

Compounds	Nominal [ng/mL]	Measured [ng/mL]	Precision (%)	Accuracy (%)
Fentanyl	0.0625	0.0584	10.8	93.4
	0.25	0.249	8.6	99.7
	12.5	12.46	0.5	99.7
Sufentanil	0.025	0.028	10.5	111.2
	0.25	0.252	2.0	100.7
	6.25	6.272	0.4	100.4
Loperamide	0.025	0.0221	5.6	88.4
	0.25	0.246	1.2	98.4
	6.25	6.24	0.2	99.8
Remifentanil	0.0625	0.0607	6.9	97.1
	1.25	1.228	1.5	98.3
	25	24.96	0.9	99.8
Alfentanil	0.025	0.0236	3.4	94.5
	0.25	0.251	0.6	100.3
	12.5	12.50	0.4	99.9

REFERENCES

Anderson DT and Muto JJ (2000) Duragesic transdermal patch: postmortem tissue distribution of fentanyl in 25 cases. *J Anal Toxicol.* **24**:627-634.

Bjorksten AR, Chan C and Crankshaw DP (2002) Determination of remifentanil in human blood by capillary gas chromatography with nitrogen-selective detection. *Journal of Chromatography B* **775**:97-101.

Cone E, Fant R, Rohay J, Caplan Y, Ballina M, Reder R and Haddox J (2004) Oxycodone involvement in drug abuse deaths. II. Evidence for toxic multiple drug-drug interactions. *J Anal Toxicol.* **Oct;28**:616-624.

Darwin WD, Murphy CM, Lambert WE and Huestis mA (2003) Urine drug trsting for opioids, cocaine, and metabolites by direct injection liquid chromatography/tandem mass spectrometry. *Rapid Communications in Mass Spectrometry* **17**.

Day J and al e (2003) *Journal of Toxicology* **27**:513-516.

Day J, Slawson M, Lugo R and Wilkins D (2003) Analysis of fentanyl and norfentanyl in human plasma by liquid chromatography-tandem mass spectrometry using electrospray ionization. *Journal of Analytical Toxicology* **27**:513-516.

Kabbaj M and Varin F (2003) Simultaneous solid-phase extraction combined with liquid chromatography with ultraviolet absorbance detection for the determination of

remifentanil and its metabolite in dog plasma. *Journal of Chromatography B* **783**:103-111.

Koch DE, Isaza R, Carpenter JW and Hunter RP (2004) Simultaneous extraction and quantitation of fentanyl and norfentanyl from primate plasma with LC/MS detection. *J Pharm Biomed Anal.* **34**:577-584.

Kuhlman JJJ, McCaulley R, Valouch TJ and S. BG (2003) Fentanyl use, misuse, and abuse: a summary of 23 postmortem cases. *J Anal Toxicol.* **27**:499-504.

Kumar K, Ballantyne JA and Baker AB (1996a) A sensitive assay for the simultaneous measurement of alfentanil and fentanyl in plasma. *Journal of Pharmaceutical and Biomedical Analysis* **14**:667-673.

Kumar K, Ballantyne JA and Baker AB (1996b) A sensitive assay for the simutaneous measurement of alfentanil and fentanyl in plasma. *Journal of Pharmaceutical and Biomedical Analysis* **14**:667-673.

Lambropoulos J, Spanos GA and Lazaridis NV (2000) Development and validation of an HPLC assay for fentanyl, alfentanil, and sufentanil in swab samples. *Journal of Pharmaceutical and Biomedical Analysis* **23**:421-428.

Lambropoulos J, Spanos GA, Lazaridis NV, Ingallinera TS and Rodriguez VK (1999) Development and validation of an HPLC assay for fentanyl and related substances in fentanyl citrate injection, USP. *Journal of Pharmaceutical and Biomedical Analysis* **20**:705-716.

Metz C, Gobel L, Gruber M, Hoerauf K and Taeger K (2000a) Pharmacokinetics of Human Cerbral Opioids Extraction. *Anesthesiology* **92**:1559-1567.

Metz C, Gobel L, Gruber M and Hoerauf KH (2000b) Pharmacokinetics of Human Cerebral Opioids Extraction. *Anesthesiology* **92**:1559-1567.

palleschi L, Lucentini L, Ferretti E and Anastasi F (2003) Quantitative determination of sufentanil in human plasma by liquid chromatography-tandem mass spectrometry. *Journal of Pharmaceutical and Biomedical Analysis* **32**:329-336.

Ropero-Miller JD, Lambert MK and Winecker RE (2002) Simultaneous quantitation of opioids in blood by GC-EI-MS analysis following deproteination, detautomerization of keto analytes, solid-phase extraction, and trimethylsilyl derivatization. *J Anal Toxicol.* **26**:524-528.

Selinger K, Lanzo C and Sekut A (1994) Determination of remifentanil in human and dog blood by HPLC with UV detection. *Journal of Pharmaceutical and Biomedical Analysis* **12**:243-248.

Shou W and al e (2001) A highly automated 96-well solid phase extraction and liquid chromatography/tandem mass spectrometry method for the determination of fentanyl in human plasma. *Rapid Communications in Mass Spectrometry* **15**:466-476.

Shou W, Jiang X, Beato BD and Naidong W (2001) A highly automated 96-well solid phase extraction and liquid chromatography/tandem mass spectrometry method for the determination of fentanyl in human plasma. *Rapid Communications in Mass Spectrometry* **15**:466-476.

Szeitz A, Riggs KW and Harvey-Clark C (1996) Sensitive and selective assay for fentanyl using gas chromatography with mass selective detection. *Journal of Chromatography B* **675**:33-42.

Tu Y-H, Allen JLV and Wang D-P (1989) Stability of loperamide hydrochloride in aqueous solutions as determined by high performance liquid chromatography. *International Journal of Pharmaceutics* **Volume 51**:157-160.

Wasels R and Belleville F (1994) Gas-Chromatographic Mass-Spectrometric Procedures Used for the Identification and Determination of Morphine, Codeine and 6-Monoacetylmorphine. *Journal of Chromatography A* **674**:225-234.

Weng N and al e (2002) Simultaneous development of six LC-MS-MS methods for the determination of multiple analytes in human plasma. *Journal of Pharmaceutical and Biomedical* **28**:1115-1126.

Woestenborghs RJ, Timmerman PM, Cornelissen ML, Van Rompaey FA, Gepts E, Camu F, Heykants JJ and Stanski DR (1994) Assay methods for sufentanil in plasma. Radioimmunoassay versus ga chromatography-mass spectrometry. *Anesthesiology* **80**:666-670.

CDER (2001) U.S. Department of Health and Human Services, Food and Drug Administration, Center for Drug Evaluation and Research and Center for Veterinary Medicine (CVM). Guidance for the Industry. Bioanalytical Method Validation, May 2001. (www.fda.gov/cder/)

Müller C, Schäfer P, Störtzel M, Vogt S, Weinmann W. Ion suppression effects in liquid chromatrography-electrospray-ionization transport-region collision induced dissociation mass spectrometry with different serum extraction methods for systematic toxicological analysis with mass spectra libraries. *J Chromatogr B.* 2002; 773: 47-52.

Christians U, Jacobsen W, Serkova N, *et al.* Automated, fast and sensitive quantification of drugs in blood by liquid chromatography-mass spectrometry with on-line extraction: immunosuppressants. *J Chromatogr B.* 2000; 748: 41-53.

Jacobsen W, Unger M, Niemann C, Baloum M, Hirai S, Benet LZ, Christians U. Automated, Fast and Sensitive Quantification of Drugs in Human Plasma by LC/LC-MS: Simultaneous Quantification of Six Protease Inhibitors and Three Non-Nucleoside Transcriptase Inhibitors. Ther Drug Monit 2004; 26: 546-562.

Huber R, Zech K. Determination of drugs and their metabolites in biological samples by fully automated HPLC with on-line extraction and pre-column switching. In: Selective Sample Handling and Detection in High- Performance Liquid Chromatography. R.W. Frei and K. Zech, eds. Journal of Chromatography Library, Elsevier, Vol. 39A, Amsterdam, 1988, pp 81-144.

CHAPTER 3

The effect of verapamil on the distribution kinetics of fentanyl and loperamide to lung and brain in Sprague Dawley rats.

Iman A. Elkiweri, Martha C. Tissot van Patot, Yan Ling Zhang, Uwe Christians and Thomas K. Henthorn

Department of Anesthesiology, University of Colorado Denver Health Sciences Center, Denver, Colorado (IAE, MCTvP, YLZ, UC, TKH).

Supported by grant No. R01- GM47502.09 from the National Institutes of Health and in part by the Nema Foundation, Malaysia.

Fentanyl is a widely used, potent, synthetic opioid analgesic, which was introduced into clinical practice in the early 1960s and represented a major increase in potency in comparison with clinically important opiate agonists of the time. It acts at the μ-opioid receptor and is used as analgesic to supplement general anesthesia for various surgical procedures or as a primary anesthetic agent in very high doses during cardiac surgery. For long term analgesia and sedation in intensive care patients, fentanyl is administered via intravenous infusion (Stanley, 1992; Ball and Westhorpe, 2002; Stanley, 2005). Fentanyl demonstrates extensive first-pass uptake into lung following intravenous administration (Roerig et al., 1994). Distribution to the brain is also extensive. Fentanyl distribution to tissue was considered to be a result of its lipid solubility (Bjorkman et al., 1994), however, we have previously demonstrated that a saturable energy-dependent process mediates lung and brain uptake of fentanyl – perhaps by an unidentified inward transporter that is inhibited by verapamil *in vitro* (Henthorn et al., 1998; Henthorn et al., 1999; Waters et al., 1999).

By contrast, loperamide is a potent opioid that is widely used for treatment of diarrhea. It primarily acts through activation of opioid receptors in the intestinal tract (Heykants et al., 1974; Heel et al., 1978). Loperamide is actively extruded from many tissues, including the brain by the outward transporter P-glycoprotein (P-gp) (Dagenais et al., 2004). Data are inconsistent as to whether loperamide has a central effect.

Because we previously demonstrated that verapamil blocked fentanyl uptake *in vitro,* and verapamil is a potent P-gp inhibitor, we studied the variable transport of fentanyl and

loperamide to the lung and brain of rats and hypothesized differential effects of verapamil on opioid concentrations in the lung and brain.

Materials and Methods

Materials. Fentanyl citrate was purchased from Abbott Laboratories (North Chicago, IL, USA), loperamide hydrochloride was obtained from Sigma Aldrich Inc. (St Louis, MO, USA) and verapamil hydrochloride was purchased from Abbott Laboratories (North Chicago, IL, USA).

Animals. Male Sprague-Dawley rats weighing 300-350 g were purchased from Harlan (Madison, Wisconsin) with indwelling cannulae (jugular venous catheters for drug infusion and a carotid artery catheter for blood collection). The rats were housed in the University of Colorado Health Sciences Center animal facility. They were kept on a 12-hour light/dark cycle and were fed standard laboratory chow. Experiments were carried out according to the guidelines provided by Institutional Animal Care and Use Committee (University of Colorado Health Sciences Center).

Infusions. The animals received a five-minute (from time t = 0 to 5 minutes) intravenous infusion of fentanyl citrate (5.25 μg/kg/min) or loperamide hydrochloride (0.475mg/kg/min). The dose for fentanyl is based on doses used in human anesthesia and the dose for loperamide is the dose at which brain activity is affected, as measured by EEG. On a separate occasion, a target-controlled infusion (TCI) of verapamil hydrochloride was administered for five minutes at a target concentration of 1 mg/ml prior to the opioid infusion and continued ten minutes after the opioid infusion (from time t = -5 to 10). The TCI was accomplished using a Harvard 22 syringe pump (Harvard Apparatus, Holliston, Massachusetts), controlled via a serial connection to a Pentium-

based computer running the TCI software STANPUMP (written by Steven L. Shafer, MD) and using a 3-compartment pharmacokinetic model for verapamil derived from a one-compartment rat model for verapamil and a similar 3-compartmental model for thiopental in the rat (Gustafsson et al., 1992; Bhatti and Foster, 1997). Four rats per time period were euthanized by guillotine at 0, 1, 5, 6, 8, 10, or 60 minutes. Blood (5 mL) was collected from the carotid catheter prior to decapitation and drawn into tubes containing citrate as anticoagulant. Plasma was separated following a standard centrifugation protocol (400 g, 10 min, 4°C). The skull was opened immediately after decapitation. Brain tissue was collected and was flash-frozen in liquid nitrogen. A thoracotomy was performed to allow extraction of the lungs which were immediately frozen in liquid nitrogen. Plasma, lung, and brain tissue were stored at –80°C until analysis using specific and highly sensitive high-performance liquid chromatography/ mass spectrometry assays for fentanyl and loperamide.

Analytical Methods Plasma and tissue fentanyl concentration of all samples obtained at the times delineated above were measured by a high-performance liquid chromatography/ mass spectrometry (LC/LC, MS/MS) technique developed in our laboratory.

Instrumentation. The extracts were analyzed using an LC/LC-MS/MS system. The two HPLC systems consisted of the following components (all series 1100, Agilent Technologies, Palo Alto, CA): HPLC I: G1312A binary pump, G1379A degasser and a LEAP autosampler (PAL, Zürich, Switzerland); HPLC II: G1312A binary pump, and a G1316A column thermostat. A Sciex API 4000 triple-stage quadrupole mass spectrometer was used as detector (Applied Biosystems, Foster City, CA). The HPLC systems were connected *via* a 6-port column-switching valve mounted on a step motor

(Rheodyne, Cotati, CA). The connections of the switching valve and the solvent flow in the two valve positions are shown in figure 3.1.

Sample Preparation. Rat brain and lung (approximately 10 mg) were weighed and homogenized with 2 ml KH_2PO_4 buffer pH = 7.4 (1 M) using a teflon-glass manual homogenizer. Homogenized samples were stored at -80°C before analysis. On the day of analysis, plasma and homogenized brain and lung were thawed on ice. Samples were prepared by adding 200 μL of plasma, or homogenates of lung or brain to 400 μL of internal standard solution (0.06 M $ZnSO_4$ solution contained water and methanol (30:70, v/v), and 10 μL of the internal standard alfentanil resulting in a final concentration of 50 ng/mL. After vortexing (2 min), the samples were centrifuged (13000 g, 5 min) to remove precipitated proteins. One hundred μL of the supernatant was directly injected into the HPLC system (1100 HP Agilent, Waldbronn, Germany) through a Leap autosampler.

For on-line sample clean-up, supernatants were loaded onto the extraction column (4.6 × 12.5 mm, 5 μm particle size, Eclipse XDB-C8, Agilent) and were washed with a high flow of 5 mL/min, 80% 0.1% formic acid/ 20% methanol for 1 min. Then the switching valve was activated and the analytes were back-flushed onto the C8 analytical column (4.6 × 12.5 mm, 5 μm particle size, Eclipse XDB-C8, Agilent). A linear gradient was used: methanol increased from 55% to 100% in 4 min and was kept at 100% methanol for 1 min. Flow rate was 1 mL/min and column temperature was maintained at 40°C.

The analytes that eluted from the HPLC column were introduced into the turbo-ion spray source. Zero-grade air for the nebulizing and turbo gasses was provided by a Zero Air Generator (Analytical Gas Systems). Ultra-high-purity nitrogen (99.999%) was used as

collision activated dissociation (CAD) gas and the curtain gas provided by a nitrogen generation systems purchased (Agilent, Palo Alto, CA). Ionization was achieved in the positive Multiple Reaction Monitory (MRM) mode. MRM sensitivities for each analyte were simultaneously optimized by direct infusion of each compound (0.1 μg/mL, in 80% methanol/20% 0.1% formic acid). The mass spectrometer, HPLC components, LEAP autosampler and all data processing were controlled through the ABI/Sciex "Analyst" software version 1.3. (Applied Biosystems, Foster City, CA).

For the quantification of all opioids, the MRM parameters used were: the source temperature was set to 480°C, and the ion spray voltage was 5000V, gases were set at 20 for nebulizer gas, 15 for turbo gas, curtain gas was 15 and the setting for the CAD gas was 8 (all arbitrary units). The declustering potential (DP) was 50V. The dwell time for each transition was 200 ms. Data was collected and the major product ion transitions were monitored: fentanyl *m/z* 337.5 → 188.4, loperamide *m/z* 477.5 → 266.1, and the internal standard alfentanil *m/z* 417.4 → 197.3.

Assay validation. The assay was completely validated following current FDA guidelines (CDER (2001) U.S. Department of Health and Human Services, Food and Drug Administration, Center for Drug Evaluation and Research and Center for Veterinary Medicine (CVM), Guidance for the Industry, Bioanalytical Method Validation, May 2001. (www.fda.gov/cder, accessed 5-24-2005). Key method performance parameters were: linear range from 0.033 to 16.67 ng/mL for in rat plasma, lung and brain). The regression coefficients (r) were always better than 0.999. The lower limits of quantitation (LLOQ) on column was 3.3 pg. Intra-day accuracies were between 81.8% (brain) and 119.7% (lung), and intra-day precisions were between 2.3% (plasma) and 20.4% (lung) at

the lower limit of quantitation (LLOQ). At the upper limit of quantitation (ULOQ), intra-day accuracies and precisions were between 99.4%-100.3% and 0.9%-3.9% in plasma and tissues, respectively. Inter-day accuracies were between 80.5%-119.5% at LLOQ, 99%-100.8% at ULOQ, and inter-day precisions were between 3.6%-18.0% at LLOQ, and 2.1%-3.8% at ULOQ. There were no matrix interferences, carry-over or ion suppression.

Data Analysis. The pharmacokinetics were analyzed using the SAAM II software (SAAM Institute, Seattle, WA) using a naive pooled-data technique. Model parsimony was tested using the Akiake information criterion (AIC) (Ludden et al., 1994). The data from the fentanyl or loperamide infusion alone and the fentanyl or loperamide infusion with verapamil treatment where lumped into separate models with linked parameters. Plasma kinetics were modeled with a two-compartment open model in which intercompartmental clearance (Cl_I) was assumed to be 0.1 ml/kg/min for fentanyl and 0.01 ml/kg/min for loperamide and the remaining parameters; volume1, volume2 and elimination clearance (V_1, V_2, Cl_E) were fit to the plasma fentanyl or plasma loperamide concentration-time data. Data fit with this model had lower AIC than either a one-compartment model or a two-compartment model in which Cl_I was an adjustable parameter.

To test the hypothesis that verapamil affects the plasma pharmacokinetics of fentanyl or loperamide, all data were first fit to a unified pharmacokinetic model for fentanyl or loperamide alone and then each of the adjustable parameters (V_1, V_2, Cl_E) where fit so that each parameter could have a covariate parameter for the experimental condition in which verapamil was infused. Whether a covariate for the verapamil condition produced

a statistically significant change in the pharmacokinetic parameter was tested by comparing the AIC with the added covariate in the model versus the AIC the simpler model without the covariate.

Lung and brain concentration-time data were modeled by adding partition coefficients, P_B and P_L, to describe the ratio between plasma fentanyl or loperamide concentrations and those in brain and lung, respectively. To test the hypothesis that verapamil changes plasma: tissue partitioning in the brain and lung, all data were first fit to a unified pharmacokinetic model for fentanyl or loperamide alone and then each of the plasma: tissue partition coefficients (P_B, P_L) where fit so that each coefficient could have a covariate parameter for the experimental condition in which verapamil was infused. Whether a covariate for the verapamil condition produced a statistically significant change in the partition coefficient was tested by comparing the AIC with the added covariate in the model versus the AIC the simpler model without the covariate.

Results.

Effect of verapamil on fentanyl pharmacokinetics. Rat arterial plasma, lung and brain fentanyl concentrations in the absence and presence of verapamil versus time relations were well-characterized by the model from the moment of injection (Figures 3.2-3.3). Visual comparison of the measured and predicted fentanyl concentration versus time relationships revealed no model misspecification.

Fentanyl plasma pharmacokinetics were described using a two-compartment open model After all data were fit to a unified pharmacokinetic model for fentanyl, the adjustable parameters (V_1, V_2, Cl_E) were fit so that each parameter could have a verapamil covariate for the experimental condition in which verapamil was infused. The reported results are

those of model 3, which had the lowest AIC (Table 3.1). Data resulting from model 3 indicated that verapamil treatment increased V_1 by 2.2-fold, had no effect on V_2 and increased Cl_E by 23% (Table 3.3).

Lung and brain concentration-time data were modeled by adding partition coefficients, P_L and P_B, to describe the ratio between plasma fentanyl concentrations and those in lung and brain, respectively. After all data were fit to a unified pharmacokinetic model for fentanyl alone, then each of the plasma: tissue partition coefficients (P_B, P_L) where fit so that each coefficient could have a covariate parameter for the experimental condition in which verapamil was infused. As shown in table 1 model 6 had the lowest AIC. Data resulting from model 6 indicated that verapamil had no effect on fentanyl partitioning in lung, however; partitioning in brain P_B decreased by 43 % (Table 3.3).

Effect of verapamil on loperamide pharmacokinetics. Loperamide concentrations in rat arterial plasma, lung, and brain were well characterized by the model from the moment of infusion through 10 minutes post-loperamide infusion (Figure 3.4A and 3.5); however, at 60 minutes post-infusion the model did not characterize the actual measured loperamide concentrations, as revealed by visual comparison. Rat arterial plasma, lung and brain loperamide concentrations in the presence of verapamil versus time relations were well-characterized by the model from the moment of injection through 60 minutes post-infusion (Figure 3.4B and 3.5).

Loperamide plasma pharmacokinetics were modeled using the same process as previously described. The results reported and discussed herein are those of model 4, which had the lowest AIC (Table 3.2). Verapamil caused no change in V_1, increased V_2 by 89% and decreased Cl_E by 49.5% (Table 3.3).

Loperamide lung and brain concentration-time data were modeled as previously described. The results reported and discussed are those of model 8, which had the lowest AIC (Table 3.2). Verapamil increased loperamide P_L by 427% while P_B increased by 80.7% (Table 3.3).

Comparison of fentanyl and loperamide pharmacokinetics. Pharmacokinetic modeling indicated significant differences between fentanyl and loperamide (Table 3.3). Fentanyl and loperamide demonstrated rapid uptake into rat lung and brain tissue, but the partitioning of fentanyl into these tissues was more extensive than that of loperamide. The blood brain partition coefficient was greater for fentanyl than for loperamide, while the blood lung partition coefficient for fentanyl was less than that for loperamide. Plasma volumes of fentanyl and loperamide were similar. The elimination clearance of fentanyl was greater than that of loperamide.

In the presence of verapamil, fentanyl uptake was inhibited in the brain whereas loperamide uptake was promoted in the lung and brain. For fentanyl, the uptake-inhibiting effect of verapamil was in the brain whereas for loperamide, the uptake-promoting effect was in the brain and lung.

Discussion.

We wished to measure the distribution of fentanyl and loperamide and to determine whether there may be differences in their transport in to the lung and brain, *in vivo*, in the presence of verapamil. In addition, we wished to evaluate fentanyl and loperamide pharmacokinetics using a high resolution recirculatory model to examine carefully any possible differences in disposition that could reasonably be attributed to differential handling of the two opioids.

Our results indicating that verapamil decreased partitioning of fentanyl into brain (P_B) by 42% are in support of our previous *in vitro* results (Henthorn et al., 1999). However, verapamil had no effect on fentanyl partitioning into lung (P_L). In contrast to fentanyl, loperamide P_L and P_B *increased* in the presence of verapamil (Table 3.3). Fentanyl and loperamide uptake into lungs and brains of Sprague Dawley rats occurred within 5 minutes (Figure 3.3 and 3.5), but the partitioning of fentanyl into brain was more extensive than that of loperamide (Table 3.3).

Previously, we showed that uptake of fentanyl in brain occurred via an unidentified inward transporter which was blocked by verapamil (Henthorn et al., 1999). Recently, organic anion transporter polypeptides (Oatp/OATP) were found in endothelial cells lining capillaries in the brain of rats and humans (Gao et al., 1999; Hagenbuch and Meier, 2003) and were reported to serve as inward transporters for the opioid deltorphin (Gao et al., 2000). A number of the Oatp/OATP transporters appear to have shared drug substrates with the efflux transporter P-gp, such as opioids (Gao et al., 2000; Cvetkovic et al., 1999). Fentanyl and verapamil are known substrates of the P-gp efflux transporter, yet the present study showed that verapamil decreased fentanyl partitioning in brain of rats suggesting that verapamil and fentanyl may be substrates of inward Oatp transporters in rat brain. Therefore, our data suggest that Oatp/OATP transporters may play a role in the uptake of fentanyl into brain. Further work is needed to establish whether or not one of the Oatp/OATP transporters, is responsible for fentanyl uptake into brain.

In contrast to results from human pulmonary artery endothelial cell culture indicating that verapamil decreased fentanyl uptake (Waters et al., 2000), our results showed that verapamil had no effect on fentanyl partitioning in Sprague Dawley rat lungs. Because P-gp inhibition by verapamil had no effect on lung partitioning, it is likely that P-gp does not play a role in the kinetics of first-pass pulmonary uptake of fentanyl in rats. Further research is needed to identify the inward transport mechanism responsible for fentanyl uptake in the lungs observed *in vivo*.

Loperamide, a μ-opioid agonist, was thought not to cross the blood-brain barrier and therefore lacked central effects after systemic administration (Nozaki-Taguchi and Yaksh, 1999). In contrast, we showed that following intravenous administration, loperamide demonstrated rapid uptake into Sprague Dawley rat brains (Figure 3.4). However, our data indicating that P-gp inhibition by verapamil increased loperamide partitioning in the brain, are supported by previous research indicating that administration of quinidine, a P-gp substrate, with loperamide resulted in an opioid central effect (Sadeque et al., 2000).

P-gp efficiently extrudes loperamide from brain and lung (Schinkel et al., 1996; Ayrton and Morgan, 2001; Dagenais et al., 2004). We have demonstrated that in the presence of the P-gp inhibitor verapamil there was a greater than 5.27-fold increase in pulmonary uptake of loperamide, and a 1.8-fold increase in brain uptake. These data suggest that P-gp plays an important role in the pulmonary uptake kinetics for loperamide. Further

research is necessary to determine if the inhibition of P-gp resulting in elevated brain partitioning of loperamide is sufficient to produce a central effect.

As reported in the results, the model predicted partitioning estimates did not characterize loperamide tissue partitioning. This indicates that loperamide tissue uptake and equilibration is slower than fentanyl and loperamide when P-gp is blocked. Full characterization of loperamide partitioning in tissue require longer and more frequent blood and tissue sampling.

In conclusion, our results indicate that loperamide crosses the blood-brain barrier following systemic administration. Further, verapamil, known inhibitor of the P-gp efflux transporter, accordingly increased loperamide partitioning, but decreased fentanyl partitioning into brain, *in vivo*, suggesting that verapamil and fentanyl may be substrates of both inward and outward transporters.

Table 3.1. Akiake information criterion (AIC) for pharmacokinetic models of study drug alone (control) and with verapamil

Fentanyl	*Model 1* Control plasma	*Model 2* CL_E	*Model 3** CL_E+V_1	*Model 4* $CL_E+V_1+V_2$	*Model 5* Control plasma+ lung +brain	*Model 6** P_B	*Model 7* P_{B+} P_L
AIC	3.6635 $x10^{-3}$	3.597 $x10^{-3}$	3.585 $x10^{-3}$	3.595 $x10^{-3}$	2.709 $x10^{-3}$	2.660 $x10^{-3}$	2.663 $x10^{-3}$

* Models selected for fentanyl.
Cl_E = elimination clearance
V_1 and V_2 = volumes of rapidly equilibrating and slowly equilibrating compartments respectively
P_B = plasma: brain partition coefficient
P_L = plasma: lung partition coefficient

Table 3.2. Akiake information criterion (AIC) for pharmacokinetic models of study drug alone (control) and with verapamil.

Loperamide	*Model 1* Control plasma	*Model 2* CL_E	*Model 3* CL_E+V_1	*Model 4†* CL_E+V_2	*Model 5* $CL_E+V_1+V_2$	*Model 6* Control plasma+ lung +brain	*Model 7* P_B	*Model 8†* P_B, P_L
AIC	6.762 $x10^{-3}$	6.607 $x10^{-3}$	6.621 $x10^{-3}$	6.577 $X10^{-3}$	6.598 $x10^{-3}$	6.003 $x10^{-3}$	5.988 $x10^{-3}$	5.951 $x10^{-3}$

† Model selected for loperamide
Cl_E = elimination clearance
V_1 and V_2 = volumes of rapidly equilibrating and slowly equilibrating compartments respectively
P_B = plasma: brain partition coefficient
P_L = plasma: lung partition coefficient

Table 3.3. Pharmacokinetic variables for fentanyl and loperamide in the absence and presence of verapamil (n = 4), using data from models described in Tables 3.1 and 3.2

Treatment	P_B	P_L	Cl_E ml/kg/min	V_1 ml	V_2 ml
Fentanyl	0.1424	0.3672	0.0866	0.3403	1.9425
Fentanyl + Verapamil	0.0818	0.3672	0.1069	0.768	1.9425
Loperamide	0.0057	1.0897	0.000973	0.1010	0.0177
Loperamide + Verapamil	0.0103	5.7432	0.000491	0.1010	0.0335

P_B = plasma: brain partition coefficient
P_L = plasma: lung partition coefficient
Cl_E = elimination clearance
V_1 and V_2 = volumes of rapidly equilibrating and slowly equilibrating compartments respectively

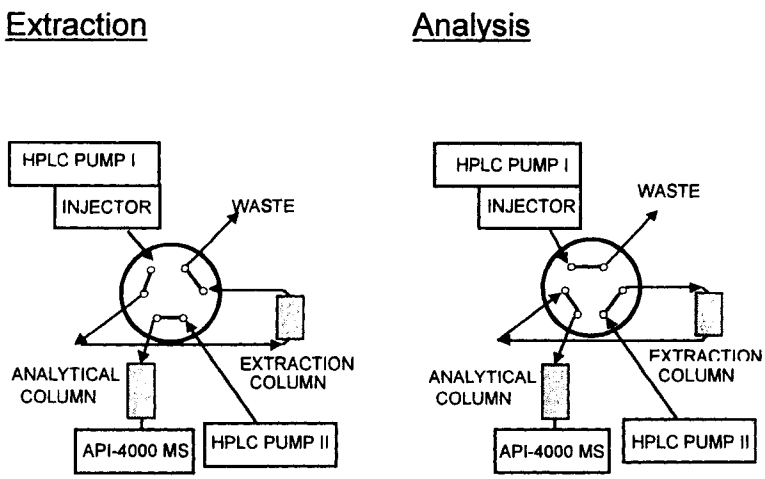

Figure 3.1. Connections and solvent flow of the HPLC switching valve.

A

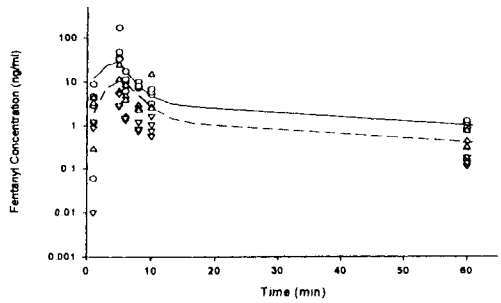

B

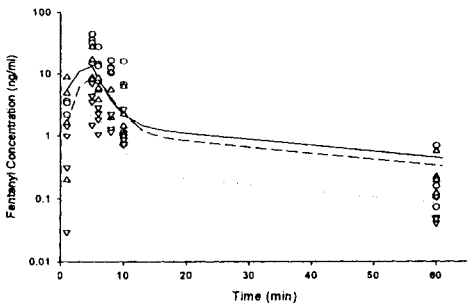

Figure 3.2. Fentanyl concentration in Sprague-Dawley rats arterial plasma, lung, and brain in absence of verapamil (A) and in the presence of verapamil (B). The symbols represent measured drug concentrations, whereas the lines represent concentrations predicted by the model. Predicted plasma drug concentrations (solid line), measured plasma drug concentration (circle), predicted lung drug concentrations (dashed line), measured lung drug concentration (triangle up), predicted brain drug concentration (dotted line), measured brain concentration (triangle down).

A

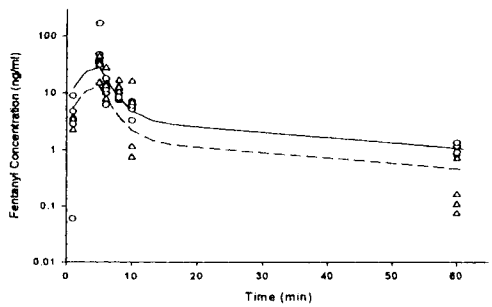

B.

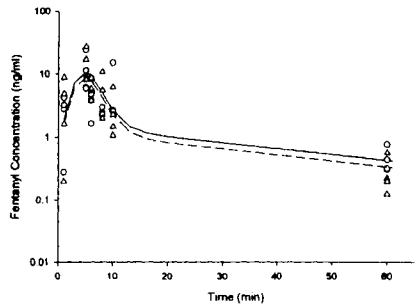

C

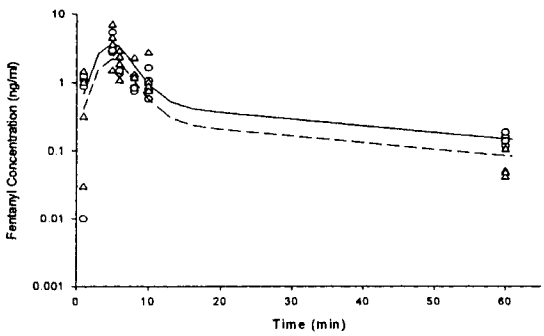

Figure 3.3. Fentanyl concentration in Sprague-Dawley rats arterial plasma (A), lung (B), and brain (C) in the absence and presence of verapamil. The symbols represent measured drug concentrations, whereas the lines represent concentrations predicted by the model. Predicted drug concentrations in absence of verapamil (solid line), measured drug concentration in absence of verapamil (circle), predicted drug concentrations in presence of verapamil (dashed line), measured drug concentrations in presence of verapamil (triangle).

A

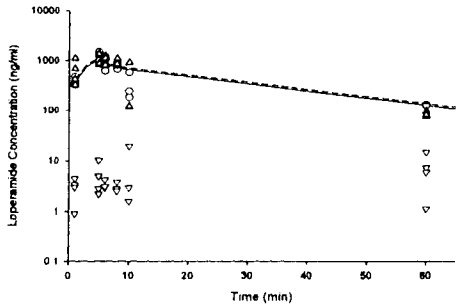

B

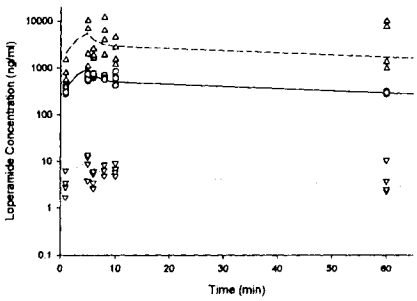

Figure 3.4. Loperamide concentration in Sprague-Dawley rats arterial plasma, lung, and brain in the absence (A) and presence (B) of verapamil. The symbols represent measured drug concentrations, whereas the lines represent concentrations predicted by the model. Predicted plasma drug concentrations (solid line), measured plasma drug concentration (circle), predicted lung drug concentrations (dashed line), measured lung drug concentration (triangle up), predicted brain drug concentration (dotted line), measured brain concentration (triangle down).

A

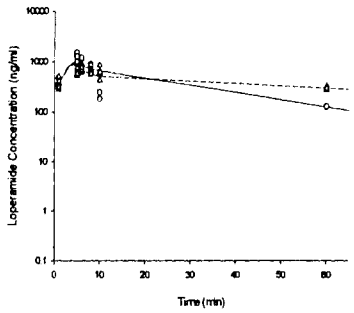

B.

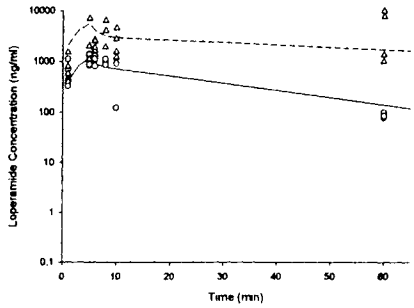

C

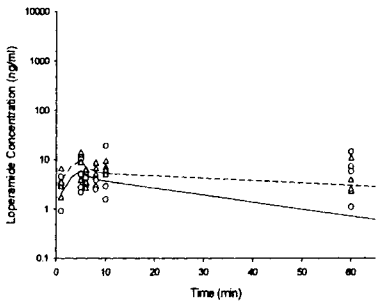

Figure 3.5. Loperamide concentration in Sprague-Dawley rats arterial plasma (A), lung (B), and brain (C) in the absence and presence of verapamil. The symbols represent measured drug concentrations, whereas the lines represent concentrations predicted by the model. Predicted drug concentrations in absence of verapamil (solid line), measured drug concentration in absence of verapamil (circle), predicted drug concentrations in presence of verapamil (dashed line), measured drug concentration in presence of verapamil (triangle).

REFERENCES

Ayrton A and Morgan P (2001) Role of transport proteins in drug absorption, distribution and excretion. *Xenobiotica* **31**:469-497.

Ball C and Westhorpe R (2002) Intravenous induction agents: opioids. *Anaesthesia & Intensive Care* **30**:717.

Bhatti MM and Foster RT (1997) Pharmacokinetics of the enantiomers of verapamil after intravenous and oral administration of racemic verapamil in a rat model. *Biopharmaceutics & Drug Disposition* **18**:387-396.

Bjorkman S, Wada DR, Stanski DR and Ebling WF (1994) Comparative physiological pharmacokinetics of fentanyl and alfentanil in rats and humans based on parametric single-tissue models.[erratum appears in J Pharmacokinet Biopharm 1995 Aug;23(4):438]. *Journal of Pharmacokinetics & Biopharmaceutics* **22**:381-410.

Cvetkovic M, Leake B, Fromm MF, Wilkinson GR and Kim RB (1999) OATP and P-glycoprotein transporters mediate the cellular uptake and excretion of fexofenadine. *Drug Metabolism & Disposition* **27**:866-871.

Dagenais C, Graff CL and Pollack GM (2004) Variable modulation of opioid brain uptake by P-glycoprotein in mice. *Biochemical Pharmacology* **67**:269-276.

Gao B, Hagenbuch B, Kullak-Ublick GA, Benke D, Aguzzi A and Meier PJ (2000) Organic anion-transporting polypeptides mediate transport of opioid peptides across blood-brain barrier. *Journal of Pharmacology & Experimental Therapeutics* **294**:73-79.

Gao B, Stieger B, Noe B, Fritschy JM and Meier PJ (1999) Localization of the organic anion transporting polypeptide 2 (Oatp2) in capillary endothelium and choroid plexus epithelium of rat brain. *Journal of Histochemistry & Cytochemistry* **47**:1255-1264.

Gustafsson LL, Ebling WF, Osaki E, Harapat S, Stanski DR and Shafer SL (1992) Plasma concentration clamping in the rat using a computer-controlled infusion pump. *Pharmaceutical Research* **9**:800-807.

Hagenbuch B and Meier PJ (2003) The superfamily of organic anion transporting polypeptides. *Biochimica et Biophysica Acta* **1609**:1-18.

Heel RC, Brogden RN, Speight TM and Avery GS (1978) Loperamide: a review of its pharmacological properties and therapeutic efficacy in diarrhoea. *Drugs* **15**:33-52.

Henthorn TK, Krejcie TC, Avram MJ, Jensen TR and Waters CM (1998) Transporter-mediated pulmonary endothelial uptake of fentanyl. *International Journal of Clinical Pharmacology & Therapeutics* **36**:74-75.

Henthorn TK, Liu Y, Mahapatro M and Ng KY (1999) Active transport of fentanyl by the blood-brain barrier. *Journal of Pharmacology & Experimental Therapeutics* **289**:1084-1089.

Heykants J, Michiels M, Knaeps A and Brugmans J (1974) Loperamide (R 18 553), a novel type of antidiarrheal agent. Part 5: the pharmacokinetics of loperamide in rats and man. *Arzneimittel-Forschung* **24**:1649-1653.

Ludden TM, Beal SL and Sheiner LB (1994) Comparison of the Akaike Information Criterion, the Schwarz criterion and the F test as guides to model selection. *Journal of Pharmacokinetics & Biopharmaceutics* **22**:431-445.

Nozaki-Taguchi N and Yaksh TL (1999) Characterization of the antihyperalgesic action of a novel peripheral mu-opioid receptor agonist--loperamide. *Anesthesiology* **90**:225-234.

Roerig DL, Ahlf SB, Dawson CA, Linehan JH and Kampine JP (1994) First pass uptake in the human lung of drugs used during anesthesia. *Advances in Pharmacology* **31**:531-549.

Sadeque AJ, Wandel C, He H, Shah S and Wood AJ (2000) Increased drug delivery to the brain by P-glycoprotein inhibition. *Clinical Pharmacology & Therapeutics* **68**:231-237.

Schinkel AH, Wagenaar E, Mol CA and van Deemter L (1996) P-glycoprotein in the blood-brain barrier of mice influences the brain penetration and pharmacological activity of many drugs. *Journal of Clinical Investigation* **97**:2517-2524.

Stanley TH (1992) The history and development of the fentanyl series. *Journal of Pain & Symptom Management* **7**:S3-7.

Stanley TH (2005) Fentanyl. *Journal of Pain & Symptom Management* **29**:S67-71.

Waters CM, Avram MJ, Krejcie TC and Henthorn TK (1999) Uptake of fentanyl in pulmonary endothelium. *Journal of Pharmacology & Experimental Therapeutics* **288**:157-163.

Waters CM, Krejcie TC and Avram MJ (2000) Facilitated uptake of fentanyl, but not alfentanil, by human pulmonary endothelial cells. *Anesthesiology* **93**:825-831.

CHAPTER 4

Pharmacokinetic, pharmacodynamic modeling of the electroencephalogram effect of fentanyl and loperamide: Contrasting roles of P-glycoprotein inhibitor, verapamil.

Iman A. Elkiweri, Martha C. Tissot van Patot, Uwe Christians and Thomas K. Henthorn

Department of Anesthesiology, University of Colorado Denver Health Sciences Center, Denver, Colorado (IAE, MCTvP, UC, TKH), Department of Biomedical Sciences, Colorado State University, Fort Collins, Colorado (IAE)

Supported by grant No. R01- GM47502.09 from the National Institutes of Health and in part by the Nema Foundation, Malaysia.

Fentanyl is a widely used, potent, synthetic opioid analgesic that was introduced into clinical practice in the early 1960s and represented a major increase in potency in comparison with clinically important opiate agonists of the time. It acts at the μ-opioid receptor and is used as an analgesic to supplement general anesthesia for various surgical procedures or as a primary anesthetic agent in very high doses during cardiac surgery (Stanley, 1992; Ball and Westhorpe, 2002; Stanley, 2005). We have recently demonstrated *in vitro* that fentanyl is transported into the brain by a saturable energy-dependent process, in contrast to the widely held belief that fentanyl was passively transported as a result of its lipid solubility. This data opened the potential to develop therapies to control opioid central activity.

We further demonstrated that verapamil inhibited fentanyl active uptake by brain endothelium, despite its well-recognized role as an inhibitor of the outward transporter, P-glycoprotein (P-gp) (Henthorn et al., 1999). Other opioids are strong P-gp substrates and in contrast to fentanyl, inhibition of the P-gp transporter by verapamil may increase their central effect. Loperamide is one such opioid (Dagenais et al., 2004) that is widely used for treatment of diarrhea, as it primarily acts through activation of opioid receptors in the intestinal tract (Heykants et al., 1974; Heel et al., 1978). Therapeutics designed to inhibit P-gp transport may have variable effects on opioid intrinsic brain activity, depending on the opioid administered.

Therefore, we hypothesized that verapamil would have a variable effect on intrinsic brain activity when co-administered with fentanyl in comparison to loperamide. Quantative

electroencephalogram (EEG) monitoring has been used successfully to characterize the time course of opioid pharmacological actions after intravenous administration of anesthetic doses. By application of pharmacokinetic-pharmacodynamic modeling it was demonstrated that the value of certain EEG parameters can be directly related to the concentration at a hypothetical effect site on the basis of the sigmoidal E_{max} pharmacodynamic model (Scott et al., 1985; Scott et al., 1991). We continuously measured a processed EEG signal in rats on occasions when animals are not pretreated (fentanyl or loperamide only) or pretreated with verapamil.

Materials and Methods

Materials. Miniature screws for skull purchased from Small Parts, Inc (Miami Lake, Fl, USA) and solder gun from Radio Shack (Denver, Co, USA). Electroencephalogram (EEG) transmitters (CTA-F40), receivers, and telemetry system purchased from Data Sciences International (Arden Hills, MN, USA). Dental acrylic powder purchased from Stoelting Co (Wood Dale, Illinois, USA). Fentanyl citrate purchased from Abbott Laboratories (North Chicago, IL, USA) and loperamide hydrochloride obtained from Sigma Aldrich Inc. (St Louis, MO, USA). Verapamil hydrochloride purchased from Abbott Laboratories (North Chicago, IL, USA).

Animals. Male Sprague-Dawley rats weighing 300-350 g were purchased from Harlan (Madison, Wisconsin) with indwelling cannulae (jugular venous catheters for drug infusion and a carotid artery catheter for blood collection). The rats were housed in the University of Colorado Health Sciences Center animal facility. They were kept on a 12-hour light/dark cycle and were fed standard laboratory chow, and experiments were

carried out according to the guidelines provided by Institutional Animal Care and Use Committee (University of Colorado Health Sciences Center).

Preparing transmitters. One day prior to surgery, one centimeter of transmitter wire (Figure 4.1C) on each lead was exposed by cutting off the surrounding teflon using razor blade. The end of the coiled wire was stretched to form a loop to accommodate the screw. The screw and wire were placed in contact with a preheated soldering iron and thus soldered and secured both mechanically and electrically.

Surgery. On the day of the surgery animals were given 75 mg of ketamine hydrochloride and 15 mg of xylazine hydrochloride per kg body weight, intraperitoneally. The animal was placed in a stereotaxic apparatus (Stoelting Co, Wood Dale, Illinois, USA) and a straight midline skin incision was made from the bridge of the nose to halfway down the neck. The skin was held at four "corner positions" by the weight of "bulldog" vascular clamps attached to the edge of the skin and draped along the side of the head. The fascia and muscle insertions were displaced from the skull surface by blunt probing with cotton-tipped applicators. Once the entire top surface of the skull and both lateral ridges were exposed, a small amount of hydrogen peroxide (30%) was applied to lift any remaining surface tissue, rinsed with 70% isopropyl alcohol and dried with cotton-tipped applicators, leaving a clean, dry and porous surface on the skull. The skull sutures became prominent as white irregular lines tracing a midline and two transverse gridlines (bregma and lambda). Two holes were drilled in the skull, 2 mm on either side of midline and 2 mm anterior to the bregma suture, using a dremel tool with a 1/8 inch bit, as shown in Figure 4.1A. The holes were drilled through the skull, and care was taken to avoid injuring the underlying dura and brain tissue. The skin dorsal to the neck was bluntly

dissected forming a subcutaneous pouch just large enough for the placement of the transmitter (Figure 4.1B). Once the bone was totally dry the screws soldered to the end of the transmitter leads were placed into the holes. A small amount of dental acrylic cement was applied to seal the holes and fix the screws in place. The excess wire was placed under the skin. The wound was sutured shut with 3.0 silk and bacitracin was applied to the wound.

Experiment. One day after surgery, EEG signals were recorded. The rats and their respective transmitters and receivers were entered into the telemetry system (Figure 1D). Signals were recorded for fifteen minutes to establish a baseline EEG before start of opioid infusion. Signals were continuously recorded for sixty minutes after the start of drug infusion. EEG signals were captured, low and high filters were set at 0.5 and 100 Hz respectively and immediately recorded with model A 1000 spectral EEG monitor coupled to Data logger with EEG data handling software (Data Sciences International, Arden Hills, MN, USA) for offline analysis. The delta wave was then extracted from the raw data using Brain Vision Analyzer Software, Brain Product GmbH, München, Germany.

Infusions. The animals received a five-minute (from time t = 0 to 5 minutes) intravenous infusion of fentanyl citrate (5.25 μg/kg/min) or loperamide hydrochloride (0.95 or 0.475 mg/kg/min). On a separate occasion, a target-controlled infusion (TCI) of verapamil hydrochloride was administered for five minutes at a target concentration of 1 mg/ml prior to the opioid infusion and continued ten minutes after the opioid infusion (from time t = -5 to 10). The TCI was accomplished using a Harvard 22 syringe pump (Harvard Apparatus, Holliston, Massachusetts), controlled via a serial connection to a Pentium-based computer running the TCI software STANPUMP (written by Steven L. Shafer,

MD) and using a 3-compartment pharmacokinetic model for verapamil derived from a one compartment rat verapamil model and a similar 3-compartmental model for thiopental in the rat.

Results.

Effect of verapamil on fentanyl effect site concentration and EEG effect. A sigmoid E_{max} pharmacodynamic model was used to describe the relationship between effect site drug concentration and EEG effect: $E_C = E_0 + \frac{E_{max} \bullet C^s}{EC^s_{50} + C^s}$ (Figure 4.2A& B), as previously reported (Minto et al., 2003). In which E_C is the EEG effect at drug effect site concentration C, E_0 is the no-drug effect, E_{max} is the intrinsic activity maximum effect, EC_{50} is the drug concentration at 50% maximum effect, and s is the Hill coefficient, which was fixed (Ebling et al., 1990). The parameters of this model (volumes and clearances) were analyzed across treatments with covariates for the presence of verapamil. This model, coupled with the equilibration rate (k_{e0}) will yield estimates of effect site concentrations that would be proportional to blood concentrations at steady state. Results using the model described above indicated that verapamil decreased E_{max} by 42%, and increased EC_{50} and k_{e0} by 74% and 80% respectively (Table 4.1).

Effect of verapamil on loperamide effect site concentration and EEG effect. The pharmacodynamic model described above was also used to describe the relationship between effect site loperamide concentration and EEG effect (Figure 4.3A, B, C &D). In the presence of verapamil E_{max} increased by 142%, however EC_{50} and k_{e0} decreased by 44% and 60% respectively (Table 4.2).

Discussion.

Our results indicated that verapamil decreased fentanyl brain distribution volume, and hence EC_{50} was greater and E_{max} decreased (Table 4.1) suggesting that less fentanyl was in the CNS at any given steady-state blood concentration. However, in the presence of verapamil, a potent P-gp inhibitor, loperamide brain distribution volume increased resulting in a smaller EC_{50} and a greater E_{max} (Table 4.2) suggesting that P-gp inhibition allowed increased access of loperamide to the brain. Time to maximal EEG effect was faster for fentanyl and slower for loperamide when verapamil was present.

These results support our previous results which showed that *in vivo* the uptake of fentanyl in brain occurred via an unidentified inward transporter which was blocked by verapamil (Henthorn et al., 1999). Organic anion transporter polypeptides (Oatp/OATP) were found in endothelial cells lining capillaries in the brain rats and humans (Gao et al., 1999; Hagenbuch and Meier, 2003) and were reported to serve as inward transporters for the opioid deltorphin (Gao et al., 2000). Verapamil and fentanyl are substrates of the efflux transporter P-gp which appear to have shared drug substrates with a number of the Oatp/OATP transporters. The present study showed that less fentanyl was in the CNS at any given steady-state blood concentration suggesting that verapamil and fentanyl may be substrates of inward Oatp transporters in rat brain. Therefore, our data suggest that Oatp/OATP transporters may play a role in the uptake of fentanyl in brain. Further work is needed to establish whether or not one of the Oatp/OATP transporters, is responsible for fentanyl uptake in brain.

Loperamide, a μ-opioid agonist, was thought not to cross the blood-brain barrier and therefore lacked central effects after systemic administration (Nozaki-Taguchi and Yaksh, 1999). In contrast, we showed that following intravenous administration, loperamide elicited EEG effect in Sprague Dawley rat (Figure 4.3). However, our data indicating that P-gp inhibition by verapamil increased loperamide access into the EEG effect site (Table 4.2), are supported by previous research indicating that administration of quinidine, a P-gp substrate, with loperamide resulted in an opioid central effect (Sadeque et al., 2000).

Because of loperamide's handling by P-gp at the blood-brain barrier, P-gp inhibition by verapamil allowed increased access of loperamide to the brain resulting in increased E_{max} and decreased EC_{50}. The EC_{50} is smaller because more loperamide is in the CNS at any given steady-state blood concentration, not because of changed neural effects such as opioid receptor binding.

In conclusion, our results indicate that loperamide crosses the blood-brain barrier following systemic administration. Further, verapamil, inhibition of P-gp efflux transporter, increased loperamide concentration and intrinsic activity in the brain at any given steady-state blood concentration, but reduced fentanyl concentration and intrinsic activity in the brain at any given steady-state blood concentration, *in vivo*. These data suggest that P-gp efflux play an important role in loperamide transport in rat brain but not fentanyl transport and that verapamil and fentanyl may be substrates of both inward and outward transporters.

Table 4.1. Fentanyl concentration at 50% maximum effect (EC_{50}) and maximum effect (E_{max}) n=2.

Treatment	**EC_{50}** ng/ml	**k_{e0}** ml/kg/min	**T_{max}** Min	**E_{max} (Rat 1)**	**E_{max} (Rat 2)**
Fentanyl	14.035	0.335	1.32	35.75	181.83
Fentanyl+ Verapamil	24.435	0.626	0.27	20.45	104.01

EC_{50} is the drug concentration at 50% maximum effect.
E_{max} is the maximum effect.
k_{e0} is the equilibration rate effect
T_{max} is the time to maximal effect

Table 4.2. Loperamide concentration at 50% maximum effect (EC_{50}) and maximum effect (E_{max}) n=4.

Treatment	EC_{50} ng/ml	k_{e0} ml/kg/min	T_{max} min	E_{max} (Rat 1)	E_{max} (Rat 2)	E_{max} (Rat 3)	E_{max} (Rat 4)
Loperamide	116.67	1.562	1.07	34.38	101.17	86.90	44.88
Loperamide+ Verapamil	64.52	0.618	1.84	83.54	245.84	211.67	109.06

EC_{50} is the drug concentration at 50% maximum effect.
E_{max} is the maximum effect.
k_{e0} is the equilibration rate effect
T_{max} is the time to maximal effect

A. B.

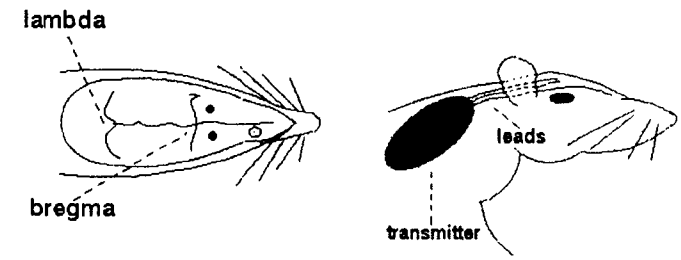

C.

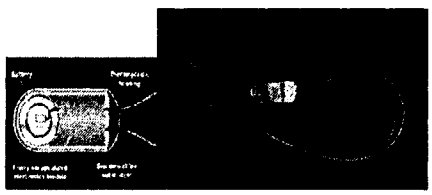

D.

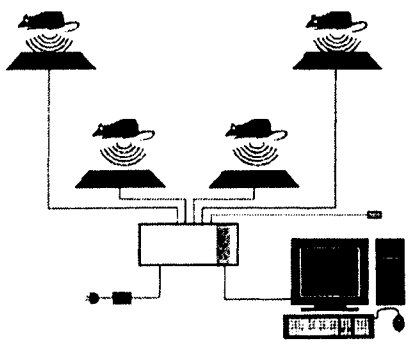

Figure 4.1. (A) Sites of screw placement in rat skull. (B) Transmitter placed in subcutaneous pouch. (C) Transmitter. (D) Telemetry system (from Data Sciences International at www.dsci.com).

A.

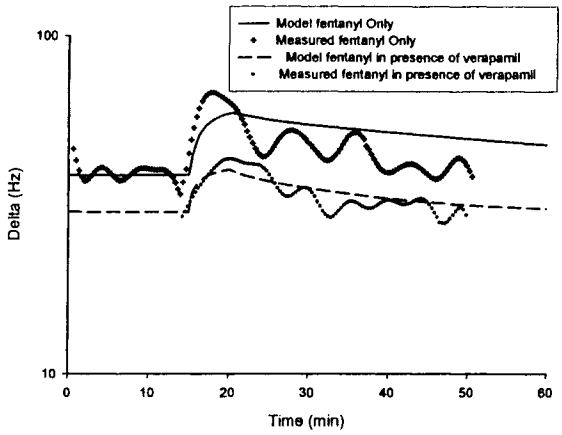

B.

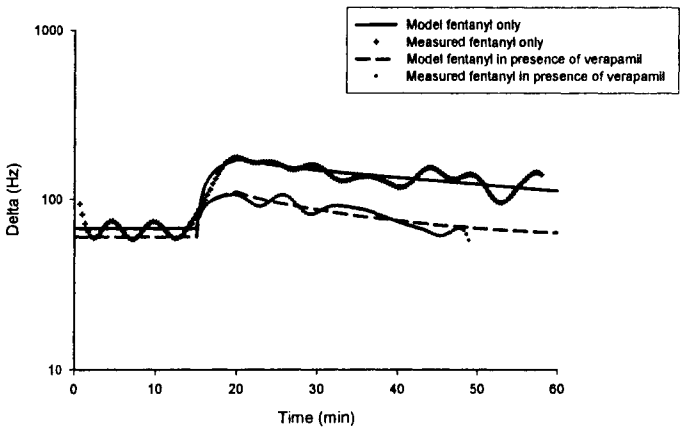

Figure 4.2. Fentanyl EEG effect in the absence and presence of verapamil in Sprague Dawley rats. Rat 1(A) and rat 2 (B).

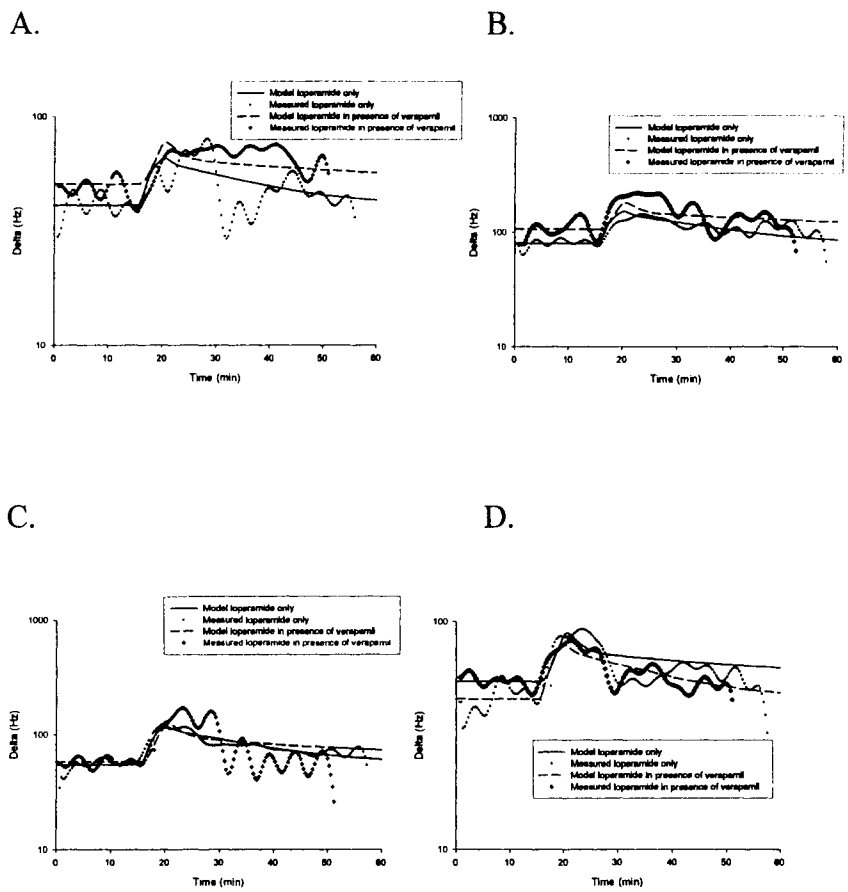

Figure 4.3. Loperamide EEG effect in the absence and presence of verapamil in Sprague Dawley rats. Rat 1(A), rat 2 (B), rat 3 (C) and rat 4 (D).

REFERNCES

Ball C and Westhorpe R (2002) Intravenous induction agents: opioids. *Anaesthesia & Intensive Care* **30**:717.

Dagenais C, Graff CL and Pollack GM (2004) Variable modulation of opioid brain uptake by P-glycoprotein in mice. *Biochemical Pharmacology* **67**:269-276.

Ebling WF, Lee EN and Stanski DR (1990) Understanding pharmacokinetics and pharmacodynamics through computer stimulation: I. The comparative clinical profiles of fentanyl and alfentanil. *Anesthesiology* **72**:650-658.

Gao B, Hagenbuch B, Kullak-Ublick GA, Benke D, Aguzzi A and Meier PJ (2000) Organic anion-transporting polypeptides mediate transport of opioid peptides across blood-brain barrier. *Journal of Pharmacology & Experimental Therapeutics* **294**:73-79.

Gao B, Stieger B, Noe B, Fritschy JM and Meier PJ (1999) Localization of the organic anion transporting polypeptide 2 (Oatp2) in capillary endothelium and choroid plexus epithelium of rat brain. *Journal of Histochemistry & Cytochemistry* **47**:1255-1264.

Hagenbuch B and Meier PJ (2003) The superfamily of organic anion transporting polypeptides. *Biochimica et Biophysica Acta* **1609**:1-18.

Heel RC, Brogden RN, Speight TM and Avery GS (1978) Loperamide: a review of its pharmacological properties and therapeutic efficacy in diarrhoea. *Drugs* **15**:33-52.

Henthorn TK, Liu Y, Mahapatro M and Ng KY (1999) Active transport of fentanyl by the blood-brain barrier. *Journal of Pharmacology & Experimental Therapeutics* **289**:1084-1089.

Heykants J, Michiels M, Knaeps A and Brugmans J (1974) Loperamide (R 18 553), a novel type of antidiarrheal agent. Part 5: the pharmacokinetics of loperamide in rats and man. *Arzneimittel-Forschung* **24**:1649-1653.

Minto CF, Schnider TW, Gregg KM, Henthorn TK and Shafer SL (2003) Using the time of maximum effect site concentration to combine pharmacokinetics and pharmacodynamics.[see comment]. *Anesthesiology* **99**:324-333.

Nozaki-Taguchi N and Yaksh TL (1999) Characterization of the antihyperalgesic action of a novel peripheral mu-opioid receptor agonist--loperamide. *Anesthesiology* **90**:225-234.

Sadeque AJ, Wandel C, He H, Shah S and Wood AJ (2000) Increased drug delivery to the brain by P-glycoprotein inhibition. *Clinical Pharmacology & Therapeutics* **68**:231-237.

Scott JC, Cooke JE and Stanski DR (1991) Electroencephalographic quantitation of opioid effect: comparative pharmacodynamics of fentanyl and sufentanil. *Anesthesiology* **74**:34-42.

Scott JC, Ponganis KV and Stanski DR (1985) EEG quantitation of narcotic effect: the comparative pharmacodynamics of fentanyl and alfentanil. *Anesthesiology* **62**:234-241.

Stanley TH (1992) The history and development of the fentanyl series. *Journal of Pain & Symptom Management* **7**:S3-7.

Stanley TH (2005) Fentanyl. *Journal of Pain & Symptom Management* **29**:S67-71.

CHAPTER 5

The effect of loperamide and fentanyl on the distribution kinetics of verapamil to lung and brain in Sprague Dawley rats.

Iman A. Elkiweri, M.S., £* Martha C. Tissot van Patot, Ph.D., † Yan Ling Zhang, Ph.D., ‡ Uwe Christians, Ph.D., § and Thomas K. Henthorn, M.D., ¥

*Research Associate, †Assistant Professor, ‡Research Associate, §Associate Professor, ¥Chairman and Professor, Department of Anesthesiology, University of Colorado Denver Health Sciences Center, Denver, Colorado, £ Graduate student, Department of Biomedical Sciences, Colorado State University, Fort Collins, Colorado.

Supported by grant No. R01- GM47502.09 from the National Institutes of Health and in part by the Nema Foundation, Malaysia.

Verapamil, a phenylalkylamine calcium channel antagonist, is widely used for the treatment of various cardiovascular disorders. Following intravenous bolus administration verapamil undergoes significant pulmonary uptake in human lung with about 50% of the drug accumulating in lung tissue during the first pass (Roerig et al., 1989). Many basic lipophilic amines such as the opioid analgesic fentanyl (Roerig et al., 1987; Taeger et al., 1988) are known to have significant, reversible, pulmonary uptake following intravenous administration. This extensive first-pass uptake of verapamil and fentanyl has been thought to be due to the high lipid solubility of the drugs. However, pulmonary uptake of the opioid analgesic fentanyl has been recently shown to be the result of a saturable specific uptake mechanism that is blocked by verapamil (Henthorn et al., 1998; Waters et al., 1999; Waters et al., 2000). Further, we have demonstrated that cultured bovine brain micro vascular endothelial cells also have a saturable energy-dependent process mediating uptake of fentanyl perhaps by an unidentified inward transporter that is inhibited by verapamil (Henthorn et al., 1999).

Verapamil is also a substrate/inhibitor of the efflux transporter P-glycoprotein (P-gp) and has been used in many clinical trials to facilitate transport of anticancer drugs across the blood brain barrier, which would otherwise be effluxed by P-gp. Recently we discovered that *in vivo*, verapamil inhibits fentanyl uptake in the brain, but inhibits efflux of another P-gp mediated opioid, loperamide (unpublished observations). Because of the varying effect of verapamil on opioid transport, we hypothesized that fentanyl would reduce verapamil uptake in lung and brain, but loperamide, as a P-gp substrate, would reduce clearance of verapamil in the lung and brain. Therefore, we studied lung and brain

uptake, distribution and elimination of verapamil in the presence and absence of fentanyl and loperamide in Sprague Dawley rats.

Methods

Experimental Protocol

After Institutional Animal Care and Use Committee approval, adult male Sprague-Dawley rats weighing 300-350 g were purchased with indwelling cannulae (jugular venous catheters for drug infusion and a carotid artery catheter for blood collection) from Harlan (Madison Wisconsin). The rats were housed in the UCHSC animal facility. They were kept on a 12-hour light/dark cycle and were fed standard laboratory chow. A target concentration controlled infusion of verapamil hydrochloride (Abbott Laboratories, North Chicago, IL) was administered for five minutes at a target concentration of 1 mg/mL prior to initiation of opioid infusion and was continued for ten minutes (from time t = -5 to 10 min). The initiation of opioid infusion was defined as time 0 min of the experiment. Verapamil and opioids were infused *via* the jugular venous catheter. Target concentration controlled infusion was accomplished using a Harvard 22 syringe pump (Harvard Apparatus, Holliston, Massachusetts) that was controlled *via* a serial interface by a personal computer running the STANPUMP target concentration controlled infusion software (written by Dr. S.L. Shafer). The infusion software was assuming a 3-compartment pharmacokinetic model for verapamil (Gustafsson et al., 1992; Bhatti and Foster, 1997). The animals received a 5-min intravenous infusion (from time t = 0 to 5 minutes) of either fentanyl citrate (Abbott Laboratories, North Chicago, IL) using an infusion rate of 5.25 μg/kg/min) or loperamide hydrochloride (Sigma Aldrich, St. Louis, MO) using an infusion rate of 0.475 mg/kg/min. Rats were euthanized by decapitation at -5, 5, 6, 8, 10, or 60 min (n = 4 per time point). Blood (5 mL) was collected from the

carotid catheter prior to decapitation and drawn into tubes containing citrate as anticoagulant. Plasma was separated following a standard centrifugation protocol (400 g, 10 min, 4°C). The skull was opened immediately after decapitation; brain tissue was collected and was flash-frozen in liquid nitrogen. Hereafter, a thoracotomy was performed to collect lung tissues that also were immediately frozen in liquid nitrogen. Plasma, lung, and brain tissues were stored at –80°C until analysis of drug concentrations using a validated high-performance liquid chromatography/ tandem mass spectrometry (LC-MS/MS) assay.

Analytical Methods

Prior to LC-MS/MS analysis, rat brain and lung (approximately 10 mg) were weighed and homogenized with 2 mL KH_2PO_4 buffer pH = 7.4 (1M) using a teflon-glass manual homogenizer. Homogenized samples were stored at -80°C before analysis. On the day of analysis, plasma, homogenized brain or lung were thawed on ice. Four hundred µL of a precipitation solution consisting of 0.06 M $ZnSO_4$ solution and methanol (3:7, v/v) as well as 10 µL of the internal standard were added to 200 µL of plasma or tissue homogenates. (±)-Methoxy verapamil hydrochloride (Sigma Aldrich) was used as internal standard. The final concentration in the extracted samples was 50ng/mL. After vortexing for 2 min, samples were centrifuged (13000 g × 5 min, 4°C) to remove precipitated proteins. One hundred µL of the supernatant was directly injected into the HPLC system (series 1100, Agilent, Waldbronn, Germany) using a Leap autosampler (CTC Analytics AG, Zwingen, Switzerland) equipped with a cool stack. Extracted samples were kept at +4°C in the autosampler.

Supernatants were loaded onto an extraction column (4.6 × 12.5 mm, 5 μm particle size, Eclipse XDB-C8, Agilent) and were washed with a high flow of 5 mL/min, 80% 0.1% formic acid/ 20% methanol for 1 min. Then the switching valve was activated and the analytes were back-flushed onto a C8 analytical column (4.6 × 12.5 mm, 5 μm particle size, Eclipse XDB-C8, Agilent). A linear gradient was used for separation: methanol increased from 55% to 100% in 4 min and was kept at 100% methanol for 1 min. The flow rate was 1 mL/min. Column temperature was maintained at 40°C.

An MDS Sciex API4000 triple-stage quadrupole mass spectrometer (Applied Biosystems, Foster City, CA) was used as detector. The mass spectrometer as well as the HPLC was controlled and data was processed using the Analyst software (version 1.3., Applied Biosystems). The analytes eluted from the HPLC column into a turbo-ion spray source. Nitrogen was provided by a Zero Air Generator (Analytical Gas Systems) Nitrogen (>99.999% purity) was used as collision activated dissociation (CAD), spray and curtain gas. Positive ions were monitored using Multiple Reaction Monitoring (MRM). During assay development, MRM parameters for each analyte were adjusted by directly infusing verapamil or its internal standard solution (0.1 μg/ mL, 80% methanol/ 20% 0.1% formic acid) into the electrospray source using a syringe infusion pump ((KD Scientific, Holliston, MA). The following MRM parameters were found to give the best sensitivities: The source temperature was set to 480°C and the ion spray voltage was 5000V. Gases were adjusted to 20 for nebulizer gas, 15 for turbo gas, 15 for curtain gas and 8 for CAD gas (all arbitrary units as used in the Analyst software). The declustering potential was set to 50V. The dwell time for each transition was 200 ms. Data was

collected and the major product ion transitions were monitored: verapamil $m/z = 455.6 \rightarrow 165.6$ and $m/z = 485.6 \rightarrow 333.5$ for the internal standard (±)-methoxy verapamil.

Data Analysis. Pharmacokinetics were analyzed using the SAAM II software (SAAM Institute, Seattle, WA) using a naive pooled-data technique. Model parsimony was tested using the Akiake information criterion (AIC) (Ludden et al., 1994). The data from the verapamil infusion alone and verapamil infusion with either fentanyl or loperamide treatment where lumped into separate models with linked parameters. Plasma kinetics were modeled with a one-compartment open model in which volume of distribution (V_1) and elimination clearance (Cl_E) were fit to the plasma verapamil concentration-time data. Data fit with this model had a lower AIC than the two-compartment model.

To test the hypothesis that either fentanyl and loperamide affects the plasma pharmacokinetics of verapamil, all data were first fit to a unified pharmacokinetic model for verapamil alone and then each of the adjustable parameters (V_1, Cl_E) where fit so that each parameter could have a covariate parameter for the experimental condition in which either fentanyl or loperamide was infused. Whether a covariate for the fentanyl or loperamide condition produced a statistically significant change in the pharmacokinetic parameter was tested by comparing the AIC with the added covariate in the model versus the AIC in the simpler model without the covariate. The model with the lowest AIC was then chosen as shown in tables 5.1 and 5.2.

Lung and brain concentration-time data were modeled by adding partition coefficients, P_B and P_L, to describe the ratio between plasma verapamil concentrations and those in brain and lung, respectively. To test the hypothesis that either fentanyl or loperamide changes plasma: tissue partitioning in the brain and lung, all data were first fit to a unified

pharmacokinetic model for verapamil alone and then each of the plasma: tissue partition coefficients (P_B, P_L) where fit so that each coefficient could have a covariate parameter for the experimental condition in which either fentanyl or loperamide was infused. Whether a covariate for either fentanyl or loperamide condition produced a statistically significant change in the partition coefficient was tested by comparing the AIC with the added covariate in the model versus the AIC the simpler model without the covariate. Model 7 had the lowest AIC as shown in tables 5.1 .and 5.2.

Results

Effect of fentanyl on verapamil pharmacokinetics. Rat arterial plasma, lung and brain verapamil concentrations in the absence and presence of fentanyl versus time relations were well-characterized by the model from the moment of injection. Visual comparison of the measured and predicted verapamil concentration versus time relationships revealed no model misspecification (Figures 5.1 and 5.2).

The pharmacokinetic parameters of verapamil were described by a one-compartment model, with elimination clearance (Cl_E) from the central compartment, blood partition coefficients for lung (P_L), and brain (P_B) and volume of distribution (V_1). In the presence of the centrally acting opioid, fentanyl, the same one-compartment model applied but fentanyl covariates were added to the parameters (Table 5.1). The results indicated that fentanyl reduced verapamil V_1 and Cl_E by 69% and 43% respectively, had no effect on P_B and P_L *increased* by 15% (Table 5.3).

Effect of loperamide on verapamil pharmacokinetics. Rat arterial plasma, lung and brain verapamil concentration in the absence and presence of loperamide versus time relations

were well-characterized by the model from the moment of injection. Visual comparison of the measured and predicted verapamil concentration versus time relationships revealed no model misspecification (Figures 5.3 and 5.4).

The pharmacokinetic parameters of verapamil were described by a one-compartment model, with elimination clearance (Cl_E) from the central compartment, blood partition coefficients for brain (P_B) and lung (P_L), and volume of distribution (V_1) In the presence of the 'peripherally' acting opioid, loperamide, the same one-compartment model applied but loperamide covariates were added to the parameters (Table 5.2) . The results demonstrated that in the presence of loperamide, verapamil P_B and P_L increased by 3.7 and 1.6 fold respectively, and Cl_E and V_1were unchanged (Table 5.3).

Discussion

We wished to determine if fentanyl or loperamide altered brain or lung partitioning of verapamil *in vivo*. In addition, we wished to evaluate verapamil pharmacokinetics using a high-resolution recirculatory model to examine carefully any possible differences in disposition that could reasonably be attributed to the presence of the two opioids.

Our results indicated that fentanyl reduced verapamil V_1, Cl_E and increased P_L. Also, loperamide increased verapamil P_B and P_L. Essentially, in the presence of fentanyl, verapamil lung concentrations were slightly increased, while loperamide increased verapamil brain and lung concentrations.

In contrast to our hypothesis, fentanyl increased verapamil partitioning in the lung. Verapamil and fentanyl are known substrates of the P-gp efflux transporter (Henthorn et al., 1999), suggesting that in Sprague Dawley rats fentanyl inhibition of the outward P-gp

mediated transporter will increase lung verapamil concentration. The present study suggests that P-gp may play an important role in verapamil pulmonary uptake.

The efflux transporter, P-glycoprotein, efficiently extrudes loperamide from brain and lung (Schinkel et al., 1996; Ayrton and Morgan, 2001; Dagenais et al., 2004) and verapamil is a known substrate/competitive inhibitor of P-gp (Verschraagen et al., 1999; Ayrton and Morgan, 2001). Our data indicating that loperamide significantly increased verapamil partitioning in lung and brain, confirms findings of others that verapamil and loperamide are substrates of the outwardly directed P-gp. Further, we have demonstrated that in the presence of loperamide there was a 3.7-fold increase in brain uptake of verapamil, and a 1.6 -fold increase in brain uptake. These data suggest that P-gp plays an important role in the brain uptake kinetics for intravenous verapamil.

Because this study was designed to give opioids for five minutes only and to measure lung and brain concentrations at 1, 5, 6, 10, and 60 minutes, further research is needed in which opioids are administered continuously with verapamil for fifteen minutes. Also, a greater number of sampling points between 10 and 60 minutes are needed to clearly delineate the pharmacokinetics of these drug interactions.

In conclusion, fentanyl increased verapamil partitioning in lung, *in vivo*, and loperamide increased verapamil lung and brain partitioning. These observations suggest that fentanyl only blocks P-gp efflux in the lung, not brain and confirm that verapamil and loperamide are substrates of the efflux transporter P-gp in brain and lung.

Table 5.1. Akiake information criterion (AIC) for pharmacokinetic models of study drug alone (control) and with fentanyl.

Verapamil + Fentanyl	***Model 1*** Control plasma	***Model 2*** CL_E	***Model 3**** $CL_E + V_1$	***Model 4*** Control plasma+ lung +brain	***Model 5*** P_B	***Model 7**** P_{B+} P_L
AIC	3.08 X 10^{-3}	1.6103 X 10^{-3}	1.548 X 10^{-3}	5.437 X 10^{-3}	5.424 X 10^{-3}	5.408 X 10^{-3}

* Model selected for verapamil in presence of fentanyl
Cl_E = elimination clearance
V_1 = volume of distribution
P_B = plasma: brain partition coefficient
P_L = plasma: lung partition coefficient

Table 5.2. Akiake information criterion (AIC) for pharmacokinetic models of study drug alone (control) and with loperamide.

Verapamil + loperamide	***Model 1*** Control plasma	***Model 2*** CL_E	***Model 3†*** $CL_E + V_1$	***Model 4*** Control plasma+ lung +brain	***Model 5*** P_B	***Model 7†*** $P_{B+} P_L$
AIC	4.536 X 10^{-3}	4.423 X 10^{-3}	4.422 X 10^{-3}	1.744 X 10^{-3}	1.743 X 10^{-3}	1.169 X 10^{-3}

† Model selected for verapamil in presence of loperamide
Cl_E = elimination clearance
V_1 = volume of distribution
P_B = plasma: brain partition coefficient
P_L = plasma: lung partition coefficient

Table 5.3. Pharmacokinetic variables for verapamil in the absence and presence of fentanyl or loperamide (n = 4).

Treatment	P_B	P_L	Cl_E ml/kg/min	V_1 ml
Verapamil	0.020	1.27	0.051	1.77
Verapamil + Fentanyl	0.017	1.46	0.029	0.55
Verapamil + Loperamide	0.063	2.4	0.048	1.81

P_B = plasma: brain partition coefficient
P_L = plasma: lung partition coefficient
Cl_E = elimination clearance
V_1 = volume of distribution

A

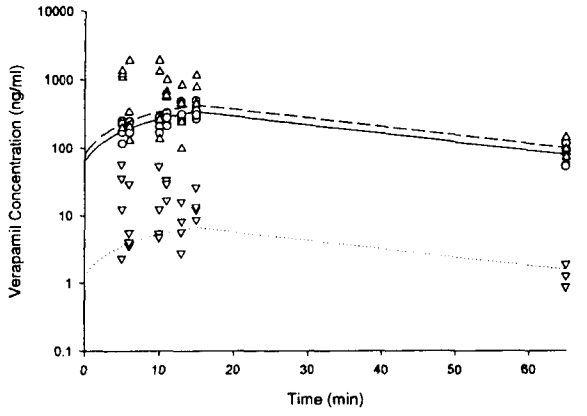

B

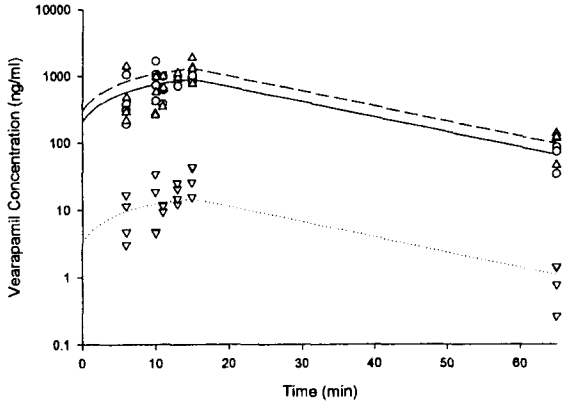

Figure 5.1. Verapamil concentration in Sprague Dawley rats arterial plasma, lung, and brain verapamil only (A), with fentanyl (B). The symbols represent drug concentrations, whereas the lines represent concentrations predicted by the model. Predicted plasma drug concentrations (solid line), measured plasma drug concentration (opened circle), predicted lung drug concentrations (dashed line), measured lung drug concentration (triangle up), predicted brain drug concentration (dotted line), measured brain concentration (triangle down).

A

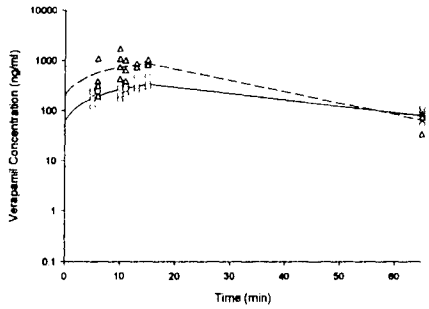

B

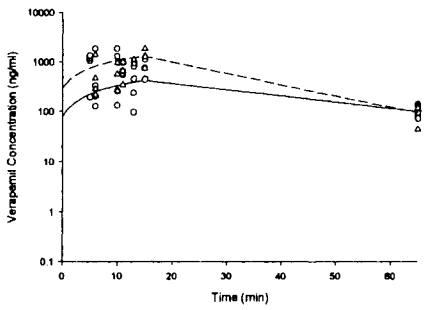

C

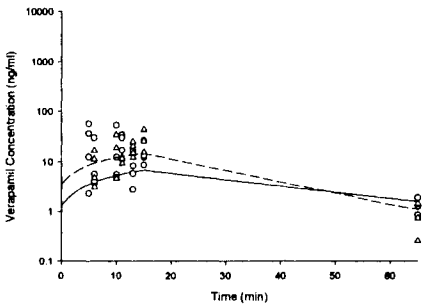

Figure 5.2. Verapamil concentration in Sprague Dawley rats arterial plasma (A), lung (B), and brain (C), in the absence and presence of fentanyl. The symbols represent drug concentrations, whereas the lines represent concentrations predicted by the model. Predicted drug concentrations in absence of fentanyl (solid line), measured drug concentration in absence of fentanyl (circle), predicted drug concentrations in presence of fentanyl (dashed line), measured drug concentration in presence of fentanyl (triangle).

A

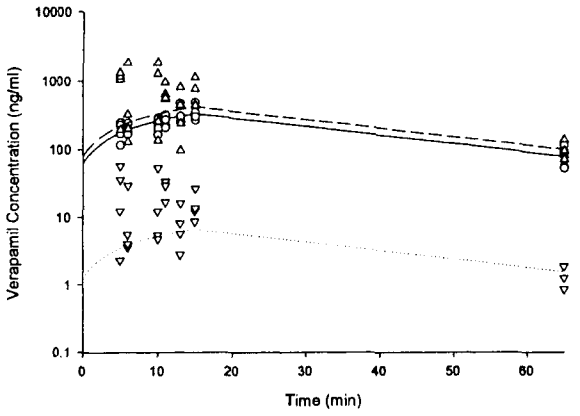

B

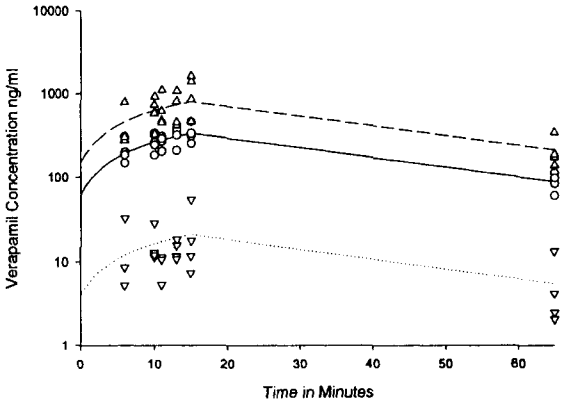

Figure 5.3. Verapamil concentration in Sprague Dawley rats arterial plasma, lung, and brain verapamil only (A), with loperamide (B). The symbols represent drug concentrations, whereas the lines represent concentrations predicted by the model. Predicted plasma drug concentrations (solid line), measured plasma drug concentration (opened circle), predicted lung drug concentrations (dashed line), measured lung drug concentration (triangle up), predicted brain drug concentration (dotted line), measured brain concentration (triangle down).

A

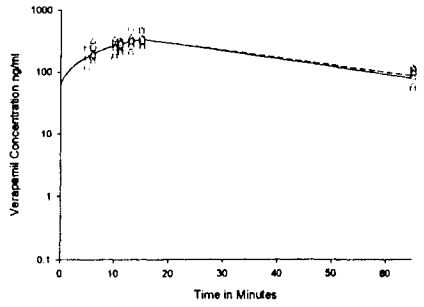

B

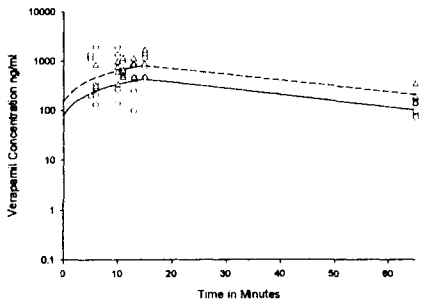

C

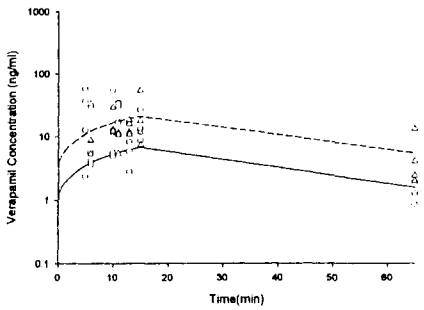

Figure 5.4. Verapamil concentration in Sprague Dawley rats arterial plasma (A), lung (B), and brain (C), in the absence and presence of loperamide. The symbols represent drug concentrations, whereas the lines represent concentrations predicted by the model. Predicted drug concentrations in absence of loperamide (solid line), measured drug concentration in absence of loperamide (circle), predicted drug concentrations in presence of loperamide (dashed line), measured drug concentration in presence of loperamide (triangle).

REFERNCES

Ayrton A and Morgan P (2001) Role of transport proteins in drug absorption, distribution and excretion. *Xenobiotica* **31**:469-497.

Bhatti MM and Foster RT (1997) Pharmacokinetics of the enantiomers of verapamil after intravenous and oral administration of racemic verapamil in a rat model. *Biopharmaceutics & Drug Disposition* **18**:387-396.

Dagenais C, Graff CL and Pollack GM (2004) Variable modulation of opioid brain uptake by P-glycoprotein in mice. *Biochemical Pharmacology* **67**:269-276.

Gustafsson LL, Ebling WF, Osaki E, Harapat S, Stanski DR and Shafer SL (1992) Plasma concentration clamping in the rat using a computer-controlled infusion pump. *Pharmaceutical Research* **9**:800-807.

Henthorn TK, Krejcie TC, Avram MJ, Jensen TR and Waters CM (1998) Transporter-mediated pulmonary endothelial uptake of fentanyl. *International Journal of Clinical Pharmacology & Therapeutics* **36**:74-75.

Henthorn TK, Liu Y, Mahapatro M and Ng KY (1999) Active transport of fentanyl by the blood-brain barrier. *Journal of Pharmacology & Experimental Therapeutics* **289**:1084-1089.

Ludden TM, Beal SL and Sheiner LB (1994) Comparison of the Akaike Information Criterion, the Schwarz criterion and the F test as guides to model selection. *Journal of Pharmacokinetics & Biopharmaceutics* **22**:431-445.

Roerig DL, Kotrly KJ, Dawson CA, Ahlf SB, Gualtieri JF and Kampine JP (1989) First-pass uptake of verapamil, diazepam, and thiopental in the human lung. *Anesthesia & Analgesia* **69**:461-466.

Roerig DL, Kotrly KJ, Vucins EJ, Ahlf SB, Dawson CA and Kampine JP (1987) First pass uptake of fentanyl, meperidine, and morphine in the human lung. *Anesthesiology* **67**:466-472.

Schinkel AH, Wagenaar E, Mol CA and van Deemter L (1996) P-glycoprotein in the blood-brain barrier of mice influences the brain penetration and pharmacological activity of many drugs. *Journal of Clinical Investigation* **97**:2517-2524.

Taeger K, Weninger E, Schmelzer F, Adt M, Franke N and Peter K (1988) Pulmonary kinetics of fentanyl and alfentanil in surgical patients. *British Journal of Anaesthesia* **61**:425-434.

Verschraagen M, Koks CH, Schellens JH and Beijnen JH (1999) P-glycoprotein system as a determinant of drug interactions: the case of digoxin-verapamil. *Pharmacological Research* **40**:301-306.

Waters CM, Avram MJ, Krejcie TC and Henthorn TK (1999) Uptake of fentanyl in pulmonary endothelium. *Journal of Pharmacology & Experimental Therapeutics* **288**:157-163.

Waters CM, Krejcie TC and Avram MJ (2000) Facilitated uptake of fentanyl, but not alfentanil, by human pulmonary endothelial cells. *Anesthesiology* **93**:825-831.

CHAPTER 6

Pravastatin and naloxone reduce fentanyl brain and lung uptake in Sprague Dawley rats.

Iman A. Elkiweri, M.S., £* Martha C. Tissot van Patot, Ph.D., † Yan Ling Zhang, Ph.D., ‡ Uwe Christians, Ph.D., § and Thomas K. Henthorn, M.D., ¥

*Research Associate, †Assistant Professor, ‡Research Associate, §Associate Professor, ¥Chairman and Professor, Department of Anesthesiology, University of Colorado Denver Health Sciences Center, Denver, Colorado, £ Graduate student, Department of Biomedical Sciences, Colorado State University, Fort Collins, Colorado.

Supported by grant No. R01- GM47502.09 from the National Institutes of Health and in part by the Nema Foundation, Malaysia.

Fentanyl is a widely used, potent, synthetic opioid analgesic, which acts at the μ-opioid receptor and is used as an analgesic to supplement general anesthesia for various surgical procedures or as a primary anesthetic agent in very high doses during cardiac surgery. For long term analgesia and sedation in intensive care patients, fentanyl is administered via intravenous infusion (Ball and Westhorpe, 2002; Stanley, 2005). Fentanyl distribution to tissue was considered to be a result of its lipid solubility(Roerig et al., 1994); however, we have previously demonstrated *in vitro* that a saturable energy-dependent process mediates lung and brain uptake of fentanyl – perhaps by an unidentified inward transporter (Henthorn et al., 1998; Henthorn et al., 1999; Waters et al., 1999). Recently, organic anion transporter polypeptides (Oatp/OATP) were found in endothelial cells lining capillaries in the brain and lung of rats (Oatp) and humans (OATP) (Gao et al., 1999; Hagenbuch and Meier, 2003). Evidence suggests that Oatp/OATP may be an important influx system for a wide range of substrates including analgesic opioids, in the brain (Gao et al., 2000) and lung. Pravastatin, the HMG-CoA reductase inhibitor, and naloxone, an opioid receptor antagonist, are either transported by or directly inhibit Oatp/OATP transport respectively (Tokui et al., 1999); (Gao et al., 2000) and may be used to block Oatp/OATP transport, *in vivo*.

Therefore, we hypothesized that pravastatin and naloxone would inhibit fentanyl uptake by the brain and lung *in vivo*. Our aim was to determine fentanyl plasma: brain and plasma: lung partition ratios as well as the global pharmacokinetics (pk) parameters of volume of distribution and elimination clearance in the absence and presence of pravastatin and naloxone.

Methods

Experimental Protocol. After Institutional Animal Care and Use approval adult male Sprague- Dawley rats weighing 300-350 g were purchased from Harlan (Madison, Wisconsin) with indwelling cannulae (jugular venous catheters for drug infusion and a carotid artery catheter for blood collection). The rats were housed in the UCHSC animal facility. They were kept on a 12-hour light/dark cycle and were fed standard laboratory chow. The animals received a five minute (from time t=0 to 5 minutes) intravenous infusion of the centrally acting study drug fentanyl citrate purchased from Abbott Laboratories (North Chicago, IL, USA) (5.25 μg/kg/min). On a separate occasion, pravastatin sodium purchased from Bristol Primary Care (1.3 mg/kg/min) or naloxone hydrochloride purchased from Abbott Laboratories (North Chicago, IL, USA) (0.1mg/kg/min) was administered for five minutes prior to the opioid infusion and continued ten minutes after the opioid infusion (from time t = -5 to 10). The infusion was accomplished using a Harvard 22 syringe pump (Harvard Apparatus, Holliston, Massachusetts). Four rats per time period were euthanized by guillotine at 1, 5, and 10 minutes. Blood (5 mL) was collected from the carotid catheter prior to decapitation and drawn into tubes containing citrate as anticoagulant. Plasma was separated following a standard centrifugation protocol (400 g, 10 min, 4°C). The skull was opened immediately after decapitation. Brain tissue was collected and was flash-frozen in liquid nitrogen. A thoracotomy was performed to allow extraction of the lungs which were immediately frozen in liquid nitrogen. Plasma, lung, and brain tissue were stored at –80°C until analysis using a specific and highly sensitive high-performance liquid chromatography/ mass spectrometry assay.

Analytical Methods Plasma and tissue fentanyl concentration of all samples obtained at the times delineated above were measured by a high-performance liquid chromatography/ mass spectrometry technique developed in our laboratory.

Instrumentation. The extracts were analyzed using an LC/LC-MS/MS system. The two HPLC systems consisted of the following components (all series 1100, Agilent Technologies, Palo Alto, CA): HPLC I: G1312A binary pump, G1379A degasser and a LEAP autosampler (PAL, Zürich, Switzerland); HPLC II: G1312A binary pump, and a G1316A column thermostat. A Sciex API 4000 triple-stage quadrupole mass spectrometer was used as detector (Applied Biosystems, Foster City, CA). The HPLC systems were connected *via* a 6-port column-switching valve mounted on a step motor (Rheodyne, Cotati, CA). The connections of the switching valve and the solvent flow in the two valve positions are shown in figure 6.1.

Sample Preparation. Rat brain and lung (approximately 10 mg) were weighed and homogenized with 2 ml KH_2PO_4 buffer pH=7.4 (1 M) using a teflon-glass manual homogenizer. Homogenized samples were stored at -80°C before analysis. On the day of analysis, plasma and homogenized brain and lung were thawed on ice. Samples were prepared by adding 200 µL of plasma, or homogenates of lung or brain to 400 µL of internal standard solution (0.06 M $ZnSO_4$ solution contained water and methanol (30:70, v/v), and 10 µL of the internal standard alfentanil resulting in a final concentration of 50 ng/mL. After vortexing (2 min), the samples were centrifuged (13000 g × 5 min) to remove precipitated proteins. One hundred µL of the supernatant was directly injected into the HPLC system (1100 HP Agilent, Waldbronn, Germany) through a Leap autosampler.

For on-line sample clean-up, supernatants were loaded onto the extraction column (4.6 × 12.5 mm, 5 μm particle size, Eclipse XDB-C8, Agilent) and were washed with a high flow of 5 mL/min, 80% 0.1% formic acid/ 20% methanol for 1 min. Then the switching valve was activated and the analytes were back-flushed onto the C8 analytical column (4.6 × 12.5 mm, 5 μm particle size, Eclipse XDB-C8, Agilent). A linear gradient was used: methanol increased from 55% to 100% in 4 min and was kept at 100% methanol for 1 min. Flow rate was 1 mL/min. Column temperature was maintained at 40°C.

The analytes that eluted from the HPLC column were introduced into the turbo-ion spray source. Zero-grade air for the nebulizing and turbo gasses was provided by a Zero Air Generator (Analytical Gas Systems). Ultra-high-purity nitrogen (99.999%) was used as collision activated dissociation (CAD) gas and the curtain gas provided by a nitrogen generation systems purchased (Agilent, Palo Alto, CA). Ionization was achieved in the positive Multiple Reaction Monitory (MRM) mode. MRM sensitivities for each analyte were simultaneously optimized by direct infusion of each compound (0.1 μg/mL, in 80% methanol/20% 0.1% formic acid). The mass spectrometer, HPLC components, LEAP autosampler and all data processing were controlled through the ABI/Sciex "Analyst" software version 1.3. (Applied Biosystems, Foster City, CA).

For the quantification of fentanyl the MRM parameters used were: the source temperature was set to 480°C, and the ion spray voltage was 5000V, gases were set at 20 for nebulizer gas, 15 for turbo gas, curtain gas was 15 and the setting for the CAD gas was 8 (all arbitrary units). The declustering potential (DP) was 50V. The dwell time for each transition was 200 ms. Data was collected and the major product ion transitions were

monitored: fentanyl *m/z* 337.5 → 188.4, and the internal standard alfentanil *m/z* 417.4 → 197.3.

Data Analysis. The pharmacokinetics were analyzed using the SAAM II software (SAAM Institute, Seattle, WA) using a naive pooled-data technique. Model parsimony was tested using the Akiake information criterion (AIC) (Ludden et al., 1994). The data from the fentanyl infusion alone and the fentanyl infusion with pravastatin or naloxone treatment where lumped into separate models with linked parameters. Plasma kinetics were modeled with a one-compartment open model in which volume of distribution (V_1) and elimination clearance (Cl_E) were fit to the plasma fentanyl concentration-time data.

To test the hypothesis that pravastatin or naloxone affect the plasma pharmacokinetics of fentanyl, all data were first fit to a unified pharmacokinetic model for fentanyl and then each of the adjustable parameters V_1 and Cl_E where fit so that each parameter could have a covariate parameter for the experimental condition in which pravastatin or naloxone was infused. Whether a covariate for the pravastatin or naloxone condition produced a statistically significant change in the pharmacokinetic parameter was tested by comparing the AIC with the added covariate in the model versus the AIC the simpler model without the covariate (Table 6.1-6.2).

Lung and brain concentration-time data were modeled by adding brain (P_B) and lung (P_L) partition coefficients, to describe the ratio between plasma fentanyl concentrations and those in brain and lung, respectively. To test the hypothesis that pravastatin or naloxone changes plasma: tissue partitioning in the brain and lung, all data were first fit to a unified pharmacokinetic model for fentanyl alone and then each of the plasma: tissue partition coefficients (P_B, P_L) where fit so that each coefficient could have a covariate parameter

for the experimental condition in which pravastatin or naloxone was infused. Whether a covariate for the pravastatin or naloxone condition produced a statistically significant change in the partition coefficient was tested by comparing the AIC with the added covariate in the model versus the AIC the simpler model without the covariate (Table 6.1-6.2).

Results

Effect of pravastatin on fentanyl pharmacokinetics. Rat arterial plasma, lung and brain fentanyl concentrations in the absence and presence of pravastatin versus time relations were well-characterized by the model from the moment of injection (Figures 6.2-6.3). Fentanyl plasma pharmacokinetics were described using a one-compartment open model in which the parameters V_1 and Cl_E, were fit to the plasma concentration-time data. As shown in table 6.1 model 2 had the lowest AIC and was the model chosen to report the results herein. Pravastatin treatment had no effect on Cl_E yet it increased V_1 by 5.27-fold (Table 6.3).

Lung and brain concentration-time data were modeled by adding partition coefficients of lung (P_L) and brain (P_B) to describe the ratio between plasma fentanyl concentrations and those in lung and brain, respectively. Model 6 was chosen to report the results herein because it had the lowest AIC (Table 6.1). Pravastatin decreased P_L and P_B by 56% and 76% respectively (Table 6.3).

Effect of naloxone on fentanyl pharmacokinetics. Rat arterial plasma, lung and brain fentanyl concentrations in the absence and presence of naloxone versus time relations were well-characterized by the model from the moment of injection (Figures 6.4-6.5).

Fentanyl plasma pharmacokinetics in presence of naloxone were described using a one-compartment open model similar to that described above. Model 3 is the model with the lowest AIC and hence was chosen to report the results herein (Table 6.2). Naloxone increased V_1 and Cl_E by 1.6-fold and 3.2-fold respectively (Table 6.3).

Fentanyl lung and brain concentration-time data in presence of nalaxone were modeled similar to that described for fentanyl in presence of pravastatin. Model 6 had the lowest AIC and chosen to report the results herein (Table 6.2). Naloxone decreased P_L and P_B by 83% and 68% respectively (Table 6.3).

Discussion

We wished to determine the effect of pravastatin and naloxone on the distribution of fentanyl in lung and brain of rats. Our results showed that pravastatin and naloxone reduced P_L and P_B of fentanyl. Further pravastatin and naloxone increased V_1 and naloxone increased Cl_E of fentanyl, *in vivo*.

Previously, we showed that uptake of fentanyl in lung and brain occurred via an unidentified inward transporter which overshadows efflux transport by P-gp (Henthorn et al., 1998; Henthorn et al., 1999; Waters et al., 1999). Recently, Oatp/OATP transporter proteins were found in endothelial cells lining capillaries in the brain and lung of rats and humans (Gao et al., 1999; Hagenbuch and Meier, 2003) and were reported to serve as inward transporters for opioids (Gao et al., 2000). Evidence from others suggests that pravastatin is a substrate of Oatp (Tokui et al., 1999) and naloxone inhibits opioid uptake by Oatp (Gao et al., 2000). The reduction in lung and brain fentanyl partitioning ratios reported in the current study in the presence of pravastatin and naloxone suggests that

fentanyl uptake in lung and brain may be mediated by the inward transporter Oatp/OATP. Further that pravastatin is a substrate/inhibitor of the inward transporter Oatp/OATP.

In conclusion, co-administration of fentanyl with pravastatin or naloxone reduces lung and brain fentanyl partitioning ratios in Sprague Dawley rats. These data suggest that Oatp/OATP transport may be involved in cerebral and pulmonary uptake of opioids and that pravastatin is a substrate/inhibitor of Oatp/OATP.

Table 6.1. Akiake information criterion (AIC) for pharmacokinetic models of fentanyl alone (control) and with pravastatin.

Treatment	*Model 1* Control plasma (fentanyl alone)	*Model 2** V_1	*Model 3* V_1+CL_E	*Model 4* Control plasma+ lung +brain (fentanyl alone)	*Model 5* P_B	*Model 6** P_{B+} P_L
AIC	3.518×10^{-3}	3.251×10^{-3}	3.260×10^{-3}	2.724×10^{-3}	2.616×10^{-3}	2.600×10^{-3}

* Model selected for fentanyl in presence of pravastatin.
Cl_E = elimination clearance
V_1 = volume of distribution
P_B = plasma: brain partition coefficient
P_L = plasma: lung partition coefficient

Table 6.2. Akiake information criterion (AIC) for pharmacokinetic models of fentanyl alone (control) and with naloxone.

Treatment	***Model 1*** Control plasma (fentanyl alone)	***Model 2*** CL_E	***Model 3†*** CL_E+V_1	***Model 4*** Control plasma+ lung +brain (fentanyl alone)	***Model 5*** P_B	***Model 6†*** $P_{B+}P_L$
AIC	3.277×10^{-3}	3.251×10^{-3}	3.118×10^{-3}	2.726×10^{-3}	2.604×10^{-3}	2.542×10^{-3}

† Model selected for fentanyl in presence of naloxone.
Cl_E = elimination clearance
V_1 = volume of distribution
P_B = plasma: brain partition coefficient
P_L = plasma: lung partition coefficient

Table 6.3. Pharmacokinetic variables for fentanyl and loperamide in the absence and presence of pravastatin and naloxone (n = 4), using data from models described in Tables 6.1 and 6.2.

Treatment	P_B	P_L	Cl_E ml/kg/min	V_1 ml
Fentanyl	0.115	0.413	0.12	0.39
Fentanyl + Pravastatin	0.0275	0.183	0.12	2.055
Fentanyl+ Naloxone	0.036	0.0699	0.198	1.248

P_B = plasma: brain partition coefficient
P_L = plasma: lung partition coefficient
Cl_E = elimination clearance
V_1 = volume of distribution

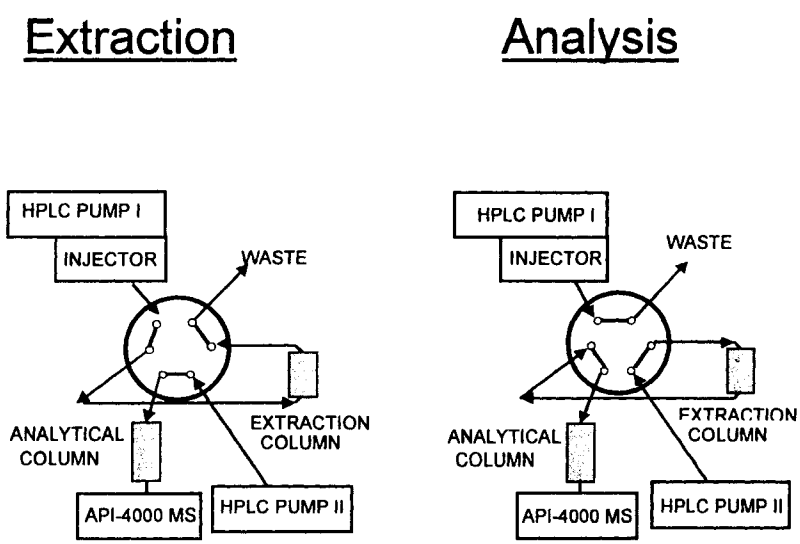

Figure 6.1. Connections and solvent flow of the HPLC switching valve.

A

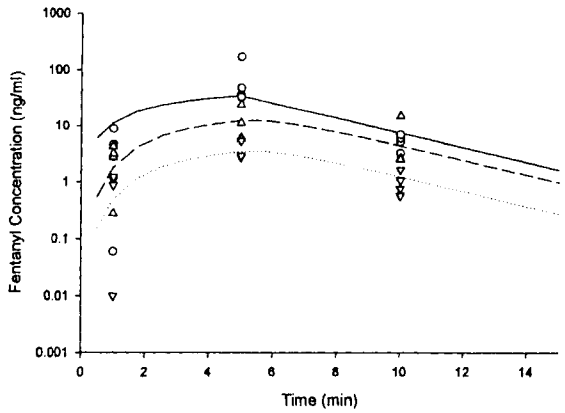

B

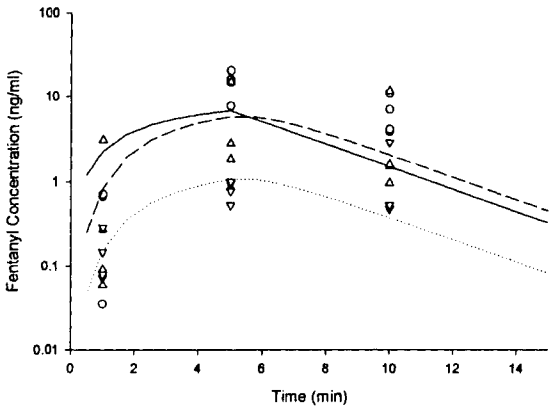

Figure 6.2. Fentanyl concentration in Sprague-Dawley rats arterial plasma, lung, and brain in the absence (A) and presence (B) of pravastatin. The symbols represent measured drug concentrations, whereas the lines represent concentrations predicted by the model. Predicted plasma drug concentrations (solid line), measured plasma drug concentration (circle), predicted lung drug concentrations (dashed line), measured lung drug concentration (triangle up), predicted brain drug concentration (dotted line), measured brain concentration (triangle down).

A

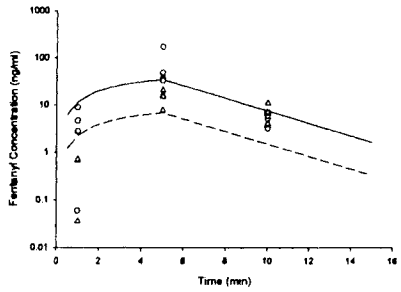

B

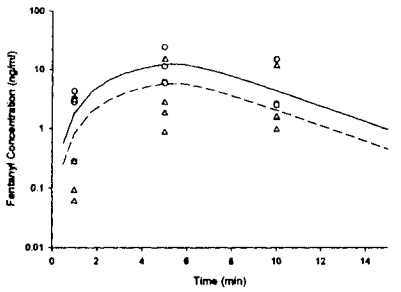

C

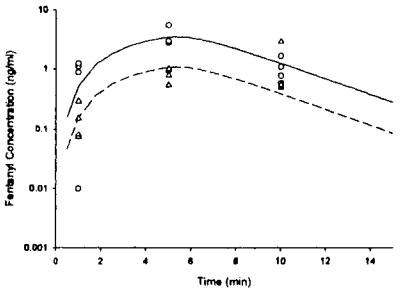

Figure 6.3. Fentanyl concentration in Sprague-Dawley rats arterial plasma (A), lung (B), and brain (C) in the absence and presence of pravastatin. The symbols represent measured drug concentrations, whereas the lines represent concentrations predicted by the model. Predicted drug concentrations in absence of pravastatin (solid line), measured drug concentration in absence of pravastatin (circle), predicted drug concentrations in presence of pravastatin (dashed line), measured drug concentrations in presence of pravastatin (triangle).

A

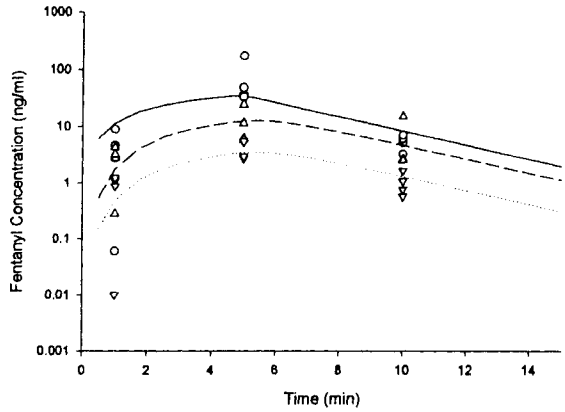

B

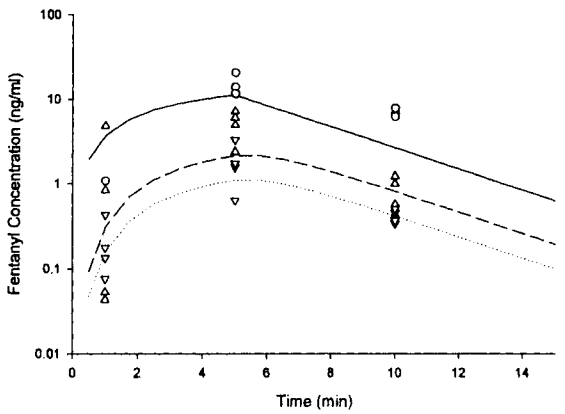

Figure 6.4. Fentanyl concentration in Sprague-Dawley rats arterial plasma, lung, and brain in the absence (A) and presence (B) of naloxone. The symbols represent measured drug concentrations, whereas the lines represent concentrations predicted by the model. Predicted plasma drug concentrations (solid line), measured plasma drug concentration (circle), predicted lung drug concentrations (dashed line), measured lung drug concentration (triangle up), predicted brain drug concentration (dotted line), measured brain concentration (triangle down).

A

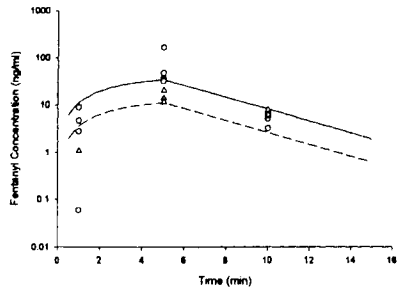

B

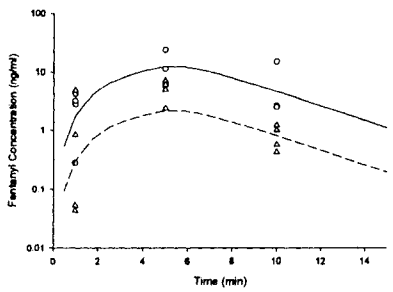

C

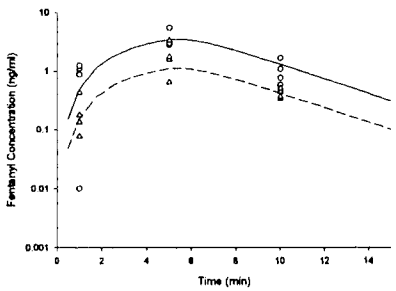

Figure 6.5. Fentanyl concentration in Sprague-Dawley rats arterial plasma (A), lung (B), and brain (C) in the absence and presence of naloxone. The symbols represent measured drug concentrations, whereas the lines represent concentrations predicted by the model. Predicted drug concentrations in absence of naloxone (solid line), measured drug concentration in absence of naloxone (circle), predicted drug concentrations in presence of naloxone (dashed line), measured drug concentrations in presence of naloxone (triangle).

RFERENCES

Ball C and Westhorpe R (2002) Intravenous induction agents: opioids. *Anaesthesia & Intensive Care* **30**:717.

Gao B, Hagenbuch B, Kullak-Ublick GA, Benke D, Aguzzi A and Meier PJ (2000) Organic anion-transporting polypeptides mediate transport of opioid peptides across blood-brain barrier. *Journal of Pharmacology & Experimental Therapeutics* **294**:73-79.

Gao B, Stieger B, Noe B, Fritschy JM and Meier PJ (1999) Localization of the organic anion transporting polypeptide 2 (Oatp2) in capillary endothelium and choroid plexus epithelium of rat brain. *Journal of Histochemistry & Cytochemistry* **47**:1255-1264.

Hagenbuch B and Meier PJ (2003) The superfamily of organic anion transporting polypeptides. *Biochimica et Biophysica Acta* **1609**:1-18.

Henthorn TK, Krejcie TC, Avram MJ, Jensen TR and Waters CM (1998) Transporter-mediated pulmonary endothelial uptake of fentanyl. *International Journal of Clinical Pharmacology & Therapeutics* **36**:74-75.

Henthorn TK, Liu Y, Mahapatro M and Ng KY (1999) Active transport of fentanyl by the blood-brain barrier. *Journal of Pharmacology & Experimental Therapeutics* **289**:1084-1089.

Ludden TM, Beal SL and Sheiner LB (1994) Comparison of the Akaike Information Criterion, the Schwarz criterion and the F test as guides to model selection. *Journal of Pharmacokinetics & Biopharmaceutics* **22**:431-445.

Roerig DL, Ahlf SB, Dawson CA, Linehan JH and Kampine JP (1994) First pass uptake in the human lung of drugs used during anesthesia. *Advances in Pharmacology* **31**:531-549.

Stanley TH (2005) Fentanyl. *Journal of Pain & Symptom Management* **29**:S67-71.

Tokui T, Nakai D, Nakagomi R, Yawo H, Abe T and Sugiyama Y (1999) Pravastatin, an HMG-CoA reductase inhibitor, is transported by rat organic anion transporting polypeptide, oatp2. *Pharmaceutical Research* **16**:904-908.

Waters CM, Avram MJ, Krejcie TC and Henthorn TK (1999) Uptake of fentanyl in pulmonary endothelium. *Journal of Pharmacology & Experimental Therapeutics* **288**:157-163.

CHAPTER 7

Summary and Conclusions

Previous research by our group and others has indicated that opioid transport into the brain is highly variable between individuals and is mediated by active uptake and efflux transporters (Henthorn et al., 1998; Henthorn et al., 1999; Waters et al., 2000). Data depicting the intricacies of opioid transport mechanisms may lead to development of therapies designed to normalize individual response to opioid infusion. To approach this goal, we first developed a semi-automated LC/LC-MS/MS platform for the simultaneous quantification of opioids and validated for alfentanil, fentanyl, loperamide, remifentanil and sufentanil in minute volumes of various biological samples (rat plasma, tissues and human plasma). We then used these methods to investigate the role of opioid transport inhibitors in lung and brain of Sprague Dawley rats using pharmacokinetic and pharmacodyanamic (EEG) modeling techniques.

Initially, we wished to evaluate the effect of verapamil on fentanyl and loperamide partitioning in lung and brain, *in vivo* and hypothesized differential effects of verapamil on these processes. Using a high resolution recirculatory model, we showed that fentanyl and loperamide demonstrated rapid uptake into lung and brain tissue but the partitioning of fentanyl was more extensive. Verapamil slightly decreased brain partition coefficient

for fentanyl, whereas the lung (P_L) and brain (P_B) partition coefficients of loperamide increased to a much larger extent (Table 7.1A). For fentanyl, the uptake-inhibiting effect of verapamil was in the brain whereas for loperamide, the uptake-promoting effect was greater in the lung. These results confirm our previous findings that fentanyl brain uptake is mediated by an active inward transport process that is inhibited by verapamil *in vitro* (Henthorn et al., 1999). Furthermore, we demonstrated that in contrast to previous reports (Heykants et al., 1974; Heel et al., 1978) that loperamide is devoid of central opiate-like effect; loperamide may pass the blood brain barrier and elicit such effect.

We then sought to determine the physiologic effect of altered partitioning and clearance of opioids in the presence of verapamil by measuring a continuously processed electroencephalogram in Sprague Dawley rats. The differential effects of verapamil on intrinsic brain activity of the opioids, fentanyl and loperamide were determined. Results were then modeled using a sigmoidal E_{max} pharmacodynamic model. Verapamil increased the equilibration rate effect of fentanyl (k_{e0}) by 80% and EC_{50} increased by 74%, for loperamide k_{e0} decreased by 60% and EC_{50} decreased 44% (Table 7.1B). This is the first report to demonstrate that loperamide has a central effect when administered intravenously. Further, we showed that P-gp inhibition by verapamil increased loperamide access into brain confirming findings of others indicating that administration of quinidine, a P-gp substrate, with loperamide resulted in an opioid central effect. However, we report that there is less fentanyl in the CNS at any given steady-state blood concentration in the presence of verapamil.

Because our data suggested that verapamil was both an inhibitor and a substrate of inward and outward transporters, we investigated the effect of opioids on verapamil disposition in lung and brain, *in vivo*. We used a recirculatory model to evaluate verapamil pharmacokinetics in the absence and presence of fentanyl or loperamide. We found that fentanyl slightly increased the lung partition coefficient and loperamide increased verapamil lung *and* brain partitioning (Table 7.1C). We also demonstrated that fentanyl reduced verapamil volume of distribution (V_I) and elimination clearance (Cl_E). These results confirm that verapamil and loperamide are substrates of the efflux transporter P-glycoprotein (P-gp) and suggest that verapamil and fentanyl may be substrates of a yet unidentified inward transporter.

Because our results indicated that verapamil had slight effect on fentanyl partitioning and clearance, we hypothesized that inhibition of Oatp influx transporter by pravastatin or naloxone may reduce lung and brain fentanyl partitioning ratios, *in vivo*. We report that in the presence of pravastatin, fentanyl P_L and P_B decreased by 56% and 76% respectively. Further naloxone reduced fentanyl P_L and P_B by 83% and 68% respectively (Table7.1D).

Our data indicated that the effect of verapamil on opioid uptake and intrinsic brain activity is dependent on the opioid used as it can inhibit uptake of fentanyl and efflux of loperamide. Further, the effectiveness of verapamil activity was organ specific; verapamil had an effect on fentanyl partition in the brain while it had no effect on fentanyl partitioning into lung yet for loperamide the greater effect was in the lung. Both fentanyl and loperamide had central effects, and verapamil mediated changes in brain intrinsic

activity confirming partitioning data for both opioids. Pursuing evidence suggesting the presence of an active inward transporter for fentanyl, our investigations provided data suggesting that the Oatp transporter plays such a role. Further investigations are needed to confirm these data. Overall, data are promising that opioid effect may be modulated by therapies targeting opioid uptake and/or efflux, yet a greater understanding of transport mechanisms is necessary before such therapies are designed.

Table 7.1 Summary of Results

A. Fentanyl/loperamide partitioning and global pharmacokinetics in presence of verapamil.

Treatment	P_B	P_L	Cl_E	V_1	V_2
Fentanyl+ Verapamil	Decreased 42.6%	No change	Increased 23%	Increased 125% (2.2-fold)	No change
Loperamide+ Verapamil	Increased 80.7% (1.8 fold)	Increased 427% (5.27fold)	Decreased 49.5%	No Change	Increased 89.3%

B. EEG parameters

Treatment	EC_{50}	k_{e0}
Fentanyl+ Verapamil	Increased 74%	Increased 80%
Loperamide+ Verapamil	Decreased 44%	Decreased 60%

C. Verapamil partitioning and global pharmacokinetics in presence of opioids.

Treatment	P_B	P_L	Cl_E	V_1
Verapamil + Fentanyl	Slight decrease	Increase 15%	Decrease 43%	Decrease 69%
Verapamil + Loperamide	Increase 3.7-fold	Increase 1.6-fold	Slight decrease	Slight decrease

D. Fentanyl partitioning and global pharmacokinetics in presence of pravastatin or naloxone.

Treatment	P_B	P_L	Cl_E	V_1
Fentanyl + pravastatin	Decreased 76%	Decreased 56%	No change	Increased
Fentanyl + naloxone	Decreased 68%	Decreased 83%	Increased 1.6-fold	Increased 3.2-fold

REFERNCES

Heel RC, Brogden RN, Speight TM and Avery GS (1978) Loperamide: a review of its pharmacological properties and therapeutic efficacy in diarrhoea. Drugs **15**:33-52.

Henthorn TK, Krejcie TC, Avram MJ, Jensen TR and Waters CM (1998) Transporter-mediated pulmonary endothelial uptake of fentanyl. International Journal of Clinical Pharmacology & Therapeutics **36**:74-75.

Henthorn TK, Liu Y, Mahapatro M and Ng KY (1999) Active transport of fentanyl by the blood-brain barrier. Journal of Pharmacology & Experimental Therapeutics **289**:1084-1089.

Heykants J, Michiels M, Knaeps A and Brugmans J (1974) Loperamide (R 18 553), a novel type of antidiarrheal agent. Part 5: the pharmacokinetics of loperamide in rats and man. Arzneimittel-Forschung **24**:1649-1653.

Waters CM, Krejcie TC and Avram MJ (2000) Facilitated uptake of fentanyl, but not alfentanil, by human pulmonary endothelial cells. Anesthesiology **93**:825-831.